

**Evaluation of Commercial Sorbents for Separation of Ultrashort-, Short-, and Long-chain Per- and Polyfluoroalkyl Substances (PFAS) from Municipal Wastewater Effluent**

Kovas Saulius Žygas

A thesis  
submitted in partial fulfillment of  
the requirements for the degree of

Master of Science

University of Washington  
2025

Committee:  
Jessica Ray  
Edward Kolodziej

Program Authorized to Offer Degree:  
Civil and Environmental Engineering

©Copyright 2025  
Kovas Saulius Žygas

University of Washington

**Abstract**

Evaluation of Commercial Sorbents for Separation of Ultrashort-, Short-, and Long-chain Per- and Polyfluoroalkyl Substances (PFAS) from Municipal Wastewater Effluent

Kovas Saulius Žygas

Chair of the Supervisory Committee:  
Jessica Ray  
Civil and Environmental Engineering

PFAS are a diverse class of synthetic compounds that, are persistent, mobile, and have been detected ubiquitously in the environment in all parts of the world. In addition to the continued detection of "legacy PFAS" such as, PFOA and PFOS, there is increasing awareness and concern over ultrashort-chain and short-chain perfluoroalkyl acids (PFAAs) in treated wastewater effluent. Traditional adsorptive media such as granular activated carbon (GAC) and ion exchange (IX) resins have demonstrated inhibited PFAS removal due to the presence of organic matter (OM), co-occurring ionic constituents, and relatively poor uptake of short- and ultrashort-chain PFAAs.

This study evaluated commercially available sorbent media for the removal of ultrashort-, short-, and long-chain per- and polyfluoroalkyl substances (PFAS) from a variety of aquatic matrices including ultrapure water, synthetic wastewater effluent and treated municipal wastewater effluent – with a focus on addressing the influence of matrix interferences in the form of wastewater effluent-derived organic matter and co-occurring constituents on PFAS removal. The adsorptive media we evaluated included GACs, non-selective and "PFAS-selective" ion exchange resins (IX), and two alternative adsorbent materials that are commercially marketed as PFAS treatment technologies: an anonymized surface-modified clay (SMC), and a  $\beta$ -cyclodextrin-based polymeric adsorbent (DEXSORB<sup>®</sup>, Cyclopure<sup>®</sup>). Batch adsorption capacity and kinetics tests

were conducted in both ultrapure (UP) and synthetic wastewater (SW) matrices to characterize PFAS removal prior to continuous-flow rapid small-scale column tests (RSSCTs) using artificially spiked tertiary treated municipal wastewater effluent from an ultrafiltration (UF) membrane pilot system.

In UP water, long-chain PFAS outcompeted and displaced (ultra)short-chain PFAS across all sorbents, suppressing (ultra)short-chain uptake and driving strong preferential adsorption of long-chain PFASs and PFCAs. While GAC and DEXSORB® exhibit pronounced chain-length-dependent sorption dominated by hydrophobic interactions, the IX resins show more balanced uptake across PFAS chain-lengths, reflecting the greater role of electrostatic interactions in their removal. Despite strong adsorption in ultrapure water, IRA910 IX performed similarly to GAC in the SW matrix, demonstrating inhibited adsorption kinetics and capacities across all PFAS chain-lengths, especially for PFCAs and short- and ultrashort-chain PFAS, while PFA694 IX and DEXSORB® were least affected by the SW matrix. In the RSSCTs, the PFA694 IX resin treated the suite of 18 PFAS to the lowest effluent concentrations for the longest operational times compared to DEXSORB, F400 GAC, and non-selective IRA910 IX resin. Although, PFA694 IX only exhibited incremental improvement over GAC for treating short- and ultrashort-chain PFCAs.

Agreement between SW batch tests and column results underscores the need to evaluate PFAS treatment media under realistic wastewater conditions. Fundamentally, further characterization and elucidation of the physical and chemical characteristics of the adsorbent media, particularly the proprietary PFAS-selective IX resins, in addition to evaluations of single-PFAS solute systems in ultrapure and complex aqueous matrices, will help improve the mechanistic understanding of the removal of ultrashort-, short-, and long-chain PFAAs and other PFAS widespread in the environment and municipal wastewater effluents. The results of this study

suggest that in an ideally designed treatment train scenario installation of a PFAS-selective IX resin employed as a polishing step following tertiary treatment of secondary wastewater effluent could be a feasible method to target PFAS for removal from municipal wastewater.

## **Acknowledgements**

First and foremost, I would like to thank Dr. Jess Ray for her leadership, mentorship, guidance, and support through all phases of this research. Thank you for enthusiastically sharing your knowledge and expertise with me and the rest of the AIMS Lab, and for assisting tremendously in my development and growth as a scientist and engineer through the opportunity to work on this project. I am grateful for the opportunity provided by the King County-UW Technology Research Fellowship program, which provided the funding for this research. Thank you to Bob Bucher, Pardi Sukapanpotharam, Eron Jacobsen and the rest of the King County staff who provided their insight and guidance, as well as attending my research updates.

Thank you to the other members of the AIMS Lab, Reagan Beers, Alanna Hildebrandt, Kaylyn Stewart, Aparna Lobo, Priya Seetharaman, Jen Hooper, Fanny Okaikue-Woodi, Amy Quintanilla, and Jess Steigerwald for all of the assistance with laboratory work, discussions, training, coordinating supplies and ordering, and helpful advice you all shared with me over the past year-and-a-half. Thank you, also, to all of the AIMS Lab's stellar undergraduate research assistants. Particularly, thank you to Evan Eadie for all of your assistance in completing much of the crucial laboratory procedures that were a significant contribution to the completion of this research - as well as Finn and Cedric who were vital in collecting samples for the RSSCTs. I would also like to thank Dr. Martin Sadilek and Brandon Bolb at the University of Washington Department of Chemistry Mass Spectrometry Facility for their knowledge, assistance and support in training me to conduct LC-MS/MS quantification of PFAS and always being willing to help with troubleshooting. And I cannot forget to thank Dr. Ed Kolodziej, for sitting on my defense committee, as well as all of the staff and faculty in the Civil & Environmental Engineering Department for making my UW experience a great learning opportunity

I would like to thank my family and friends for not only their support over the past year-and-a-half, but throughout my past who have helped me get to this stage in my life and academic career. Mostly, thank you to my mom Dalia for supporting me through my youth and through my undergrad experience and beyond; for always encouraging me to do my best; and for instilling in me a deep-seated interest in chemistry, water, and science.

Finally, I do not have enough words to describe how influential and crucial to my life - as a student at UW, and over the past 9 years, that my amazing partner Rosa has been. Thank you, Rosa, for your incredible, kind, loving belief in me.

<b><u>EVALUATION OF COMMERCIAL SORBENTS FOR SEPARATION OF ULTRASHORT-, SHORT-, AND LONG-CHAIN PER- AND POLYFLUOROALKYL SUBSTANCES (PFAS) FROM MUNICIPAL WASTEWATER EFFLUENT</u></b>	<b>1</b>
<b><u>ABSTRACT</u></b>	<b>3</b>
<b><u>ACKNOWLEDGEMENTS</u></b>	<b>6</b>
<b><u>LIST OF FIGURES</u></b>	<b>10</b>
<b><u>LIST OF TABLES</u></b>	<b>10</b>
<b><u>1. EXPANDED INTRODUCTION</u></b>	<b>11</b>
1.1. PFAS INTRODUCTION	11
1.2. LEGACY PFAS	15
1.3. ULTRASHORT-CHAIN PFAS	18
1.4. PFAS OCCURRENCE IN WASTEWATER TREATMENT PLANTS	21
1.5. PFAS TREATMENT METHODS	22
1.5.1. PFAS ADSORPTION FROM AQUEOUS MATRICES	23
1.5.1.1. GRANULAR ACTIVATED CARBON (GAC)	23
1.5.1.2. ION EXCHANGE (IX) RESINS	26
1.5.1.3. ALTERNATIVE ADSORBENTS	30
1.6. STUDY OBJECTIVES AND HYPOTHESES	35
1.6.1. Media Selected for Evaluation	37
1.6.2. <i>PFAS SELECTED FOR EVALUATION</i>	47
<b><u>2. MANUSCRIPT: EVALUATING COMMERCIAL SORBENTS FOR REMOVAL OF ULTRASHORT-, SHORT-, AND LONG-CHAIN PER- AND POLYFLUOROALKYL SUBSTANCES (PFAS) FROM MUNICIPAL WASTEWATER EFFLUENTS</u></b>	<b>49</b>
2.1. OBJECTIVES AND HYPOTHESIS	49
2.2. MATERIALS AND METHODS	52
2.2.1. <i>CHEMICALS</i>	52

2.2.2.	<i>COMMERCIAL MEDIA SELECTED FOR EVALUATION</i>	54
2.2.2.1.	<i>Point of zero charge</i>	55
2.2.3.	<i>BATCH SORPTION ISOTHERM AND KINETICS TESTS IN ULTRAPURE WATER</i>	55
2.2.4.	<i>SYNTHETIC WASTEWATER (SW)-MATRIX SORPTION CAPACITY AND KINETICS TESTS</i>	56
2.2.5.	<i>RAPID SMALL-SCALE COLUMN TESTS (RSSCTS)</i>	58
2.2.5.1.	<i>Tertiary-Treatment UF-Membrane Pilot</i>	59
2.2.5.2.	<i>Wastewater Characterization</i>	60
2.2.6.	<i>PFAS QUANTIFICATION</i>	60
<b>2.3.</b>	<b>RESULTS AND DISCUSSION</b>	<b>61</b>
2.3.1.	<i>ULTRAPURE WATER ISOTHERM TESTS FOR 18-PFAS MIX—NON-SELECTIVE IX RESIN EXHIBITS GREATEST PFAS ADSORPTION CAPACITY</i>	61
2.3.1.1.	<i>GACs exhibit multi-layer adsorption at high aqueous PFAS loadings</i>	61
2.3.1.2.	<i>DEXSORB® exhibits sorption behavior dominated by hydrophobic interactions</i>	63
2.3.1.3.	<i>Non-PFAS-selective IX resin has highest PFAS adsorption capacity</i>	66
2.3.2.	<i>INTRA-PFAS COMPETITION IN AN ULTRAPURE MATRIX: LONG-CHAIN PFAS OUTCOMPETE (ULTRA)SHORT-CHAIN PFAS</i>	73
2.3.3.	<i>FAST SORPTION OF (ULTRA)SHORT-CHAIN PFAS, SUPPRESSED AND DISPLACED BY LONGER-CHAIN PFAS IN ULTRAPURE MATRIX VIA INTRA-PFAS COMPETITION</i>	80
	<i>LESS INHIBITION BY SYNTHETIC WASTEWATER MATRIX ON PFAS-SELECTIVE MEDIA SORPTION</i>	88
2.3.4.	<i>LESS INHIBITION BY SYNTHETIC WASTEWATER MATRIX ON PFAS-SELECTIVE MEDIA SORPTION CAPACITIES, KINETICS</i>	89
2.3.5.	<i>PFA694 IX OUTPERFORMS ALL ADSORBENTS IN RSSCTS FOR MAJORITY OF 18-PFAS MIX</i>	100
<b>2.4.</b>	<b>CONCLUSION</b>	<b>107</b>
<b>2.5.</b>	<b>RECOMMENDATIONS FOR FUTURE WORK</b>	<b>108</b>
	<b>REFERENCES</b>	<b>111</b>

## **List of Figures**

**Figure 1.1** - Ion Exchange Resin Properties and Composition

**Figure 1.2** – DEXSORB® and  $\beta$ -Cyclodextrin

**Figure 1.3** – Schematic Illustration of Polymer-Modified Clay Synthesis

**Figure 2.1** – Ultrapure Water 18-PFAS Mix Adsorption Isotherms

**Figure 2.2** – Cumulative Percentage of Mass Sorbed by group and chain-length classification

**Figure 2.3** – Ultrapure Batch Adsorption Maximum achieved adsorption capacity vs PFAS  
Molecular Weight

**Figure 2.4** – Maximum Achieved Adsorption Capacities in UP matrix versus PFAS MW

**Figure 2.5.0** - Adsorption Kinetics in Ultrapure Water

**Figure 2.5.1** – Adsorption Kinetics: UP vs SW – DEXSORB® and F400 GAC

**Figure 2.5.2** - Adsorption Kinetics: UP vs SW – IRA910 IX and PFA694 IX

**Figure 2.6** – RSSCT Breakthrough Curves

## **List of Tables**

**Table 1.1** – PFAS Evaluated in this Study

**Table 1.2** – Commercial Adsorbent Media Evaluated in this Study

## **1. Expanded Introduction**

### *1.1. PFAS Introduction*

Per- and polyfluoroalkyl substances (PFAS) are a diverse family of organic, xenobiotic, bioaccumulative, persistent, mobile, and hazardous chemicals which have been used in a wide variety of industrial applications and consumer products since the 1940's.<sup>1,2</sup> The PFAS family includes more than 4,700 compounds with unique chemical abstracts service (CAS) registry numbers; over 1,900 chemicals “without explicit structures” identified by the United States Environmental Protection Agency (US EPA); and in total, estimated to include more than 14,000 compounds.<sup>3</sup> Due to their strong resistance to biodegradation, PFAS are generally highly environmentally persistent, and have come to be known as “forever chemicals” in common discourse. Importantly, PFAS are widely considered to be potentially toxic, mutagenic, or carcinogenic in humans and other organisms.<sup>4-6</sup>

In 1968 a researcher at the University of Rochester School of Medicine and Dentistry who was investigating the effects of inorganic fluoride in drinking water, Donald Taves, first reported “the presence of a fluorocarbon molecule” in human blood serum, which more than a decade later were identified as PFAS.<sup>7</sup> Subsequently, research on the human health and environmental impacts of PFAS have steadily increased from the late 1970s through to the early 2000s,<sup>7,8</sup> including numerous studies documenting the widespread occurrence of anthropogenic fluorinated organic compounds in the environment; in the blood of marine mammals, birds, and fish in remote areas far from human industry;<sup>4,5,7,9</sup> and, most significantly, concentrations of PFAS were detected in blood serum of humans living in all regions of the United States and across the globe.<sup>6,10-12</sup> As a result, over the past two decades, regulatory bodies in the United States (U.S.), Canada, Latin America, Asia, the European Union and elsewhere have begun to address PFAS in terms of their

production, commercial and industrial uses, health effects, and occurrence in the environment—including in drinking water supplies, a potential significant source of PFAS exposure.<sup>6,9,13–16</sup>

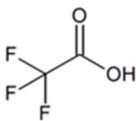
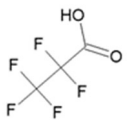
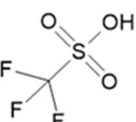
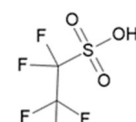
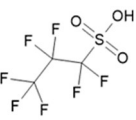
Only in 2024 did certain PFAS become regulated under the Safe Drinking Water Act (SDWA). As of April 2024, the Environmental Protection Agency (EPA) finalized National Primary Drinking Water Regulations (NPDWRs) which established legally enforceable maximum contaminant levels (MCLs) for six PFAS to be monitored in public drinking water supplies:<sup>17</sup>

- (1) perfluorooctanoic acid (PFOA),
- (2) perfluorooctanesulfonic acid (PFOS),
- (3) perfluorobutanesulfonic acid (PFBS),
- (4) perfluorononanoic acid (PFNA),
- (5) perfluorohexanesulfonic acid (PFHxS) and,

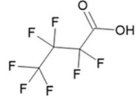
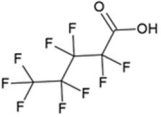
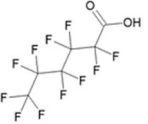
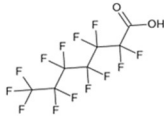
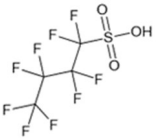
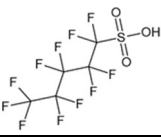
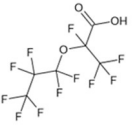
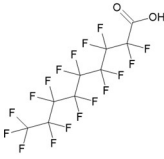
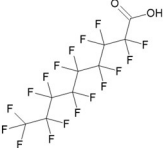
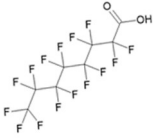
(6) “GenX Chemicals,” which refers to hexafluoropropylene dimer acid (HFPO-DA) (CAS# 13252–13–6) and its ammonium salt (CAS# 62037-80-3). It is the latter compound, which is patented by Chemours (originally, DuPont) under the tradename “GenX.”<sup>18–21</sup> **Table 1.1** contains the name, chemical structure, classification, and relevant physicochemical properties of ultra-short, short-, and long-chain PFAS, that are commonly discussed in the context of environmental regulation and water treatment. The 18 compounds listed in **Table 1.1** are those that were evaluated in the study discussed in Part 2 of this report. The new leaders of the U.S. EPA that assumed power under the 2025 administration, however, have rescinded the MCLs for all but PFOA and PFOS despite Occurrence Data from the Unregulated Contaminant Monitoring Rule demonstrating that 113 public water systems in the United States, serving approximately 8 million

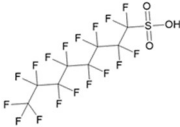
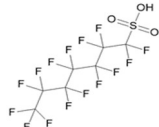
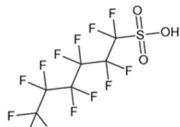
people have exceeded the no-longer-actionable MCLs for PFBS, PFNA, PFHxS, and/or HFPO-DA at least once between 2023 and 2025.<sup>22,23</sup> The modified regulation also extends the deadline for municipal public utilities to comply with the MCLs for PFOA and PFOS from 2029 to 2031. There are currently no federal guidelines requiring the monitoring of PFAS discharged from municipal wastewater treatment plants (WWTPs), but the State of Washington has begun permitting certain wastewater treatment plants to monitor for PFAS in the influent and effluent, and for the control of industrial point-source inputs to the WWTP.<sup>24</sup>

**Table 1.1** Chemical structure, name, grouping and relevant physicochemical properties of the “18 PFAS mix” evaluated in the study discussed in Part 2.

Structure	Acronym	Compound	CAS #	Formula	pK <sub>a</sub>	log K <sub>ow</sub> <sup>1</sup>	Grouping
	TFA	Trifluoroacetic Acid	76-05-1	C <sub>2</sub> HF <sub>3</sub> O <sub>2</sub>	0.3	0.91	Ultrashort-chain PFCA
	PFPrA	Perfluoropropionic Acid	422-64-0	C <sub>3</sub> HF <sub>5</sub> O <sub>2</sub>	1.37	1.61	Ultrashort-chain PFCA
	TFMS	Trifluoromethanesulfonic Acid	1493-13-6	CHF <sub>3</sub> O <sub>3</sub> S	-15	1.15	Ultrashort-chain PFSA
	PFEtS	Perfluoroethanesulfonic Acid	354-88-1	C <sub>2</sub> HF <sub>5</sub> O <sub>3</sub> S	3.31	1.23	Ultrashort-chain PFSA
	PFPrS	Perfluoropropanesulfonic Acid	423-41-6	C <sub>3</sub> HF <sub>7</sub> O <sub>3</sub> S	3.31	1.93	Ultrashort-chain PFSA

<sup>1</sup> National Center for Biotechnology Information (2025). PubChem Compound Summaries

	PFBA	Perfluorobutanoic Acid	375-22-4	C <sub>4</sub> HF <sub>7</sub> O <sub>2</sub>	0.17	2.43, 2.31 <sup>25</sup>	Short-chain PFCA
	PFPeA	Perfluoropentanoic Acid	2706-90-3	C <sub>5</sub> HF <sub>9</sub> O <sub>2</sub>	0.4	3.4, 3.01 <sup>25</sup>	Short-chain PFCA
	PFHxA	Perfluorohexanoic Acid	307-24-4	C <sub>6</sub> HF <sub>11</sub> O <sub>2</sub>	0.42	4.37, 3.71 <sup>25</sup>	Short-chain PFCA
	PFHpA	Perfluoroheptanoic Acid	375-85-9	C <sub>7</sub> HF <sub>13</sub> O <sub>2</sub>	0.47	5.33, 4.41 <sup>25</sup>	Short-chain PFCA
	PFBS	Perfluorobutanesulfonic Acid	375-73-5	C <sub>4</sub> HF <sub>9</sub> O <sub>3</sub> S	-3.57	2.41, 2.63 <sup>25</sup>	Short-chain PFSA
	PFPeS	Perfluoropentanesulfonic Acid	2706-91-4	C <sub>5</sub> HF <sub>11</sub> O <sub>3</sub> S	-3.56	3.38	Short-chain PFSA
	HFPO-DA	Hexafluoropropyleneoxide-dimer acid	13252-13-6	C <sub>6</sub> HF <sub>11</sub> O <sub>3</sub>	2.84	3.66	Short-chain perfluoroethercarboxylic Acid (PFECA)
	6:2 FTS	6:2 Fluorotelomersulfonic Acid	27619-97-2	C <sub>8</sub> H <sub>5</sub> F <sub>12</sub> O <sub>3</sub> S	1.31	3.85	Long-chain fluorotelomersulfonic Acid (FTSA)
	PFNA	Perfluorononanoic Acid	375-95-1	C <sub>9</sub> HF <sub>17</sub> O <sub>2</sub>	0.5	7.27	Long-chain PFCA
	PFOA	Perfluorooctanoic Acid	335-67-1	C <sub>8</sub> HF <sub>15</sub> O <sub>2</sub>	-0.5 to 4.2	6.3, 5.11 <sup>25</sup>	Long-chain PFCA

	PFOS	Perfluorooctanesulfonic Acid	1763-23-1	$C_8HF_{17}O_3$ S	< -1.0	5.43 <sup>25</sup>	Long-chain PFSA
	PFHpS	Perfluoroheptanesulfonic Acid	375-92-8	$C_7HF_{15}O_3$ S	-3.29	5.31	Long-chain PFSA
	PFHxS	Perfluorohexanesulfonic Acid	355-46-4	$C_6HF_{13}O_3$ S	0.14	4.34, 4.03 <sup>25</sup>	Long-chain PFSA

## 1.2. Legacy PFAS

Amongst the non-polymeric perfluoroalkyl substances, a significant group of compounds that receive the most attention in terms of regulation, concern over human health impacts, and occurrence in the environment are the perfluoroalkyl acids (PFAAs). The PFAA group includes further perfluorinated sub-groups based on the composition of terminal functional group, which can be a sulfinic (PFSIA), phosphonic (PFPA), phosphinic (PFPiA), carboxylic (PFCA), or sulfonic (PFSA) acid moiety, amongst other possible functional groups.<sup>9,26</sup> Each of these groups contain compounds with homologous structures of varying perfluorinated alkyl-chain length. Long-chain PFAS are defined based on the number of perfluorinated carbon atoms that constitute the namesake fluoroalkyl moiety.<sup>9</sup> For the perfluorosulfonic acid (PFSA) group, long-chain compounds are defined as those with  $C \geq 6$  (i.e. PFHxS, perfluoroheptanesulfonic acid [PFHpS], PFOS, etc.); while for the perfluorocarboxylic acid (PFCA) group, long-chain compounds are defined as those with  $C \geq 8$  (i.e. PFOA, PFNA, perfluorodecanoic acid [PFDA], etc.).

Long-chain PFOA has a long history and variety of uses including as an industrial surfactant, and as a processing aid in the production of fluoropolymers such as PTFE (commonly

known as “Teflon”). Similarly, long-chain PFOS, was utilized in a wide variety of applications, including water-proofing, metal plating, and in firefighting foams.<sup>4</sup> These two PFAS were the first to be confirmed as present in the blood serum of humans and mammals across the globe by at least 2003,<sup>5,7,9</sup> and are the two primary PFAS targeted for regulation across the globe and scrutinized for their toxicity and carcinogenicity to humans—thus they are known as “legacy PFAS.”<sup>27–29</sup>

Between 2000 and 2002, the US EPA reached a voluntary agreement with 3M (the sole US manufacturer of PFOS) to phase-out the production and use of PFOS and a compound used in its manufacture, perfluorooctane sulfonyl fluoride (POSF); and in 2009 the European Union listed PFOS as a Persistent Organic Pollutant (POP) under Annex B of the Stockholm Convention on POPs.<sup>1,7</sup> Furthermore, between February and March 2006, the EPA reached agreements with eight major fluorochemical manufacturers, including 3M and DuPont (now Chemours), to participate in the 2010/2015 PFOA Stewardship Program. The goals of this program were to achieve a 95% reduction (relative to 2000 levels) in the production and emissions of PFOA and PFOA-precursors to the environment by 2010; and to achieve complete elimination of PFOA and related compound emissions by 2015.<sup>9,11,29</sup> Despite the early 2000’s EPA-mediated voluntary phase-outs conducted by major U.S. manufacturers of these “legacy” PFAS, the two compounds are still widely detected in the environment in tandem with short-chain PFAS, as well numerous other distinct PFAS sub-classes.<sup>7,19,30,31</sup>

One of the main effects of phasing-out production and use of PFOA and PFOS, has been the emergence of ‘fluorinated alternative’ compounds intended to achieve many of the same desirable properties of PFOA and PFOS: hydrophobicity (water-repellency), lipophobicity (grease-repellency), high chemical and thermal stability, and high-performance dielectric and surface-tension-lowering properties.<sup>7,9,18,19,32</sup> Examples of short-chain PFAS that have been

employed as replacements for more bioaccumulative long-chain PFAS are (hexafluoropropylene oxide-dimer acid (HFPO-DA) and perfluorobutanoic acid (PFBA) as replacements for PFOA, and PFBS as a replacement for PFOS.<sup>11,21,27,33,34</sup> In a 2013 review by Wang et al. titled *A review of sources, multimedia distribution and health risks of novel fluorinated alternatives*, the authors suggest that short-chain perfluorinated alkyl chains (compared to legacy, long-chain PFAS) do not invariably impart lower bioaccumulative potential to certain compounds. PFBA, perfluorobutanesulfonic acid (PFBS), and perfluorohexanoic acid (PFHxA) were reported to have shorter half-lives in humans and other biota compared to their long-chain homologues; however, perfluorohexanesulfonic acid (PFHxS) was shown to have a half-life in human blood serum between 8 and 13 years, compared to a half-life of approximately 6 years for PFOS.<sup>35</sup> Another systematic review conducted by Gomis et al. (2018), established that the differences in toxicities between long-chain and short-chain alternatives are minimal, and that the short-chain alternatives, PFBA, PFHxA, PFBS, and GenX showed greater tendency to partition to blood serum as opposed to the liver when compared with the legacy compounds PFOA and PFOS. That review also determined that ‘fluorinated alternatives’ are likely to have similar inherent toxicity to the long-chain homologues, but apparent lower toxicities may be attributable to faster elimination from the body, and lower distribution to the liver.<sup>36</sup> The historical use of many different classes and subclasses of PFAS in the U.S., particularly long-chain PFAAs such as PFOA and PFOS, coupled with their inherent environmental persistence and mobility have contributed to long-chain PFAS becoming a trace, yet significant contaminant of concern in surface waters and groundwaters used for drinking water supplies across the globe.<sup>14,37</sup>

### 1.3. *Ultrashort-chain PFAS*

Historically, as regulation and treatment targets have focused on long-chain PFAS (and, more recently, short-chain PFAS), ultrashort-chain (C<4) PFAS have been overlooked.<sup>27,38</sup> Ultrashort-chain PFCAs include trifluoroacetic acid (TFA), the fluorinated analogue of acetic acid (commonly known as vinegar), and perfluoropropionic acid (PFPrA); while the ultrashort-chain PFSAAs (C<4) include perfluoropropanesulfonic acid (PFPrS), perfluoroethanesulfonic acid (PFEtS), and trifluoromethanesulfonic acid (TFMS), also known as perfluoromethanesulfonic acid (PFMeS) and/or triflic acid.<sup>27</sup> Ultrashort-chain PFAS are very commonly detected in rain,<sup>39</sup> bottled water,<sup>40</sup> tap water,<sup>41</sup> surface waters,<sup>38</sup> within wastewater treatment plant influents and effluents,<sup>49</sup> and in human blood and waste<sup>42</sup> from samples of each media collected across the globe. TFA in particular is gaining much attention due to the increasing recognition of its potential adverse health effects to humans and aquatic species,<sup>43</sup> its widespread occurrence,<sup>44</sup> and presence in the environment at concentrations often orders of magnitude greater than other PFAS.<sup>15,45</sup> For example, in a 2022 survey of 13 German drinking water sources evaluating for 40 distinct PFAS, Neuwald et al. reported that ultrashort-chain TFA, PFPrA, and TFMS comprised up to 98% of the total PFAS composition in the samples.<sup>15</sup>

There are still significant data gaps regarding the occurrences and sources of ultrashort-chain PFAS,<sup>46</sup> including in WWTP effluents; however, degradation of PFAA precursors present in WWTP influents is considered a significant source of PFAAs., PFAA precursors refer to the many PFAS groups, such as fluorotelomer alcohols, perfluoroalkyl ethers, or perfluorinated sulfonamides, and other polyfluoroalkyl substances have the potential for oxidative degradation to terminal persistent PFAAs.<sup>47</sup> Additionally, there is a lack of research evaluating the use of adsorbent technology to treat ultrashort-chain PFAS,<sup>38</sup> especially when considered in a mixed

system containing an extended spectrum of perfluorinated alkyl chain length compounds. While several studies conducted by Wang et al. (2020),<sup>48</sup> Murray et al. (2021),<sup>49</sup> Ellis et al. (2022),<sup>50</sup> Chow et al. (2022),<sup>51</sup> Gorji et al. (2023),<sup>52</sup> Lenka et al. (2024),<sup>53</sup> Tajdini et al. (2025),<sup>54</sup> and Lobitz (2025)<sup>55</sup> report data on the removal of at least one ultrashort-chain PFAA from various aqueous matrices by GAC, IX, and select alternative adsorbents, peer-reviewed research featuring evaluation of a mixed-system with a continuous spectrum of PFAA chain-lengths from C1-C8 are critically lacking. Several examples of studies considering adsorptive treatment of ultrashort-chain PFAS are discussed below highlighting (1) the overall increased PFAS treatment capacity of IX resins compared to GAC, and (2) the preferential removal of long-chain PFASs and PFCAs over their short- and ultrashort-chain homologues is a limitation for adsorptive media in general.<sup>51,56-60</sup>

In batch tests Wang et al. (2020)<sup>48</sup> demonstrated low removal percentages of PFPrS by GAC (4%), Purolite® “PFA694E” ion exchange (IX) resin (65%), and several  $\beta$ -cyclodextrin polymers ( $\beta$ -CDPs, 3-36%) from an aqueous firefighting foam (AFFF)-contaminated groundwater sample with a contact time of 48 hours. In a pilot-scale comparison of non-selective and PFAS-selective IX resins by Ellis et al. (2022), each of the IX resins exhibited the lowest relative PFAS removal for ultrashort-chain PFPrS relative to longer-chain PFASs. Interestingly, the removal efficiency for all investigated PFCAs (C4 PFBA to C8 PFOA) was lower than for PFPrS by all examined IX, highlighting a widely demonstrated trend that PFCAs are more recalcitrant to adsorptive treatment technologies than PFASs.<sup>50</sup> Chow et al. (2022) reported on the relatively short service times for successful treatment of PFETs, PFPeA, PFBA, and PFPrA in pilot-scale, continuous flow tests treating PFAS-impacted groundwater for PFAS-selective Purolite® PFA694 IX and Amberlite PSR2+ IX, with a substantially lower number of bed volumes (BVs) treated prior to PFAS breakthrough for Norit 1240+ GAC.<sup>51</sup> PFAS-selective IX resins treated PFETs

PFPeA, PFBA, and PFPrA occurred after treatment of 120,000 BVs, 60,000 BVs, 20,000 BVs, and <15,000 BVs, respectively, with no long-chain PFSA breakthrough above 10% after treating more than 210,000 BVs.<sup>51</sup> Comparatively, the 1240+ GAC exhibited breakthrough above 10% for PFEtS, PFPeA, PFBA, PFPrA after treatment of 13,000 BVs, 20,000 BVs, 10,000 BVs, and <5000 BVs, respectively.<sup>51</sup>

Lenka et al. (2024) evaluated one GAC, one non-PFAS-selective strong-base IX resin identified as A900 (Lenntech Ambersep® 900 OH (A900) (Netherlands), a macroporous, PS-DVB polymer with quaternary ammonium functional groups balanced with exchangeable hydroxide anions<sup>61</sup>), and two experimental weak-base IX resins for the removal of three PFAS (ultrashort-chain: PFPrA; short-chain: PFBA and PFBS) from ultrapure and 100 mM CaCl<sub>2</sub> aqueous matrices with initial PFAS concentrations ranging from 50 µg/L to 6,400 µg/L (or 6.4 mg/L) (each PFAS).<sup>53</sup> Their results demonstrate the greater adsorption capacities for the strong-base IX resin arising primarily from dominant electrostatic interactions between the anionic PFAS and positively-charged resin surface. While the relative lack of attractive electrostatic interactions between short- or ultrashort-chain PFAS and the activated carbon surface inhibit their adsorption to GACs—particularly at more environmentally-relevant PFAS concentrations. A further notable result from this study is that short-chain PFAS are preferentially adsorbed over ultrashort-chain PFAS, suggesting that hydrophobic interactions are an important mechanism of removal for short-chain PFAS from aqueous matrices, regardless of sorbent media type. Additionally, co-occurring divalent cations (e.g. CaCl<sub>2</sub>) can decrease the PFAS adsorption capacity and kinetics for both media types via direct competition, compression of the electrical double-layer surrounding dissolved PFAS ions, and adsorbent surface charge suppression.<sup>53</sup>

#### 1.4. PFAS Occurrence in Wastewater Treatment Plants

Municipal wastewater treatment plants have been identified as a major pathway of PFAS to the environment as they receive waste from diffuse sources (e.g., residences, commercial businesses, industrial facilities) which are aggregated in the wastewater influent in concentrations ranging from a few nanogram/liter (ng/L or ppt) to more than 10,000 ppt.<sup>30,62,63</sup> Data collected from wastewater treatment plants across the globe suggest that little to no removal of PFAS detected in wastewater influent sampled is being removed in the effluent. As a result, municipal wastewater effluent is considered to be an important pathway of PFAS release to freshwater sources.<sup>56,62,64,65</sup>

Short-chain ( $C \leq 5$  for PFSA and  $C \leq 7$  for PFCAs) and ultrashort-chain PFAS ( $C < 4$ ) are increasingly becoming a significant fraction of the total PFAS mass detected in WWTP effluents—partially due to the tendency of long-chain PFAS and PFAA precursors to be biologically degraded during conventional wastewater treatment processes.<sup>56,65–68</sup> A meta-analysis of the PFAS concentrations in WWTPs across the globe by Cookson and Detweiler (2022) indicates that there is negligible PFAS removal from influent to effluent in conventional treatment plants, and that the concentrations of short-chain PFAS in wastewater effluent increased from 2005 to 2020.<sup>69</sup> A similar long-term meta-analysis spanning 2012 to 2020 by Thompson et al. (2022) suggests that legacy PFOA and PFOS concentrations are decreasing in U.S. wastewater effluents; however, the concentrations of PFBA and PFBS show an increasing trend.<sup>63</sup> Similarly, studies from Schaefer et al. (2023) and Kim et al. (2022) suggest that short- and ultrashort chain PFAS will tend to exit WWTPs via aqueous effluent discharges in a higher proportion than they occur in the influent, and at higher proportions compared to long-chain PFAS which tend to partition to biosolid discharges.<sup>65,66</sup>

The persistence, distribution, and toxicity of PFAS combined with their frequent detection in WWTPs has driven extensive research on innovative approaches to separate PFAS from water in treatment and reclamation facilities.<sup>63,64,66,70-72</sup> As changing climates due to global warming threaten the sustainability and dependability of water supplies globally, direct or indirect potable reuse is becoming a more feasible approach to reclaiming water resources.<sup>73</sup> Identification of pilot-scale adsorbents that can be utilized for PFAS separation following tertiary wastewater treatment is a critical component for the implementation of cost-effective potable reuse applications.<sup>70,74,75</sup>

### *1.5. PFAS Treatment Methods*

Conventional aerated activated sludge treatment of municipal wastewater, as well as traditional drinking water treatment techniques such as coagulation, flocculation, sedimentation, sand filtration, and chlorine or UV disinfection all fail to destroy or remove PFAS from aqueous matrices.<sup>30,76-78</sup> In fact, both conventional biological wastewater treatment and many advanced oxidation processes have been shown to convert polyfluorinated precursor compounds into degradation byproducts, both of which can form into more environmentally persistent and mobile PFAAs, including short-, and ultrashort-chain PFCAs and PFSAAs.<sup>47,79,80</sup>

A variety of treatment techniques do exist for removal or destruction of PFAS in water, such as reverse osmosis (RO) or nanofiltration (NF) membrane treatment, sonolysis, electrochemical oxidation, and advanced reductive processes (ARPs);<sup>79,81</sup> however, many of these methods are not mature enough for widespread adoption or are too costly or poorly understood to feasibly implement at scale.<sup>79</sup> Adsorption-based treatments are currently the best available process due to relatively low-cost, ease of operation, and technological maturity.<sup>54,82</sup> Examples of other promising treatment techniques that could become more feasible or developed in the future are foam fractionation,<sup>83,84</sup> and advanced reduction processes (ARPs), such as the hydrothermal

alkaline treatment, which has demonstrated the capability to mineralize both PFOS and TFA under relatively mild conditions.<sup>85,86</sup>

#### 1.5.1. PFAS Adsorption from Aqueous Matrices

Dozens of modified and novel media have been developed in the past two decades for the purpose of investigating their efficacy to remove PFAS from aqueous matrices via adsorption to solid surfaces.<sup>76,87,88</sup> Despite this, traditional adsorptive media such as GAC and IX resins are two of the most well-established commercial technologies for the separation of PFAS from water due to their effectiveness, passive operation, and relatively low cost.<sup>54,56,59,70,77,89,90</sup> However, evaluations of adsorbent technologies considering the combined effects of co-occurring organic matter and inorganic ions are minimal.<sup>75,78,91</sup> Particularly, there is limited published data available for the effectiveness of GAC, IX or other novel adsorbents to remove short- and ultrashort-chain PFAS from water matrices with high wastewater-derived organic matter content, and co-occurring inorganic ions, and other co-occurring organic micro-pollutants.<sup>74,77,78,90-93</sup>

##### 1.5.1.1. Granular Activated Carbon (GAC)

The main mechanism through which GAC adsorb PFAS are through hydrophobic interactions between the nonpolar GAC surface and the hydrophobic tail of the PFAS – where hydrophobicity can be explained as the noncovalent interaction between water-repellent molecules or materials.<sup>94</sup> Specific characteristics of GAC that are important in determining their effectiveness at PFAS removal are the particle size, surface area, pore size distribution, and the surface chemistry composition.<sup>53,59,76</sup> More recently, surface basicity of activated carbon (AC) has been shown to have a significant role in the adsorption of more hydrophilic short-chain PFAS via electrostatic interaction.<sup>25,95-99</sup>

In continuous flow operation, GAC tends to exhibit much earlier breakthrough of short-chain PFAS compounds relative to long-chain PFAS, potentially resulting in higher costs for the treatment plant operators due to more frequent change-out of the GAC media.<sup>15,49</sup> For example, laboratory-scale continuous-flow tests were conducted by Murray et al. (2021) treating simulated aqueous firefighting foam (AFFF)-impacted groundwater with a series of triply-segmented columns packed with Calgon F400 GAC. The source waters were relatively low total organic carbon (TOC) containing tap water (2.6 mg/L) spiked with AFFF to concentrations consistent with real AFFF-impacted groundwaters (i.e. 12.5 µg/L PFOS, 3 µg/L PFHxS, 0.72 µg/ PFBS , 0.45 µg/L PFOA, 0.44, 0.72 µg/L PFHxA, 0.18 µg/L PFPeA etc.). They show that the F400 GAC at 50% breakthrough (i.e., when column effluent concentrations reach 50% of the contaminant influent concentrations) of the first column had an adsorption capacity of 8 µg/g for PFOA, 1.5 µg/g for PFPeA, 250 µg/g for PFOS, 60 µg/g for PFHxS, 13 µg/g for PFBS, and 5 µg/g PFPrS, highlighting the capability of GAC to preferentially treat long-chain PFAS(particularly PFASs) over short- and ultrashort-chain PFAS. In that study and others, GAC was shown to require long contact times to reach equilibrium and to have relatively poor affinity to adsorb short-chain PFAS. In pilot-scale continuous flow tests using, Kempisty et al report that PFCAs with fewer than six carbon atoms and PFASs with fewer than four carbon atoms are not viable for treatment via GAC.<sup>100</sup>

An additional well-established limitation of GAC for PFAS treatment is that they are typically inhibited in the targeted removal of trace contaminants by the presence of dissolved organic matter (DOM).<sup>76,77,79,100–104</sup> Due to the somewhat similar characteristics (i.e. net negative charge, high MW, hydrophobic structures), competitive sorption between hydrophobic PFAS and DOM typically can cause the inhibited uptake of PFAS from solution; however, DOM and PFAS

can also mutually interact hydrophobically, electrostatically (i.e. via cationic functional groups on DOM), or via cation bridging with (e.g. with  $\text{Ca}^{2+}$ ,  $\text{Fe}^{3+}$ ,  $\text{Al}^{3+}$ ), so predicting GAC inhibition is difficult to predict without characterization of DOM characteristics.<sup>58,105</sup> In an evaluation of the role of DOM in PFAS adsorption to GAC utilizing rapid small-scale column tests (RSSCTs) treating groundwater (0.7 mg-C/L TOC) and surface waters (2-2.7 mg-C/L TOC) with Calgon Carbon Filtrasorb 600 GAC (F600 GAC) and Norit 1240 GAC.<sup>100</sup> They determined that GAC treated approximately 50-60% more volume of the groundwater compared to the surface water, and that GAC treatment is only economically feasible for long-chain PFAAs.<sup>100</sup> DOM has also been shown to variably impact the removal of long-chain PFAS, sometimes improving hydrophobic PFAS removal via DOM-PFAS associations. For example, Kothawala et al. (2017) conducted batch sorption tests using F400 GAC for removal of a range of 12 short- and long-chain PFAAs and perfluorooctanesulfonamide (FOSA) while varying the concentration and characteristics of the DOM in the system. They determined that both the quantity and quality of the DOM can increase removal of the most hydrophobic long-chain PFAS, while simultaneously removing DOC from solution.<sup>58</sup>

Significantly, GAC is least effective for the treatment of PFAS in aqueous matrices that contain low PFAS concentrations with co-occurring DOM, inorganic ions, and other co-contaminants, as would be expected in a municipal wastewater effluent.<sup>56,60,70,74,78,106-108</sup> A recently conducted evaluation using RSSCTs by Mortazavian et al. (2025) evaluated the feasibility of F400 GAC, Norit 400 GAC, and a commercial biochar for treating real samples from two wastewater treatment plants in Ontario, Canada (5.9 and 5.6 mg/L DOC) that were spiked to 200 ng/L with PFOS, PFHxS, PFOA, and PFHxA.<sup>70</sup> Each of the GACs displayed a trend of treating a greater number of BVs prior to 50% breakthrough in the order PFOS > PFHxS > PFOA > PFHxA, while

the biochar exhibited near immediate breakthrough of all four PFAS.<sup>70</sup> Overall, GAC has been shown to have relatively poor performance for the uptake of hydrophilic short-chain PFAS and this effect is amplified with increasing complexity of the water matrix.

Concern is increasing around the world about the widespread occurrence of PFAS, and more recently, the occurrence of short- and ultrashort-chain PFAS in drinking water sources.<sup>46</sup> Alternatives to GAC capable of treating (ultra)short-chain PFAS in relatively complex matrices could be a crucial development for long-term removal of PFAS from the urban water cycle.<sup>43,62,109</sup> GAC, however, may continue to be a key component of treatment train systems due to its broad selectivity for a range of PFAS compounds beyond PFAAs and anionic PFAS, such as cationic, zwitterionic, and polymeric PFAS<sup>54,74,110</sup>

#### 1.5.1.2. Ion Exchange (IX) Resins

Like GAC, contaminant adsorption via IX resin is an established treatment technique that has been evaluated for separation of PFAS from groundwaters impacted by PFAS contamination,<sup>106</sup> landfill leachate,<sup>107</sup> and primarily for treatment of drinking water sources.<sup>111–114</sup> When compared to GAC, certain IX resins demonstrate longer service lives, higher capacities to adsorb short-chain PFAS, and varying degrees of influence from co-occurring matrix constituents.<sup>78,89,92,96,115–118</sup>

Early research into IX for PFAS separation primarily focused on legacy PFAS; utilized experimental doses many orders of magnitude greater than expected environmental occurrences; and included limited evaluation of the removal of short-chain and ultrashort-chain PFAS. Significantly, research into the use of ion exchange resins between c. 2010-2020, were primarily focused on evaluating previously existing IX resins designed for treatment of non-PFAS

constituents.<sup>35,49,76,90,91,93,104,112,113,119–123</sup> Anion exchange resins can be classified as weak-base resins, or strong-base resins, depending on their functional group's tendency to lose or maintain a positive surface charge in solution at basic pH.<sup>91,93,106,122,124</sup> As indicated by their low pKa values, many PFAS, PFAAs, PFECAs, and fluorotelomer sulfonates (FTSs) tend to exist in the anionic form at environmentally relevant pH ranges. Thus anion exchange resins, typically loaded with Cl<sup>-</sup> or OH<sup>-</sup> as counter ions, are employed to target removal of PFAS as opposed to cation exchange, or non-ionic resins. IX resins can have variable physical structure, typically comprised of either a macroporous or microporous (i.e., gel-like) base polymer constituted from either polystyrene (PS), polyacrylic (PA), or polymethacrylate and functionalized with positively charged functional groups (typically quaternary ammonium or tertiary amine).<sup>55,106,125</sup>

The polymer composition of IX resins generally impacts their performance for PFAS removal, where PS IX resins have been shown to be more effective for PFAA removal due to the favorable hydrophobic interactions. PA IX resin has been shown to be more effective for uptake of DOM due to higher water content of the PA polymer, and greater ability for intraparticle diffusion.<sup>126</sup> PA IX resins have typically demonstrated lower removal capacities of PFAAs compared to PS resins particularly in the presence of DOM,<sup>127</sup> while gel-type IX composed of PS backbones crosslinked with divinylbenzene (DVB) have typically shown rapid uptake and a high capacity for PFAS sorption.<sup>76,91,122</sup> Increasing the size of the IX resin functional groups (i.e. increasing the number of methyl groups on the alkyl chains attached to the cationic group) can increase the adsorption of PFAS by increasing the non-electrostatic interactions of the resin with more hydrophobic PFAS. Specialized functional groups can be designed to selectively adsorb short-chain PFAS, as is likely the case for the emergent commercially available PFAS-selective IX resins.<sup>55,91,93,94,121,122,125,128</sup> Lobitz et al. (2025), which illustrates how a commercial IX resin can

be functionalized with novel fluorinated functional groups to enhance the adsorption capacity and kinetics of ultrashort-chain and short-chain PFAS compared to an un-modified resin.<sup>55</sup> **Figure 1.1** displays the different sub-components of the PS-divinylbenzene (PS-DVB) base polymer (top left), the structures of the functional groups for the IX resins evaluated in the study described in Part 2 (bottom left), as well as a reproduction of a figure from Lobitz et al. (2025), which illustrates how a commercial IX resin can be functionalized with novel fluorinated functional groups to enhance the adsorption capacity and kinetics of ultrashort-chain and short-chain PFAS compared to an un-modified resin.<sup>55</sup>

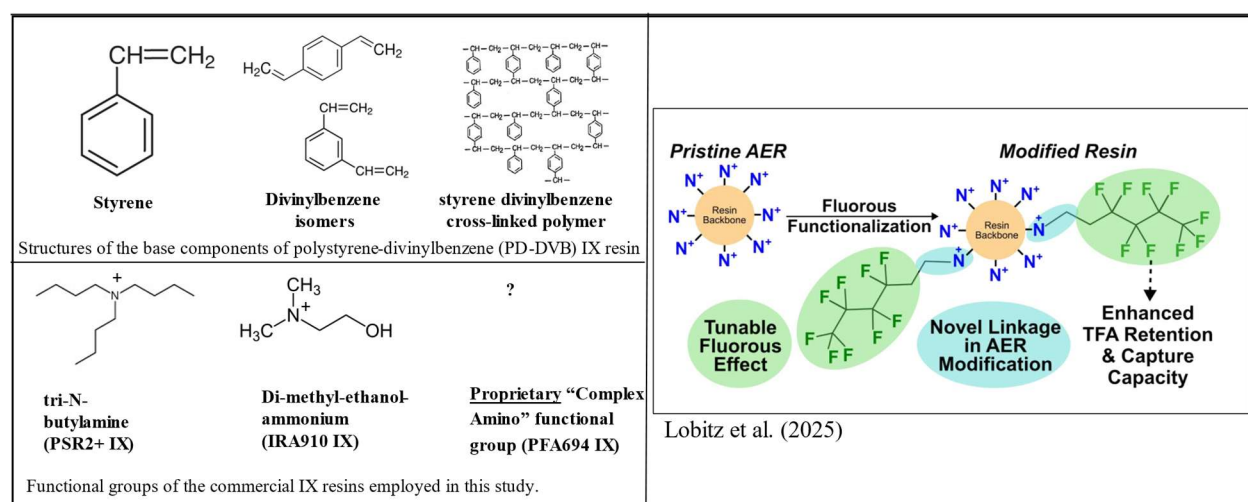


**Figure 1.1** PS-DVB IX resin structural components (top left); functional groups of the commercial IX resins evaluated in this study (bottom left); and reproduced figure from Lobitz et al. (2025) illustrating their successful modification of a commercial IX resin with fluorinated alkyl-chain functional groups, resulting in an adsorbent with enhanced capacity to adsorb ultrashort-chain PFAs, compared to un-modified IX resin.

In general, IX resins have been shown to be more successful at removing short-chain PFAS, compared to carbon-based adsorbents;<sup>34,89,111,114,127</sup> however, IX resins have not been comprehensively evaluated in the context of the removal of ultrashort-, short-, and long-chain PFAS from complex water matrices such as WWTP effluent.<sup>91,111,113,114,126</sup> In a review of PFAS removal via IX resin by Dixit et al. (2021)<sup>91</sup>, the authors highlighted that the presence of DOM can decrease PFAS removal efficacy, and that the type and composition of the DOM can influence

the degree of inhibition;<sup>91,122</sup> while some IX have been shown to be less inhibited by DOM, or effective at simultaneous removal of DOM and PFAS.<sup>34,91,127</sup> A primary knowledge gap for PFAS treatment regarding PFAS-selective IX is a lack of understanding of the impacts of dissolved ions, additional contaminants, and wastewater-derived organic matter present in the aqueous matrix.<sup>74,124</sup>

Since at least 2016, the number of peer-reviewed publications investigating IX for PFAS separation has been increasing, and there has been progression in the number of commercially manufactured “PFAS-selective” IX resins that are explicitly marketed for the removal of PFAS from aqueous matrices.<sup>54,55,125,129</sup> Examples of which include, Purolite PFA694 (wastewater), PFA694E (drinking water), and A592E (point-of-use), Amberlite PSR2+, Calgon CalRes2301, ECT2 Sorbix A3F, ResinTech SIR-110-HP, Lewatit TP 108 DW and MP 62 WS, and Resinx PFCR-1 and PFCR-2.<sup>49,54,76,88,111,124,129–131</sup> These products are purported to have high affinities for PFAS, and are reportedly designed for operation in a single-use mode, despite evidence that saline solvent washes can successfully re-generate PFAS-selective IX resins.<sup>129</sup> Single-use PFAS-selective IX, may still present site-selective operational economic benefits to treatment plant operators due to the long operational lives of IX and the expected costs associated with solvent regeneration of the resin material.<sup>59,60,91</sup>

The mechanisms through which these PFAS-selective media adsorb PFAS are a combination of hydrophobic, electrostatic, ion exchange interactions, and potentially fluorophilic interactions.<sup>55,60,91,93,94,113,115,122,125</sup> Crucially, F–F interactions are gaining attention for their potential to be employed in the design of PFAS-removing adsorbent media.<sup>94,125,128,132,133</sup> Lobitz et al. (2025) reported successful synthesis of fluoroalkyl-modified commercial IX resin, and that such an adsorbent demonstrated an increase in the sorption kinetics and a 28% increase in the adsorption

capacity of TFA.<sup>55</sup> Both of the PFAS-selective IX resins evaluated in this study are manufactured as PS-DVB polymer microporous gels; the PSR2+ IX resin has a tri-N-butylamine, while the PFA694 IX resin reportedly employs a proprietary “complex amino” functional group. The study described in Part 2 was designed partially to evaluate the performance of an industrial high-capacity non-PFAS-selective IX resin (IRA910) marketed for “general demineralization”, against the performance of two novel PFAS-selective IX resins (PFA694 and PSR2+) marketed for targeted PFAS uptake.

#### 1.5.1.3. Alternative Adsorbents

A variety of polymer-based adsorbents, biomaterials, natural materials, nanomaterials, and modified-clay minerals have been in the early-stages of research and development for PFAS adsorption from aqueous matrices within the last two decades.<sup>134</sup> Few of these media have proven efficient, economical, and feasible in terms of their large-scale application for PFAS-treatment, but in recent years, at least two commercially available adsorbent technologies specifically marketed as PFAS-selective have emerged as contenders to replace GAC or IX as sorbent media for PFAS removal and remediation from diverse aqueous matrices: Cyclopure DEXSORB® (DEXSORB) and CETCO Fluorosorb® (Fluorosorb).

DEXSORB® is a proprietary  $\beta$ -cyclodextrin-based polymeric adsorbent with fluorinated aromatic cross-linkers and quaternary ammonium functionalized comonomers (**Figure 1.2**) that is sold commercially as a component in point-of-use drinking water treatment systems,<sup>48</sup> and has been deployed in packed-bed filtration systems for treating PFAS in groundwater, drinking water, landfill leachate concentrate, and industrial and municipal wastewaters.<sup>135–139</sup>  $\beta$ -cyclodextrin is a naturally occurring cyclic oligosaccharide made up of seven  $\alpha$ -D-glucopyranoside molecules, forming a toroidal ring molecule with a central hydrophobic cavity that can encapsulate

contaminants through formation of host-guest complexes, and is utilized as the active ingredient in the commercial aerosol deodorizer Febreze.<sup>135,137,140–145</sup> The cavity on the  $\beta$ -cyclodextrin monomer is uniformly 0.78 nm in diameter, which provides molecular selectivity and simultaneously prevents pore blockage via size exclusion of DOM.<sup>135,145</sup> Similar to IX resins, it is hypothesized that the mechanisms through which  $\beta$ -cyclodextrin-based adsorbents (like DEXORB) function for PFAS-removal are hydrophobic interactions and electrostatic interactions, the formation of host-guest complexes, and fluorophilic interactions arising from the use of fluorinated cross-linkers such as tetrafluoroterephthalonitrile (TFN).<sup>52,92,144,146,147</sup>

Lin et al. (2023) demonstrated that  $\beta$ -cyclodextrin polymers functionalized with fluorinated and cationic crosslinkers and co-monomers exhibit superior performance for removal of PFOA, PFHxA, and PFHxS when operated in a packed-bed filtration column treating filtered municipal wastewater effluent, when compared to Calgon Carbon F400 GAC, and PFAS-selective IX resin Amberlite® PSR2+.<sup>139</sup> Additionally, DEXSORB® reportedly outperformed both GAC and IX without interruption from biofouling or clogging due to co-occurring matrix constituents in pilot-scale systems treating PFAS-impacted industrial wastewater and a reverse osmosis concentrate from a PFAS-contaminated surface water.<sup>148</sup>

The cyclodextrin-based product has demonstrated a capacity to treat an average influent PFOS concentration of 23 ng/L for approximately 125,000 BVs prior to initial breakthrough compared with eight different GACs which treated a maximum of 40,000 BVs prior to initial breakthrough.<sup>114</sup> In terms of the short-chain PFAS, DEXSORB® was able to treat an average influent concentration of 14.6 ng/L PFBS for approximately 30,000 BVs, compared to a maximum of 17,200 BVs for the eight GACs evaluated.<sup>114</sup> DEXSORB® also has the potential for regeneration and reuse of the media via a saline wash in a methanol solution. For example, an

early-stage  $\beta$ -cyclodextrin-based polymeric adsorbent demonstrated effective regeneration between 90-100% with no apparent loss in adsorption capacity over four cycles of adsorption/desorption batch tests evaluating for PFOA, PFHxA, and PFHxS removal from

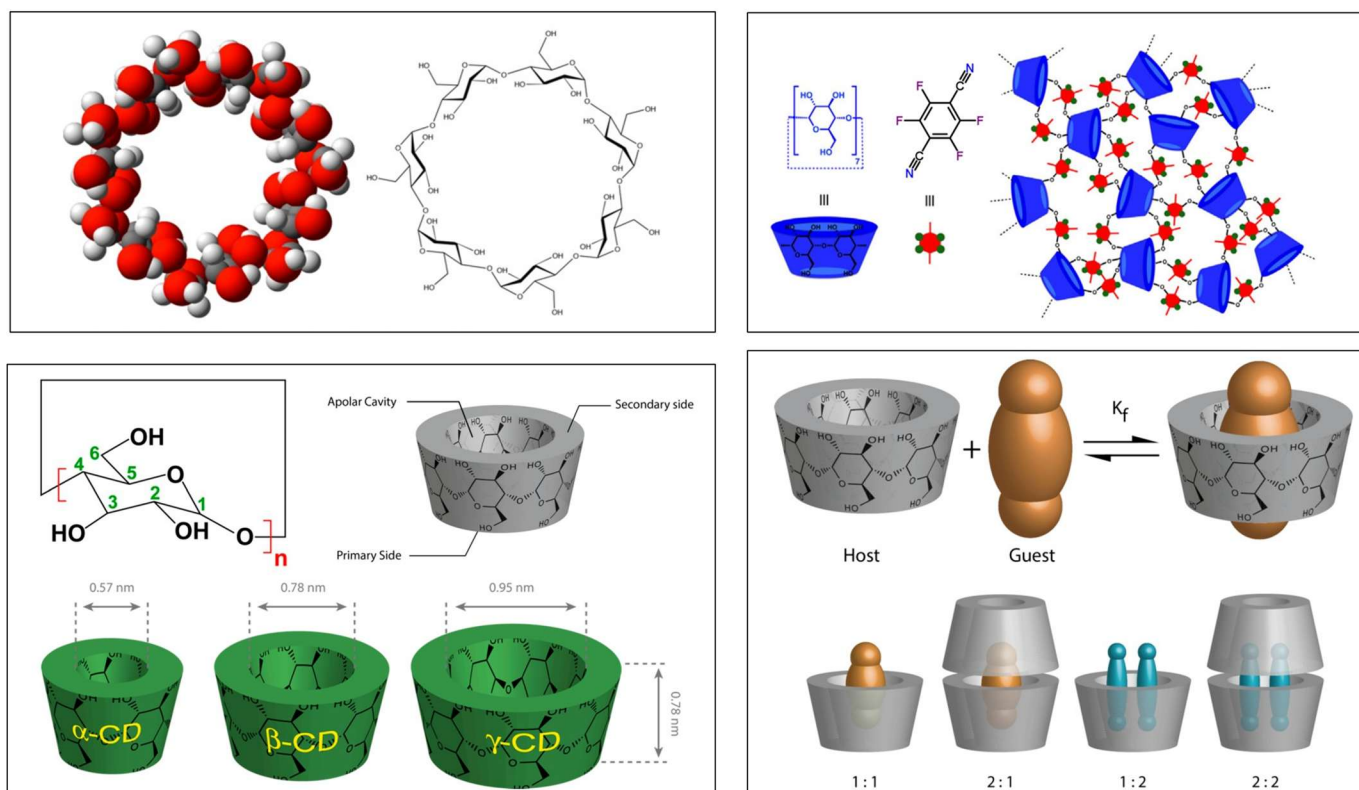


**Figure 1.2** Depictions of  $\beta$ -Cyclodextrin molecular model and structure (top left); the differential structural schemes of  $\alpha$ -, $\beta$ -,and  $\gamma$ -cyclodextrins (bottom left); a schematic illustration example of various conformations of “host-guest” interactions between cyclodextrins and target compounds. (bottom right) (images reproduced from Crini, G. (2014)).<sup>149</sup> Top right panel is a schematic of the polymerization of  $\beta$ -Cyclodextrin monomers, cross-linked with TFN; a similar composition to the evaluated sorbent, DEXSORB®.

aqueous matrices.<sup>143</sup>

Surface-modified clay (SMC) minerals have been established as a category of engineered geomedia since the early 2000s for the removal of metals and trace organic contaminants from stormwater and wastewater.<sup>150–152</sup> Synthesis of polymer-clay composites is relatively low-cost and straightforward to achieve. The process involves blending an inorganic clay mineral with cationic polymers in specified proportions to match the clay minerals’ cation exchange capacity and the

desired degree of hydrophobic interaction between the synthesized clay and target contaminant.<sup>153</sup> The mixture is separated, washed, dried, and formed into granular or pellet-like morphology.<sup>152</sup> Compared to clays or polymers alone, properly engineered composite media can exhibit greater target contaminant adsorption capacity and faster adsorption kinetics, aided by strong electrostatic interaction and increased hydrophobic interactions imparted by the intercalated surfactant.<sup>150</sup> A generalized schematic illustration of the synthesis of polymer-clay composites, modified from Okaikue-Woodi, et al. (2020)<sup>152</sup> is presented in **Figure 1.3**.

Regarding clay minerals that have been modified for purposes of PFAS-removal from aqueous matrices, recent peer-reviewed publications have reported on a variety of surface modifications to different types of clay minerals.<sup>74,131,154–156</sup> For example, Ruckbeil et al. (2025) conducted batch adsorption evaluations of two proprietary surfactant-modified bentonite clays, and two modified palygorskite clays functionalized with oleylamine and octyl amine, along with other commercial adsorbents (activated carbons, IX resins,  $\beta$ -CDPs and zeolites) for removal of PFAS from German drinking water with “elevated DOM levels” of 4.5 mg-C/L.<sup>131</sup> And, Umeh et al (2023) evaluated an anonymized “surface-modified organoclay-carbon amendment” against powdered activated carbon (PAC) for the sorption and desorption of 9 PFAS in ultrapure water or simulated groundwater.<sup>154</sup> As early as 2013, Das et al. had evaluated a commercial palygorskite-based adsorbent modified with oleylamine known as MatCARE™ for remediation of PFOS contaminated soils and wastewaters.<sup>155</sup>

A recently commercialized modified-clay mineral adsorbent, CETCO Fluorosorb® (Fluorosorb), is on the market for in situ and ex situ groundwater remediation, as well as for wastewater treatment. This product is a modified smectite clay, intercalated with a proprietary surfactant that has a positively charged functional group, leading to favorable hydrophobic and

electrostatic interaction with anionic and hydrophobic PFAS.<sup>157,158</sup> It has been evaluated in comparison to GAC in both batch and continuous flow experiments, while reportedly demonstrating fast uptake kinetics, and greater capacities for long- and short-chain PFAS. Furthermore, studies examining Fluorosorb for PFAS removal also suggest minimal inhibition co-occurring DOM and co-contaminants when compared to GACs.<sup>54,74,88,114,116,130,157,159</sup> Fluorosorb has also been deployed as an in situ adsorptive remediation technique for remediation of PFAS-contaminated groundwater plumes.<sup>117,130,160–162</sup>

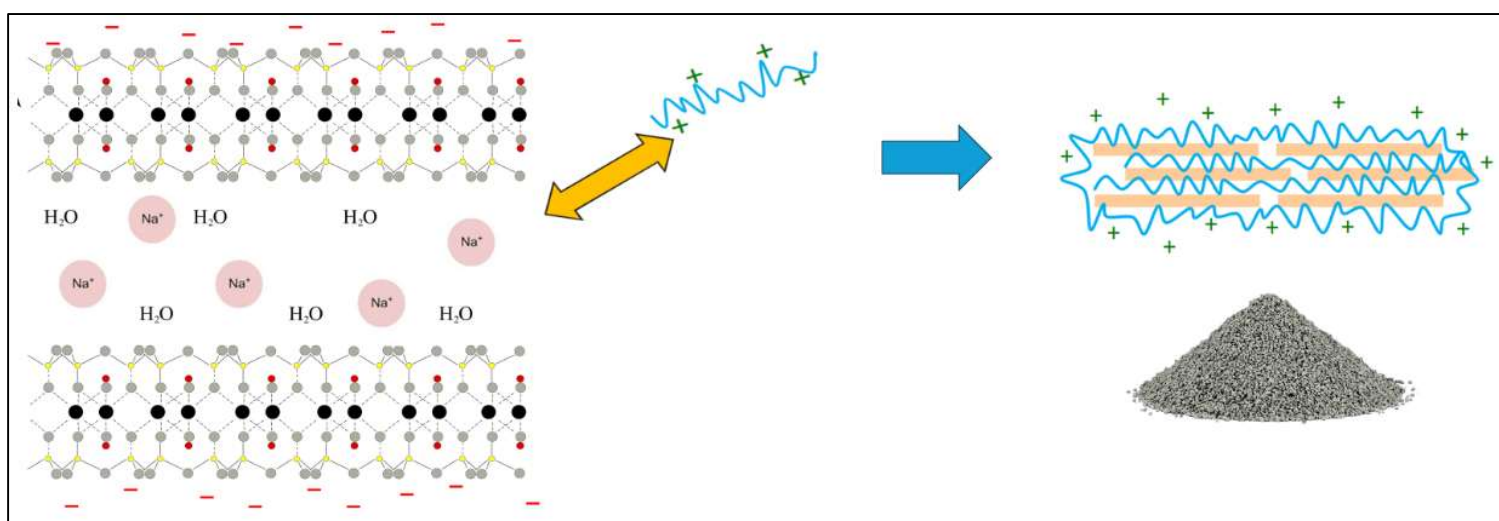


**Figure 1.3** Schematic illustration of the synthesis of a polymer-clay composite modified from Okaikue-Woodi, et al. (2020). The base mineral (left) undergoes modification with a positively charged surfactant via cation-exchange naturally present in clay minerals, which yields a functionalized adsorbent media for water treatment applications (right).

Marshall (2019) compared Fluorosorb and GAC in a lab-scale continuous flow experiment for treating 14 PFAAs in a contaminated groundwater (pH: 7.3, 4.0 mg/L TOC, 44 mg/L calcium, 12.1 µg/L arsenic, 10.5 µg/L barium, 5.7 mg/L sulfate, 1.8 mg/L nitrate, 1.6 mg/L chloride; and 14 µg/L PFHxS, 19 µg/L PFOS, 7.3 µg/L PFOA, 4.9 µg/L 6:2-FTS, etc.) including evaluation of treatment efficacies for only one ultrashort-chain PFAA, PFPrS.<sup>130</sup> That study demonstrated that Fluorosorb and GAC were both able to treat up to 2,500 BVs to non-detect levels, but that Fluorosorb removed PFAS, including PFOA and PFOS, to lower effluent concentrations over

longer operational times.<sup>130</sup> As is the case for GAC and IX, there is a pronounced lack of research evaluating modified-clay adsorbents for the removal of short- and ultrashort-chain PFAS.

#### 1.6. Study Objectives and Hypotheses

There are limited studies that directly evaluate different types of adsorbent media in real, complex aqueous matrices for their ability to treat a variety of co-occurring PFAS (e.g., ultrashort-, short-, and long-chain PFAAs) in batch and/or continuous-flow conditions. This research attempts to address this knowledge gap while simultaneously generating data to benchmark the performance of commercially available adsorbents against novel adsorbents produced in this research group and for other lab-scale PFAS sorbents under development.

Although GAC and IX resins have remained as leading technologies for PFAS treatment, there is a lack of direct GAC and IX treatment comparisons, especially those that systematically evaluate treatment techniques in continuous flow systems—even at the laboratory- and pilot-scale.<sup>49,163</sup> Studies that directly evaluate different types of adsorbent media in real, complex aqueous matrices for their ability to treat a variety of co-occurring PFAS (e.g., ultrashort-, short-, and long-chain PFAAs) are also lacking. Recent investigations by Tajdini et al. (2023), Tajdini et al. (2025), Cheng et al. (2025), Dixit et al. (2021), Chow et al. (2022), Medina et al. (2022), Ahrens et al. (2025) have comparatively assessed IX against GAC,  $\beta$ -CDPs, and SMCs for PFAS removal in continuous flowing systems in a variety of aqueous matrices of varying complexities. These investigations have various limitations in that they either focus on a small subset of long- and short-chain PFAAs, or target a wide-array of PFAS sub-groups for targeted treatment but neglect consideration of all five of the ultrashort-chain PFCAs and PFSAs (TFA, PFPrA, TFMS, PFEtS, and PFPrS) which are likely to co-occur with other targeted PFAS in realistic water treatment scenarios. Furthermore, adsorption data is less commonly reported for the complete spectrum of

long- and short-chain PFASs—often omitting PFPeS and PFHpS in favor of focusing exclusively on the more commonly investigated trio of PFBS, PFHxS, and PFOS.<sup>51,54,70,74,78,114,116,131</sup>

The purposes of this study were to identify and evaluate different types of currently available commercial adsorbent media for the efficient removal of ultrashort-, short-, and long-chain PFAS from municipal wastewater. The preliminary evaluation included batch sorption capacity and kinetics tests in both ultrapure water and a synthetic wastewater matrix, constituted from effluent organic matter (EfOM) isolated from the King County West Point WWTP (Seattle, WA) and a mixture of commonly occurring inorganic ions. The final objective for this research was to perform lab-controlled RSSCTs using the best performing media from the preliminary evaluations. RSSCTs using 1 wt% active media mass packed-bed columns were designed to assess the ability of each adsorbent to remove ultrashort-, short-, and long-chain PFAS from tertiary treated municipal effluent, mimicking a realistic process in a potential treatment train approach targeting PFAS removal via adsorption as may be encountered in advanced treatment systems designed for potable and non-potable re-use.<sup>57,74,82</sup>

Based on the literature review conducted, evaluating peer-reviewed research regarding the removal of ultrashort-, short-, and long-chain PFAS from municipal wastewater effluent, we hypothesize that ultrashort-chain PFAS will be poorly adsorbed by GAC, DEXSORB®, and the SMC due to weak electrostatic interactions relative to the ion exchange resins. We anticipate the PFAS-selective media will outperform the conventional media (i.e. GACs and non-selective IRA910 IX) in the RSSCTs for long- and short-chain PFAS typically targeted for removal due to regulatory pressures (e.g PFOS, PFOA, PFHxA, PFBS, HFPO-DA) primarily due to inhibitory effects introduced by the dissolved organic matter and co-occurring inorganic ions. Finally, previously reported results from continuous-flow tests treating multiple types of PFAS (discussed

further below), suggest that the two PFAS-selective IX resins and DEXSORB® will be the most effective adsorbent media for treating the entire suite of PFAS included in this evaluation.

### 1.6.1. Media Selected for Evaluation

A survey of peer-reviewed literature identified novel and commercial adsorbent media that have been previously evaluated for removal of PFAS in contaminated waters. Particularly, the literature review focused on identifying commercially available, readily deployable, robust adsorbent media that have demonstrated potential to efficiently and selectively separate long-, short-, and ultrashort-chain PFAS from complex water matrices. The adsorbent materials selected for this study are presented in **Table 1.2** below followed by a brief description of each. Additional sorbent media characteristics are presented in **Tables S.2A** and **S.2B**

**Table 1.2** Commercially available adsorbent media for PFAS removal selected for this study.

Type	Manufacturer	Name	PFAS-Removal Mechanisms
GAC	Calgon Carbon	F400	primary: hydrophobic interactions
	Norit	1240+	
IX	Purolite	PFA694	primary: electrostatic interactions, secondary: hydrophobic interactions
	Amberlite (Dupont)	PSR2+	
	Amberlite (Dupont)	IRA910	
Surface modified-clay (SMC)	<i>Anonymous</i>	<i>Anonymous Surface Modified-Clay</i>	primary: hydrophobic interactions, secondary: electrostatic interactions
$\beta$ -cyclodextrin-based polymer	Cyclopure	DEXSORB	hydrophobic, electrostatic, and host-guest complexation interactions

GACs: **Calgon Carbon Filtrasorb® 400 (F400)** is a broadly used GAC for the removal of a wide-range of contaminants in treating groundwaters, surface waters, and wastewaters.<sup>30,57,81,97,107</sup> It is produced from re-agglomerated bituminous coal and has been investigated in numerous studies for PFAS removal in batch and column filtration studies.<sup>164</sup> Investigations conducted by Ochoa-Herrera et al. of F400 GAC report an adsorption capacity for

PFOS of up to 236 mg/g, and for PFOA up to 112 mg/g in batch experiments in ultrapure water.<sup>165</sup> Additionally, Zhang et al. similarly demonstrate that the single solute adsorption capacity of F400 GAC in ultrapure water for PFOS was 210 mg/g, for PFOA was 136 mg/g, for PFBS was 93 mg/g, for PFBA was 47 mg/g, for 8:2-FTS was 188 mg/g, and for 4:2-FTS was 85 mg/g.<sup>98</sup> This study also demonstrated that the presence of long-chain PFAS suppressed the sorption of short-chain PFAS in bi-solute systems, but did not significantly affect the sorption of PFAS with longer perfluorinated chain lengths. Co-occurring inorganic ions inhibited the sorption of short-chain PFBA and PFBS by approximately 50%, compared to 0 to -10% inhibition for the longer-chain PFAS evaluated.<sup>98</sup>

In a continuous flow setting treating low DOC (< 1 mg/L) groundwaters from Arizona, Zeng et al. (2021) demonstrated that F400 was more effective for treating long-chain PFNA, PFOA, and PFOS compared to shorter-chain PFHxS, PFHxA, and PFBS.<sup>166</sup> Park et al. (2020) published results with similar trends for the F400 in a small-scale continuous flow study, and concluded that the F400 GAC was more efficient for treating longer-chain PFAS due to its mesoporosity. Whereas, GAC micropore surface area was a more significant characteristic for the removal of more hydrophilic PFAS for all of the evaluated GACs in that study.<sup>97</sup>

Mortazavian et al. (2025) conducted RSSCTs evaluating commercial biochar and F400 for treating artificially-spiked wastewater, and demonstrated that both PFOS and PFHxS were successfully treated by F400 GAC for longer operational times than either PFOA or PFHxA. This study also suggested that the complex water matrix—relative to published data evaluating F400 for treating PFAS in groundwaters or drinking waters—significantly hindered GAC's efficacy to treat PFAS, especially for the evaluated PFCAs.<sup>70</sup>

**Norit® GAC 1240+ (1240+)** is an acid washed GAC that is produced via steam activation of bituminous coal.<sup>167,168</sup> Croll et al. (2022) utilized this product for a pilot-scale treatment of a PFAS contaminated groundwater, and demonstrated similar breakthrough trends as described for the F400 GAC.<sup>167</sup> Long-chain PFOS exhibited no breakthrough for the duration of the tests, and the number of BVs treated prior to 20% breakthrough decreased in the order PFHxS~PFHpS > PFOA > PFPeS > PFHpA~PFBS > PFHxA~PFPrS > PFPeA > PFEtS > PFBA > PFPrA.<sup>167</sup> Chow et al. (2022) evaluated 1240+ GAC against IX resins in pilot-scale tests. 1240+ GAC treated PFOA for approximately 55,000 BVs), and PFOS for approximately 85,000 BVs prior to 10% breakthrough; while PFBA and PFBS were only treated for 11,000 and 37,000 BVs prior to 10% breakthrough.<sup>51</sup>

IX Resins: **Purolite PFA694 (PFA694)** is a commercially available IX resin that is designed and marketed for PFAS removal from wastewater as a single-use (non-regenerable) media;<sup>169</sup> whereas, the PFA694E product is marketed for PFAS removal in point-of-use treatment systems or in drinking water applications.<sup>114,169,170</sup> PFA694 is composed of a non-porous (gel) PS-DVB synthetic polymer with cationic, proprietary “complex amino” functional groups, and a manufacturer reported equilibrium exchange capacity of 0.9 eq/L for PFA694E IX. Boodoo (2017) reported that a PFA694E treatment column was able to treat 155,000 BVs to a combined breakthrough of 7 ppt for PFOA and PFOS, compared to only 19,000 BVs to a combined breakthrough of 4.6 ppt for coal-based GAC. The PFAS-selective IX resin also demonstrated approximately 10–15 times greater operating capacity than GAC for PFHpA and PFHxS.<sup>170</sup>

In batch sorption tests, Liu and Sun (2021) showed that PFA694E IX along with several other PS-DVB IX resins, were successful at removing >90% of a variety of short- and long-chain PFAAs compared to PA- and polymethacrylate-based IX resins.<sup>112</sup> Ellis et al. (2023) reported that

PFA694E IX treated greater than 700,000 BVs, 639,000 BVs, 315,000 BVs, and 67,000 BVs prior to initial breakthrough for PFOS, PFOA, PFBS, and PFBA, respectively. While, the non-PFAS-selective IX evaluated in that study, Purolite A860, treated PFOS, PFOA, PFBS, and PFBA for 3,000 BVs, <1,000 BVs, 3,700 BVs, and <1,000 BVs, respectively, prior to initial breakthrough.<sup>106</sup>

In a pilot test for a drinking water treatment of PFAS contaminated groundwater in California, Medina et al. (2022) confirmed that (1) PFAS-selective IX resins, including PFA694E IX, outperform a variety of GACs in terms of BVs treated prior to breakthrough; (2) that shorter-chain PFAS breakthrough earlier than longer-chain compounds; and that (3) PFCAs of same fluorocarbon chain length will breakthrough earlier than corresponding PFASs.<sup>114</sup> Similarly, for treating a landfill leachate, Malovany et al. (2023) demonstrated that PFA694E IX can treat PFOS for ~22,000 BVs and PFOA for ~8,000 BVs prior to breakthrough in continuous flow tests, compared to less than 2,000 BVs for each compound for the F400 GAC. The PFAS-selective resin showed little removal of DOC, compared to F400 GAC; and only slightly outperformed the GAC for removal of the sum of 11 other PFAS detected in the influent groundwater.<sup>107</sup> Ellis et al. (2025) report that, despite being marketed as a ‘single-use’ resin, spent PFA694E IX resin from a pilot system treating AFFF-impacted groundwater was successfully regenerated using an organic brine solution; however, complete regeneration of the PFAS-selective IX resins required wash solutions with large volumes of organic solvent (between 70–90% v/v).<sup>129</sup>

**Amberlite PSR2+** (formerly known as Dowex PSR2+) is another ‘single-use’ (i.e., marketed as non-regenerable), PFAS-selective IX resin, with a similar composition to PFA694, except the functional group is defined as tri-N-butylamine, and the reported equilibrium exchange capacity is 0.7 meq/mL.<sup>171</sup> Zeng et al. (2020) compared several GACs and the PFAS-selective IXs PFA694E and PSR2+ in RSSCTs using real drinking water sources for removal of PFOS, PFHxS,

PFBS, PFNA, PFOA, PFHpA, and PFHxA, where the sum of the concentration for the seven detected PFAS ranged from 0.156 to greater than 7  $\mu\text{g/L}$ , and DOC was  $<1 \text{ mg}\cdot\text{C/L}$ . Both of the IX resins treated approximately 2–4 times as many BVs as the GACs in the continuous flow tests, and they both were more effective for the treatment of PFASs rather than PFCAs. In the case of PFCAs, breakthrough first occurred for PFHxA, followed by PFHpA, PFOA, and PFNA; while for the PFASs, PFBS was first to breakthrough, followed by PFHxS and PFOA.<sup>166</sup>

Lin et al. (2023) evaluated PSR2+ IX against a quaternary amine- and styrene-modified,  $\beta$ -CDP (referred to as a “StyDex polymer” in that text), and GAC for the removal of PFOS, PFHxS, PFOA, and PFHxA along with several other trace organic contaminants from real Illinois municipal wastewaters. Evaluations were conducted using batch adsorption capacity and kinetics tests, in addition to RSSCTs.<sup>139</sup> In ultrapure water batch tests, the three adsorbent media removed between 95-100% of each PFAS, with PSR2+ IX and the GAC exhibiting marginally slower adsorption kinetics compared to the StyDex polymer. In the batch tests conducted in real wastewaters, the StyDex polymer was least inhibited in terms of PFAS adsorption capacity and kinetics, followed closely by PSR2+ IX, while the GAC had decreases in the adsorption capacities of approximately 50% for PFOA and PFHxA, and decreases of approximately 30% for PFOS and PFHxS, with significantly reduced adsorption kinetics in the real wastewaters compared to the efficacy of PSR2+ IX or the StyDex polymer. In the RSSCTs using real wastewaters, both the PSR2+ IX and the StyDex polymer were able to treat PFOA for approximately 32,000 BVs, PFHxS for approximately 36,000 BVs, and PFHxA for approximately 15,000 BVs prior to 20% breakthrough, whereas the GAC exhibited near immediate breakthrough above 20% of the influent concentration when treating the real wastewaters.<sup>139</sup>

Ellis et al. (2022) conducted pilot-scale evaluations of various PFAS-selective and non-selective IX resins treating PFAS-impacted California groundwater ( $39 \pm 9.5 \mu\text{g/L}$  total PFAS concentration;  $\sim 1 \text{ mg/L}$  DOC;  $\sim 360 \text{ mg}\cdot\text{C/L}$  total dissolved carbon). For PSR2+ IX 50% breakthrough of PFOS, PFHpS, PFHxS, PFPeS, PFBS, and PFPrS occurred after treating approximately 503,000 BVs, 432,000 BVs, 390,000 BVs, 371,000 BVs, 350,000 BVs, and 292,000 BVs, respectively. Considering PFCAs, for PSR2+ IX 50% breakthrough of PFOA, PFHpA, PFHxA, PFPeA, and PFBA occurred after treating approximately 278,000 BVs, 182,000 BVs, 108,000 BVs, 101,000 BVs, and 70,000 BVs, respectively. Overall, for the evaluated PFAS defined in the Unregulated Contaminant Monitoring Rule 3 (UCMR3) by the U.S. EPA in 2012 (i.e. PFHpA, PFOA, PFBS, PFHxS, and PFOS), the PSR2+ IX treated approximately 142,000 BVs prior to any detectable concentrations in the pilot effluent. Comparatively, PFAS-selective IX resins CalRes2301 (Calgon Carbon) also treated  $\sim 142,000$  BVs, while PFA694E treated  $\sim 157,000$  BVs; while non-selective IX resins A520E and A860 treated only 21,000 BVs, and  $< 1,000$  BVs prior to initial detection of the UCMR3-defined PFAS.<sup>50</sup> Importantly, PFAS-selective IX resins demonstrate longer operational times of successful treatment of PFAS below a certain threshold; however, their main apparent drawback is a continued preference for the removal of long-chain PFAS over short-chain PFAS, as well as preferential removal of PFSA over PFCAs, generally mirroring prominent challenges of traditional sorbents used for PFAS removal.

Pilot-scale investigations conducted by Chow et al. (2022) evaluated Norit 1240+ GAC and two PFAS-selective IX (PFA694E and PSR2+) for treating a PFAS-impacted Minnesota groundwater used as municipal drinking water source. This source water was dominated by ultrashort-chain PFAS contributions ( $0.435 \mu\text{g/L}$  PFPrA,  $0.024 \mu\text{g/L}$  PFEtS, and  $0.095 \mu\text{g/L}$  PFPrS) and short-chain PFAS ( $0.914 \mu\text{g/L}$  PFBA,  $0.059 \mu\text{g/L}$  PFPeA,  $0.044 \mu\text{g/L}$  PFHxA,  $0.006$

$\mu\text{g/L}$  PFHpA,  $0.130\mu\text{g/L}$  PFBS, and  $0.083 \mu\text{g/L}$  PFPeS) to the total PFAS concentration compared with the detected long-chain PFAS contributions ( $0.015 \mu\text{g/L}$  PFOA,  $0.048 \mu\text{g/L}$  PFHxS,  $0.001 \mu\text{g/L}$  PFHpS, and  $0.002 \mu\text{g/L}$  PFOS). Overall, the IX resins had similar performance; they treated PFEtS below 10% breakthrough for approximately 120,000 BVs and exhibited no long-chain PFSA breakthrough above 10% after treating more than 210,000 BVs. The PFAS-selective IX resins both had poorer treatment efficacy for short- and ultrashort-chain PFCAs, with 10% breakthrough of PFPeA, PFBA, and PFPrA occurring after treatment of  $<60,000$  BVs,  $<20,000$  BVs, and  $<15,000$  BVs, respectively.<sup>51</sup> The pilot-scale continuous-flow tests conducted by Ellis et al. and Chow et al. underscore the relative success of treating (ultra)short-chain PFSAs with PFAS-selective IX resin, while also demonstrating the reduced performance for the (ultra)short-chain PFCAs, PFBA, PFPrA, and TFA.

**Amberlite IRA910**<sup>172</sup> is an industrial IX resin, one of many previously investigated IX resins with peer-reviewed investigations for PFAS removal despite not being a “PFAS-selective” resin. IRA910 IX has demonstrated high adsorption capacities for long-chain PFAS, and its inclusion in this study allows for evaluation of its effectiveness compared to the relatively novel PFAS-selective IX resins.<sup>76,112,120,173</sup>

In batch test experiments conducted by Liu and Sun (2021), IRA910 similar performance to other PS-DVB IX resins, removing greater than 90% of all short- and long-chain PFAAs which were included in that study.<sup>112</sup> Further batch test experimental results from Maimaiti et al. (2018) determined the following binary separation factors ( $\alpha_{ij} = \frac{C_i * q_j}{C_j * q_i}$ ) for IRA910 IX in bisolute systems: PFBA/PFOS: 0.394; PFBS/PFOS: 0.564; PFHxS/PFOS:1.961; PFOA/PFOS: 1.444; PFOA/PFBS: 2.837; PFHxA/PFOS: 0.740; PFHxA/PFHxS: 0.509.<sup>120</sup> The authors report a

maximum adsorption capacity for PFOA and PFOS of greater than 1,400 mg/g, greater than 360 mg/g for PFBA and greater than 1,000 mg/g for PFBS – which exceed the maximum reported capacities for F400 GAC by up to a factor of 5.<sup>76,92,122</sup>

Alternative Adsorbents: **The anonymized surface-modified clay (SMC) mineral adsorbent** selected for this evaluation was acquired from the manufacturers pursuant to a Non-Disclosure Agreement (NDA) that prohibits disclosure of the product's identity; as well as prohibiting the attempted characterization of the media's composition. The SMC has a bentonite base functionalized with a quaternary ammonium surfactant intercalated via cation exchange in between the clay mineral layers. The primary mechanism through which SMC is expected to adsorb PFAS is via hydrophobic interactions with the intercalated surfactant, as well as contributions from electrostatic interactions with the quaternary ammonium group.<sup>88,174</sup> There is limited third-party data reporting its effectiveness for PFAS-removal in complex water matrices.

**DEXSORB®** is a proprietary adsorbent developed for the removal of PFAS from water consisting of a granulated  $\beta$ -cyclodextrin-based polymer ( $\beta$ -CDP) with fluorinated aromatic cross-linkers and quaternary ammonium functionalized comonomers.<sup>136,175,176</sup> The hydrophobic cavity of the  $\beta$ -cyclodextrin monomer is uniformly 0.78 nm in diameter, which reportedly provides molecular selectivity and prevents pore blockage via size exclusion of DOM.<sup>136,137,176</sup> It is hypothesized that the mechanisms through which polymeric  $\beta$ -cyclodextrin-based adsorbents, like DEXSORB, function are hydrophobic interactions and electrostatic interactions, with additional favorable interaction via formation of host-guest complexes and fluorophilic interactions induced by fluorinated polymeric co-monomers.<sup>136,137,139</sup> DEXSORB® is sold as a component in point-of-use and at-home supplemental drinking water treatment systems, has reportedly good performance for the removal of legacy PFAS from relatively complex matrices, fast adsorption kinetics, and

demonstrates size-exclusion effects to avoid inhibition from large DOM molecules.<sup>92,131,135,139,177,178</sup> Previously reported adsorption capacities of  $\beta$ -CDPs for PFAS include 1,316.7  $\mu\text{mol/g}$  for PFOA (i.e.  $\sim 545$  mg PFOA/g) and 672.6  $\mu\text{mol/g}$  for HFPO-DA (i.e.  $\sim 222$  mg HFPO-DA/g).<sup>92,179</sup>

Wu et al. (2020) evaluated activated carbons and an aminated and a permanently positively-charged  $\beta$ -CDP (referred to as aCDP and CDP+) in batch tests for the removal of 20 PFAS from artificially-spiked (0.5  $\mu\text{g/L}$  each PFAS) ultrapure water and “native-PFAS” present in real groundwater samples sourced from the northeastern U.S. (TOC 1.5 – 2.1 mg/L). They reported that each of the evaluated activated carbons with particle size  $< 212$  microns (i.e. powdered activated carbons (PACs)) and each of the  $\beta$ -CDPs were able to remove nearly 100% of the PFAS in the ultrapure water matrix, while GACs with particle sizes between 425–1000 microns (i.e. GACs) removed all the PFAS to a lower extent ( $\sim 50\%$ ) within the 4-hour equilibration time.<sup>177</sup> For the batch tests conducted in the real groundwater matrices, overall removal was inhibited, yet long-chain PFAS were removed to a greater extent for all of the evaluated activated carbons (ACs) and  $\beta$ -CDPs, suggesting that hydrophobic interactions are the main adsorption mechanism for PFAS adsorption to AC and  $\beta$ -CDP in complex water matrices. The CDP+, however, was consistently the least inhibited by the groundwater matrices for removal of short- and long-chain PFAS, suggesting that the sorbent surface charge is also a significant mechanism of removal particularly for more hydrophilic short-chain PFAS. Further, their results indicate that co-occurring divalent cations inhibit the electrostatic interaction between the PFAS and the positively-charged sorbent surface in the complex water matrix.<sup>177</sup>

In batch tests conducted by Ruckbeil et al. (2025) evaluating ACs, IX resins, and various alternative adsorbents for removal of PFAS and other organic micro-pollutants from German

drinking water (4.5 mg/L TOC), DEXSORB® demonstrated low DOC removal, but was significantly outperformed by various GACs and five PFAS-selective IX resins for the removal of short-chain PFCAs and PFSAAs and barely removed ultrashort-chain TFMS (~4% removal).<sup>131</sup> In pilot-scale evaluations treating PFAS-contaminated California groundwater conducted by Medina et al. (2022), an anonymized  $\beta$ -CDP sorbent media treated the following PFAS for the specified number of BVs prior to initial breakthrough:

- PFOA: 17,400 BVs
- PFOS: 125,000 BVs; and PFBS: 30,000 BVs

Compared to the initial breakthrough of each of the compounds for the F400 GAC:

- PFOA: 22,400 BVs
- PFOS: 35,000 BVs; and PFBS: 17,200 BVs

for Fluorosorb 200:

- PFOA: 154,000 BVs
- PFOS: no breakthrough; PFBS: 100,000 BVs

And for the PFAS-selective IX resin, PFA694E:

- PFOA: 77,000 BVs,
- PFOS: no breakthrough; and PFBS: 198,000 BVs.<sup>114</sup>

Similar results were reported from batch tests and RSSCTs conducted by Ching et al. (2023) on  $\beta$ -CDP adsorbents manufactured by Cyclopure (not specifically DEXSORB®).<sup>135</sup> For

the RSSCTs the order of PFAS breakthrough above 50% of the influent concentration was: (from latest breakthrough to earliest):

- PFOA: 500,000 BVs; PFHxA: 125,000 BVs; and PFBA: 50,000 BVs
- PFOS~PFHxS: >500,000 BVs; and PFBS - 475,000 BVs.<sup>135</sup>

### *1.6.2. PFAS Selected for Evaluation*

A continuous spectrum of PFAAs including C1–C8 PFSAAs and C2–C9 PFCAs were selected to (1) evaluate the commercial media for their ability to selectively remove ultrashort-, short-, and long-chain PFAS from municipal wastewater effluent; (2) to investigate competitive interactions amongst the selected PFAS analytes; and to (3) probe adsorption interference due to co-occurring inorganic ions, dissolved EfOM, and non-PFAS micro-contaminants (not analyzed for, but likely present in the UF membrane sample used as the influent to RSSCTs). In addition, one PFECA, hexafluoropropylene oxide-dimer acid (HFPO-DA; also known under the tradename, GenX, the ammonium salt of HFPO-DA), because it was included in the April 2024 finalized U.S. EPA National Primary Drinking Water Regulation (NPDWR),<sup>37</sup> and because it is an increasingly detected short-chain alternative compound introduced to replace PFOA.<sup>21,33,34,180,181</sup> Finally, one fluorotelomer sulfonic acid, 6:2 fluorotelomer sulfonate (6:2 FTS), was also included in the evaluation because it is a commonly occurring PFAS in the environment;<sup>182</sup> and to provide insight into the relative competition for adsorption sites between PFAAs and a polyfluoroalkyl substance. The PFAS selected for evaluation are presented in **Table 1.1**, above, along with some of their relevant physicochemical properties.



## **2. Manuscript: Evaluating Commercial Sorbents for Removal of Ultrashort-, Short-, and Long-chain Per- and Polyfluoroalkyl Substances (PFAS) from Municipal Wastewater Effluents**

### *2.1. Objectives and Hypothesis*

Per- and polyfluoroalkyl substances (PFAS) are a large class of synthetic chemicals that are estimated to include more than 14,000 compounds.<sup>3</sup> PFAS exhibit unique properties generally attributable to the high bond energies of multiple C–F bonds along the alkyl backbone,<sup>7,9</sup> and they have been utilized since the 1950s for hundreds of different uses in the oil & gas, aerospace, semiconductor, and biotechnology industries; and in the production of plastics, metals, and electronics.<sup>2,4</sup> Additionally, PFAS are or have been employed in many other consumer use categories such as personal care and cleaning products, food packaging, waterproof fabrics, electronic devices, medical utensils, and aqueous fire-fighting foams (AFFF), among many other applications.<sup>2</sup> In general, the same properties from which PFAS derive their utility, are also what make them a challenge from an environmental health standpoint—PFAS are recalcitrant to microbial, physical, thermal, or chemical degradation leading to their persistence and accumulation over long time periods in the air, soil, and in water.<sup>5,9,14,183</sup>

The widespread use and environmental occurrence of PFAS, their mobility and resistance to degradation, combined with the fact that conventional wastewater treatment plants (WWTPs) are not designed to remove PFAS, accounts for how WWTPs have come to be recognized as a significant pathway for PFAS to enter surface water bodies, and ultimately threatening drinking water supplies.<sup>13–16,46</sup> However, current treatment processes employed in WWTPs have limited effectiveness for separating PFAS from effluent discharged to surface waters. Conventional aerated activated sludge treatment of municipal wastewater, as well as traditional drinking water

treatment techniques such as coagulation, flocculation, sedimentation, sand filtration, and chlorine or UV disinfection have limited effectiveness at destroying or removing PFAS from aqueous matrices.<sup>9–12</sup> Advanced treatment methods, such as granular activated carbon (GAC) and ion exchange (IX) resins are two of the most well-established commercial adsorbent technologies for the separation of PFAS from water due to their effectiveness, passive operation, and relatively low cost.<sup>24,30,62,63,87,102,122</sup> A typical trend reported on the performance of GAC and IX resin adsorptive treatment is the preferential uptake of long-chain PFAS over (ultra)short-chain PFAS, while there is general lack of research evaluating adsorbents for treating a full-spectrum of PFAS chain-lengths.<sup>38,51,56–60</sup> Information regarding separation of short- (C4 – C6 fluorinated carbons) and ultrashort-chain (<C4 fluorinated carbons) PFAS by current and novel filtration media in WWTPs is critically lacking which is concerning considering that short- and ultrashort-chain PFAS are an increasing share of PFAS present in wastewater effluents.<sup>65,69,74,77,78,90–93</sup> For example, A study published by Kim et al (2022) demonstrated that short- and ultrashort-chain PFAS primarily exit WWTPs via aqueous effluent, whereas long-chain PFAS will tend to preferentially partition to biosolids, suggesting that targeting treatment of long-chain PFAS in wastewater effluent should not be the primary concern.<sup>15</sup> In fact, a global meta-analysis by Cookson and Detweiler (2022) shows rising short-chain PFAS levels in WWTPs from 2005–2020; and that, in the U.S., legacy PFOA and PFOS concentrations have been declining in wastewater, while concentrations of shorter PFAS like PFBA and PFBS are increasing.<sup>69</sup>

There is limited published data available for the effectiveness of GAC, IX or other novel adsorbents to remove short- and ultrashort-chain PFAS from water matrices with high wastewater-derived organic matter content, and co-occurring inorganic ions, and other organic micro-pollutants.<sup>15,51,74,78,166</sup> Significantly, the effectiveness of GAC and IX resins to remove PFAS is

diminished by interferences arising from dissolved effluent organic matter (EfOM), co-occurring ions and other potential trace contaminants.<sup>19,70,74,95</sup> Given the cost and implementation challenges associated with still-emerging PFAS destruction methods and separation techniques utilizing high-pressure membranes, it is likely that adsorbent media are the most practical, robust, and mature option for PFAS removal from municipal wastewater. Yet, there is a general lack of research evaluating the use of adsorbent technology to treat ultrashort-chain PFAS, especially when considered in a complex matrix with a mixed system containing a complete spectrum of PFAAs of varied chain-lengths.<sup>25</sup>

The objectives of this study were to identify and evaluate different types of commercial adsorbent materials (two GACs, three IX resins, one  $\beta$ -cyclodextrin-based polymer [ $\beta$ -CDP], and one surface-modified clay mineral [SMC]) for removal of ultrashort-, short-, and long-chain PFAS from municipal wastewater. The preliminary evaluation included batch sorption capacity and kinetics tests in both ultrapure water (UP) and a synthetic wastewater (SW) matrix—constituted from an effluent organic matter (EfOM) isolate—and commonly occurring inorganic ions. We performed lab-controlled rapid small-scale column tests (RSSCTs) using the best performing media from the preliminary evaluations to assess their ability to remove PFAS from a tertiary treated municipal effluent, mimicking a realistic step in a potential treatment train approach targeting PFAS removal that may be encountered in treatment trains designed for potable and non-potable re-use.<sup>57,74,82</sup>

We evaluated the efficacy of PFAS-selective media for the uptake of ultrashort-, short-, and long-chain PFAS treating a complex water matrix containing wastewater effluent-derived organic matter and co-occurring inorganic ions. Previous studies regarding the removal of ultrashort-, short-, and long-chain PFAS from aqueous matrices suggest that ultrashort-chain PFAS

will be poorly adsorbed by GAC, DEXSORB®, and the SMC due to weak electrostatic interactions relative to the ion exchange resins. We anticipate the PFAS-selective media will outperform the conventional media (i.e. GACs and non-selective IRA910 IX) in the RSSCTs for long- and short-chain PFAS typically targeted for removal due to regulatory pressures (e.g PFOS, PFOA, PFHxA, PFBS, HFPO-DA) primarily due to inhibitory effects introduced by the dissolved organic matter and co-occurring inorganic ions. Finally, previously reported results from continuous-flow tests treating multiple types of PFAS, suggest that the two PFAS-selective IX resins and DEXSORB® will be the most effective adsorbent media for treating the entire suite of PFAS in the RSSCTs with artificially-spiked, tertiary treated, real wastewater.

## 2.2. *Materials and Methods*

### 2.2.1. *Chemicals*

All chemicals used were certified ACS reagent grade or equivalent unless otherwise noted. Analytical and mass-labelled PFAS internal standards used for PFAS quantification were purchased from Wellington Laboratories (Guelph, ON), including the PFAC-MXA PFAS mixture and MPFAC-MXA mass-labelled internal standard mixture. Additional mass-labelled PFAS internal standards purchased from Wellington Laboratories included sodium 1H,1H,2H,2H-Perfluoro-1-[1,2-12C2]-octane sulfonate (<sup>13</sup>C<sub>2</sub>-6:2-FTS), and <sup>13</sup>C-hexafluoropropylene oxide – dimer acid (<sup>13</sup>C<sub>3</sub>-HFPO-DA), used in the quantification of 6:2-FTS and HFPO-DA, respectively. Further analytical standards used for PFAS quantification obtained from Wellington Laboratories (Guelph, ON) included, sodium 1H,1H,2H,2H-perfluorooctane sulfonate (6:2-FTS), and ultrashort-chain sodium perfluoroethane sulfonate (PFEtS), sodium trifluoromethane sulfonate (TFMS), and pentafluoropropionic acid (PFPrA). The other two ultrashort-chain PFAS were quantified utilizing analytical grade trifluoroacetic acid (TFA, >99% purity, product number: 74564) purchased from

Sigma Aldrich (St. Louis, MO), and analytical grade sodium perfluoro-1-propane sulfonate (PFPrS) purchased from Accustandard (New Haven, CT). Analytical grade sodium perfluoro-1-pentane sulfonate (PFPeS) was also acquired from Accustandard. Quantification of HFPO-DA was accomplished utilizing analytical grade tetrafluoro-2-(heptafluoropropoxy)propanoic acid (HFPO-DA) purchased from Cambridge Isotope Labs (Tewksbury, MA). **Table S.1** summarizes the vendor information for each compound.

Concentrated PFAS stock solutions for batch adsorption and continuous-flow experiments were prepared with Optima™ LC/MS grade Methanol purchased from Thermo Fisher Scientific. The 18 PFAS which constitute the “18-PFAS mix” used in all batch and continuous flow tests are listed in **Table 1.1** along with their group classification, and relevant physicochemical properties. Several of the PFAS analytes including, potassium perfluorooctanesulfonate (PFOS) (98% purity), potassium perfluorohexanesulfonate (PFHxS), and sodium 1H,1H,2H,2H-perfluorooctane sulfonate (6:2 FTS) were purchased in their salt forms.

Sealed vials containing methanolic solutions of each individual PFAS and the 18-PFAS mix (either 1000 µg/L, or 2 mg/L (each PFAS)) were wrapped with parafilm and stored in a refrigerator at 4 °C. Methanolic solutions of the eight perfluorocarboxylic acids (PFCAs) and one perfluoroethercarboxylic acid (i.e. HFPO-DA) were prepared with 4 molar equivalents of sodium hydroxide (NaOH; Fisher Scientific) to prevent methyl esterification of the carboxylate functional groups on the PFAS analytes.

Quantification of PFAS was achieved using a 100% acetonitrile mobile phase and a 5 mM ammonium formate (0.1% v/v formic acid) aqueous phase eluent. The methanol used was Optima® LC-MS grade and the ammonium formate was certified LC-MS grade. Both of these

chemicals were purchased from Fisher Chemical (Hampton, NH). Further details regarding the LC-MS/MS methodology are available in the SI Section S3.

Stock solutions of inorganic anions and cations were prepared and stored at 4 °C until use in the synthetic wastewater batch adsorption capacity and kinetics tests, utilizing the following chemicals and vendors. Calcium chloride ( $\text{CaCl}_2$ ) and sodium bicarbonate ( $\text{NaHCO}_3$ ) were purchased from Fisher Scientific (Hampton, NH). Sodium chloride ( $\text{NaCl}$ ) and magnesium chloride hexahydrate ( $\text{MgCl}_2 \cdot 6\text{H}_2\text{O}$ ) were purchased from VWR Chemical. Magnesium nitrate hexahydrate ( $\text{Mg}(\text{NO}_3)_2 \cdot 6\text{H}_2\text{O}$ ) was purchased from Fisher Scientific, calcium nitrate tetrahydrate ( $\text{Ca}(\text{NO}_3)_2 \cdot 4\text{H}_2\text{O}$ ) from Alfa Aesar (Haverhill, MA), sodium phosphate dibasic heptahydrate ( $\text{Na}_2(\text{PO}_4) \cdot 7\text{H}_2\text{O}$ ) from Ameresco (Solon, OH). Details on the preparation of the synthetic wastewater matrix is provided in the SI **Section S.4**. Sodium chloride ( $\text{NaCl}$ ), hydrochloric acid ( $\text{HCl}$ ) and sodium hydroxide ( $\text{NaOH}$ ) for electrophoretic mobility (EPM) analysis of the commercial sorbents were obtained from VWR Chemical (Radnor, PA).

### *2.2.2. Commercial media selected for evaluation*

The commercially available adsorbent media evaluated in this study included a  $\beta$ -cyclodextrin-based polymer ( $\beta$ -CDP), DEXSORB® produced by Cyclopure® (Evanston, IL); two GACs: Filtrasorb® 400 (F400 GAC) produced by Calgon Carbon (Moon Township, PA) and Norit® 1240+ (Marshall, Texas); two PFAS-selective IX resins: Purolite® PFA694 (King of Prussia, PA) and Amberlite™ PSR2+ (Wilmington, DE); one non-selective IX resin: Amberlite™ IRA910; and an anonymized commercial surface-modified clay mineral adsorbent (SMC). **Tables S.2A** and **S.2B** provide relevant properties and physical characteristics reported elsewhere in peer-reviewed literature of the selected media, or as reported by the manufacturers in the respective media specification data sheets.

#### 2.2.2.1. *Point of zero charge*

The media point of zero charge (PZC) was measured by quantifying the sorbent surface zeta potential across a broad range of pH values. Briefly, each of the sorbents were pulverized to a fine powder using a mortar and pestle. The crushed sorbent was added at a concentration of 500 mg/L to a pH-adjusted 10 mM NaCl solution at one of pH 2, 4, 6, 8, 10, or 12. The solution pH was measured with a Thermo Scientific (Waltham, MA) Orion™ Star A111 pH meter and adjusted to the target pH using either hydrochloric acid or sodium hydroxide. Once a stable pH reading was observed, the surface zeta potential was measured using a Zetasizer Nano ZS (Malvern Instruments, Malvern, UK). All experimental procedures for determination of the PZC were conducted in triplicate. The results of the PZC determination are presented in the SI (**Figure S.1, Table S.6**). The SMC was not characterized for its PZC due to irreproducible zeta potential readings and drifting pH measurements when preparing the solutions. This effect is possibly due to mechanical abrasion and crushing caused by the mortar and pestle, which may have weakened the surfactant's binding to the clay surface. Another potential explanation might be that the surfactant leaching from the mineral surface at acidic pH ranges.

#### 2.2.3. *Batch sorption isotherm and kinetics tests in ultrapure water*

Batch adsorption tests were conducted to determine the equilibration capacities and kinetics of PFAS uptake for the media in both an ultrapure (UP) water matrix and in a synthetic wastewater (SW) matrix in order to elucidate the effects of matrix interferences in the form of effluent organic matter (EfOM), inorganic ions, and elevated pH (~8.5 pH units). The batch adsorption tests conducted in the UP- and SW-matrices were preliminary evaluations to narrow down the number of adsorbents evaluated in the subsequent RSSCTs. All batch tests were conducted with a sorbent dose of 100 mg/L in a 50-mL polypropylene tube. After the 96-hr reaction

period, up to 5 mL aliquots from each sample were collected in a polypropylene micro-centrifuge tubes and stored at 4 °C until analysis by liquid chromatography tandem mass spectrometry (LC-MS/MS). All batch tests included control samples with no media added to account for PFAS losses to the reaction vessel walls.

The adsorption isotherms for the 18-PFAS mix (**Figure 2.1**) were generated for each of the seven adsorbent media in the UP matrix as a preliminary screening to assess PFAS removal before eliminating poor-performing media for subsequent isotherm tests. Eight different initial PFAS concentrations of the 18-PFAS mix system (nominally: 5 µg/L, 10 µg/L, 50 µg/L, 100 µg/L, 225 µg/L, 500 µg/L, 1 mg/L and 2 mg/L). were reacted over the 96-hr period with over-end mixing at 40 rpm on a Fisherbrand™ Multi-Purpose Tube Rotator (Fisher Scientific, Waltham, MA). Adsorption isotherm data for the seven media were fit to both non-linear and linear forms of the Langmuir isotherm model, and non-linear and linear forms of the Freundlich adsorption isotherm model (**Section S.6.2**).<sup>185</sup> Kinetics data from ultrapure water experiments were fit to linear and non-linear pseudo first order (PFO) kinetic model; and linear and non-linear pseudo second order (PSO) kinetics model (Section S.6)

Based on the results of the UP water matrix isotherm screening tests, we did not evaluate the adsorption kinetics of the 1240+ GAC nor the PSR2+ IX resin due to near identical sorption capacities to F400 GAC, and due to poor uptake of the ultrashort- and short-chain PFAS, respectively. All of the adsorption kinetics tests were conducted using a nominal 200 µg/L (each PFAS) initial concentration of the 18-PFAS mix.

#### *2.2.4. Synthetic wastewater (SW)-matrix sorption capacity and kinetics tests*

Following the adsorption isotherm and kinetics experiments in UP water, analogous batch tests were performed using a prepared SW effluent matrix made from an effluent organic matter

(EfOM) isolate derived from the King County West Point (Seattle, WA) wastewater treatment plant and the addition of realistic quantities of inorganic ions from aqueous stock solutions. The composition of the SW matrix used in the batch tests is presented in **Tables S.3**. All experimental conditions for SW matrix batch tests were the same as those used in the UP water batch tests, except that one more triplicate set of control samples was collected (in addition to the UP water control samples) and quantified to control for any sorption of PFAS with the EfOM.

The EfOM isolate for the synthetic wastewater matrix was produced via solid-phase extraction of a glass fiber filtered sample of pre-disinfected secondary wastewater effluent collected from the King County West Point Wastewater Treatment Plant in January 2025. Further details regarding the preparation of the EfOM isolate are provided in **Section S.4**.

F400 GAC, DEXSORB®, IRA910 IX, and PFA694 IX were the four sorbents evaluated in batch adsorption capacity and kinetics tests in the SW matrix. Only three initial concentrations of the 18-PFAS mix were evaluated for the SW adsorption capacity study: 20 µg/L, 200 µg/L, and 2 mg/L (each PFAS). During sampling, aliquots were filtered with 0.45 µm, 25 mm diameter cellulose acetate syringe filters purchased from Sigma Aldrich. Syringe filters were first primed with 5 mL of ultrapure water, then 20 mL of sample was wasted through the filter, prior to collecting up to 5 mL in a polypropylene microcentrifuge tube and storing in a refrigerator at 4 °C until preparation for analysis by LC-MS/MS (Section S.3, **Table S.7**, **Table S.8**). The overall low adsorption capacity demonstrated by the SMC in the UP water batch tests precluded it from the batch tests using the SW matrix as well as the RSSCTs. Similarly, the 1240+ GAC and PSR2+ IX resin were also not evaluated in the SW matrix batch adsorption capacity and kinetics tests nor in the RSSCTs using real wastewater.

### 2.2.5. Rapid small-scale column tests (RSSCTs)

In order to better evaluate the treatment efficacies of the different media in a continuous-flow setting and in conditions representative of real wastewater treatment plants, RSSCTs were performed using tertiary-treated (ultrafiltration [UF] membrane) wastewater treatment plant effluent spiked with 10 µg/L (each) of the 18-PFAS mix. The concentrations of PFAS in the column influent and effluent were quantified using methods developed for the LC-MS/MS. Prior to testing the media in the wastewater effluents, the source waters were characterized to assess background concentrations of PFAS, metals, organic matter, and inorganic ions (**Table S.5**). A total of two grab samples of approximately 30 gallons each of the UF membrane effluent were collected on July 7, 2025 and July 14, 2025 in clean and field-rinsed polypropylene buckets or carboys with secure lids. Samples were transported directly to storage in a 4 °C refrigerator for less than four days until used in the RSSCT experiments.

The F400 GAC, DEXSORB®, PFA694 IX, and IRA910 IX were all evaluated as reactive media in the RSSCTs. Duplicate packed bed columns were packed with 1 wt% media and 99 wt% acid-washed silica sand (**Figure S.3**). Two columns were packed with sand only (100 wt%) to serve as controls to account for PFAS losses to sorption to sand grains either directly or indirectly via association with dissolved EfOM that may subsequently associate with the sand. Parameters for the continuous flow tests are presented in **Table S.4** (i.e., column size, flow rate, mass of media, pore volumes, etc.). All columns were constructed from polypropylene or PVC pipes, tubing, and fittings acquired from McMaster-Carr (Elmhurst, IL). PharMed BPT tubing was used within the pump housing of an Ismatec (Glattbrugg, Switzerland) IP high precision multichannel peristaltic pump.

Ten of the twelve pump channels led to the bottom of each of the columns, while two of the channels were utilized to sample the concentrations of PFAS in the column influent reservoir. The average values of the sample concentration from the duplicate influent lines were used as the influent PFAS concentrations for purposes of normalizing the RSSCT breakthrough profiles. The 55-L influent reservoir was magnetically stirred during the 10-day study. After spiking the influent reservoirs with the concentrated methanolic solution of the 18-PFAS mix, the reservoirs were allowed to stir for at least one hour prior to inserting the tubing intakes for each of the test columns into the bottom of the mixed, PFAS-spiked reservoir. The influent was fed to the test columns in an up-flow configuration at a rate of 1.13 mL/min. A photo of the RSSCT set-up is provided in the SI **Figure S.3**. Conservative bromide tracer tests were carried out to determine the pore volumes for each column type (**Section S.7.1, Figure S.18**)

#### *2.2.5.1. Tertiary-Treatment UF-Membrane Pilot*

The tertiary ultrafiltration (UF) membrane pilot was being evaluated for potential application for on-site non-potable reuse to replace aging tertiary sand filters at the King County West Point Treatment Plant. The module consisted of a containerized ZeeWeed 1500 ultrafiltration system (Veolia Water Technologies, Boston, MA).<sup>186</sup> The single membrane module (600 ft<sup>2</sup> surface area) housed in a 20-ft standard shipping container operated at feed flows of ~8 GPM with a nominal pore size of 0.02  $\mu\text{m}$  and an absolute pore size of 0.1  $\mu\text{m}$ . Disinfected secondary effluent wastewater served as the influent to the UF membrane pilot. The pressurized hollow-fiber membrane operated in alternating filtration and backwash cycles supported by automated cleaning systems.

#### 2.2.5.2. *Wastewater Characterization*

The collected tertiary treated wastewater effluent was characterized for background concentrations of PFAS, inorganic ions, metals, and organic matter content. The influent feed parameters to the RSSCT columns are summarized in **Table S.5**. LC-MS/MS analyses for background PFAS concentration of the 18 PFAS analytes in this study indicated that representative PFAS were below the method limits of detection. The collected membrane effluent samples were characterized for dissolved organic carbon (DOC) concentration using a Shimadzu TOC-L analyzer (Kyoto, Japan). Concentrations of magnesium, calcium, sodium, ammonium chloride, nitrate, and sulfate were quantified via ion chromatography, and lead, aluminum and iron concentrations were determined via inductively coupled plasma-mass spectrometry (ICP-MS). Instrument and methodology details for both analyses are presented in **Section S.3, Tables S.7-8.**

#### 2.2.6. *PFAS quantification*

Concentrations of all PFAS in batch and continuous-flow tests were quantified by mass spectroscopy using a Waters Corporation (Milford, MA) triple quadrupole mass spectrometer (MS/MS) preceded by liquid chromatography (LC) using a Waters 2795 Alliance HT liquid chromatography separations module. PFAS were analyzed via LC-MS/MS using a RESTEK (Bellefonte, PA) ultra inert IBD 3  $\mu\text{m}$  high performance liquid chromatography (HPLC) column (100 x 2.1 mm, RESTEK Catalog No. 9175312-T) as the stationary phase, preceded by a 10 x 2.1 mm guard cartridge for rapid small-scale column test (RSSCT) samples to pre-filter samples using secondary effluent as the aqueous matrix. **Table S.7** and **Table S.8** provide details regarding the operational parameters for the LC gradient and for the MS/MS multiple reaction monitoring (MRM) transitional pairs. Further details provided in Section S.3.

### 2.3. Results and Discussion

For purposes of simplifying discussion, HFPO-DA will be considered as a short-chain PFCA (although it is technically a perfluoroalkyl ether carboxylic acid). Similarly, 6:2-FTS will be considered as a long-chain, PFSA in the discussion. Furthermore, the PFAS-selective PSR2+ IX resin and the SMC media demonstrated the lowest overall adsorption capacities for the spectrum of PFAS evaluated in this study (**Figure 2.1**); therefore, detailed discussion of results using these media are confined to the SI. Additionally, due to similar performances of the two evaluated GAC, discussion focused on the Norit 1240+ GAC will also be confined to the SI to allow for a more focused discussion across the different sorbent types.

#### 2.3.1. Ultrapure water isotherm tests for 18-PFAS mix—non-selective IX resin exhibits greatest PFAS adsorption capacity

##### 2.3.1.1. GACs exhibit multi-layer adsorption at high aqueous PFAS loadings

Both the F400 and 1240+ GACs exhibited comparable performances in terms of total PFAS removal percentages (**Figure S.4**), and in terms of the relative distribution of long-, short-, and ultrashort-chain compounds sorbed at the different mass loadings of PFAS in each of the batch tests conducted for UP water isotherm experiments (**Figures 2.1, 2.2, S.11, S.12**); however, they displayed much reduced adsorption capacities for the 18-PFAS mix relative to the non-selective IRA910 IX. The maximum adsorption capacity for 1240+ GAC for the 18-PFAS mix in the UP water batch tests was 81  $\mu\text{g}$  PFAS/mg, and for F400 GAC was 115  $\mu\text{g}$  PFAS/mg, which are in alignment with results reported previously reported results for F400 GAC that its adsorption capacity for PFOS is up to 236 mg/g, and up to 112 mg/g for PFOA.<sup>165</sup> Additionally, Zhang et al. demonstrated that the single solute adsorption capacity of F400 GAC in ultrapure water for PFOS

was 210 mg/g, for PFOA was 136 mg/g, for PFBS was 93 mg/g, for PFBA was 47 mg/g, for 8:2-FTS was 188 mg/g, and for 4:2-FTS was 85 mg/g.<sup>98</sup>

For both GACs, good fits to both the Langmuir and Freundlich isotherm models suggest potential interactive effects of multiple mechanisms of adsorption including electrostatic as well as hydrophobic interactions, and potentially PFAS-PFAS interactions.<sup>53,103,117</sup> The F400 GAC sorption envelope exhibited a stronger fit to the non-linear Freundlich isotherm model ( $r^2 = 0.961$ ) compared with its fit to the Langmuir model ( $r^2 = 0.860$ ); whereas the 1240+ GAC sorption envelope exhibited a better fit to the non-linear Langmuir isotherm model ( $r^2 = 0.957$ ) compared with its fit to the Freundlich model ( $r^2 = 0.921$ ). GACs commonly demonstrate good fits to both Freundlich and Langmuir models, where adherence to Langmuir-type adsorption is generally indicative of single-layer adsorption to homogeneous adsorption sites with low initial aqueous PFAS concentrations, while the Freundlich-type isotherms may provide a better fit due to formation of a PFAS bi-layer via hemicelle structures and hydrophobic interactions.<sup>59,92,97,105,187</sup> Regardless, determining goodness-of-fit to Langmuir or Freundlich models is often not enough to determine the adsorption mechanism because the two isotherm models might fit isotherm data similarly.<sup>93</sup>

Upon further inspection, both GACs appear to demonstrate “S-type” adsorption profiles when exposed to artificially high aqueous PFAS concentrations in the 1 mg PFAS/L and 2 mg PFAS/L UP water batch tests, indicative of multi-layer adsorption or a cooperative adsorption effect typical of surfactants.<sup>188–190</sup> For example, the 1240+ GAC had an average adsorption capacity of 60.1  $\mu\text{g}$  PFAS/mg and 62.1  $\mu\text{g}$  PFAS/mg in the 500  $\mu\text{g}$  PFAS/L and 1 mg PFAS/L nominal initial concentration batch tests; however, when the nominal initial concentration increased to 2 mg PFAS/L, the average adsorption capacity increased by 42% to 87.9  $\mu\text{g}$

PFAS/mg. Similarly, for the F400 GAC the total PFAS adsorption capacity increased by an average of 50% between the 500 µg PFAS/L and 1 mg PFAS/L, as well as between the 1 mg PFAS/L and 2 mg PFAS/ L nominal initial concentration batch tests. The slight differences in performance for the two GACs are potentially a result of their reported differences in pore surface area and pore volume (**Table S.6**). F400 GAC is slightly more mesoporous and may easily accommodate multiple layers of sorbed PFAS within its pore volume, compared to the more microporous 1240+ GAC which was only able to accommodate multi-layer adsorption of PFAS with additional forcing due to exceedingly high PFAS concentrations. As previously reported by Pauletto and Bardosz,<sup>191</sup> Lei,<sup>59</sup> Zhang et al.<sup>192</sup> and others, GACs with large mesopore volume and wide pore structures (such as F400 GAC), as opposed to GACs with microporous and narrow pore structures (such as 1240+ GAC) are able to accommodate the adsorption of more PFAS, and additionally tend to be less inhibited by the presence of dissolved organic matter (DOM).

#### *2.3.1.2. DEXSORB® exhibits sorption behavior dominated by hydrophobic interactions*

In the UP water isotherm tests DEXSORB® demonstrated (1) very similar trends to the GACs across the entire suite of PFAS, (2) lower PFAS adsorption capacity than the non-selective IRA910 IX resin across all batch tests, (3) lower adsorption capacity compared to PFA694 IX at relatively low aqueous PFAS loadings, and (4) greater adsorption capacities compared to the other two PFAS-selective media, PSR2+ IX and the SMC (**Figure 2.1**). DEXSORB® achieved greater than 90% removal for each the PFAS in the 10 µg/L and 200 µg/L nominal initial concentration batch tests, while exhibiting diminished removal percentages of all PFAS in the 2 mg/L UP water batch test particularly considering the uptake of all but the longest-chain PFAAs and some short-chain PFSAs (**Figure 4**), as corroborated by batch test results investigating β-CDPs conducted by Yang et al. (2020)<sup>179</sup> where PFBA was only reduced 40%, HFPO-DA was reduced 70%, while

PFHxA, PFHpA, PFOA, PFNA, PFDA, PFBS, PFHxS, and PFOS were reduced more than 95% in 48 hours from initial concentrations of 1 µg PFAS/L. Short- and ultrashort-chain PFAS remain the most challenging PFAS for uptake by β-CDP-based adsorbents.<sup>139,177,179,193</sup> Reduced uptake for (ultra)short-chain PFAS by β-CDPs remains the most significant challenge for their implementation, and is caused by intra-PFAS competition for sorption sites,<sup>48,177</sup> and the relatively weak affinities of (ultra)short-chain PFAS for β-CD relative to more hydrophobic PFAS (**Figure 2.4**).<sup>194</sup>

In a similar manner as 1240+ GAC, DEXSORB® exhibited an S-type isotherm, where the sorption capacity in the 2 mg PFAS/L batch test increased by 21% (to 59.8 µg PFAS/mg) from a previous sorption plateau of 48.6 µg PFAS/mg (**Figure 2.1**). The exceedingly high PFAS loading in the 2 mg/L UP water batch test likely forced hemicelle or a multi-layer PFAS sorption effect onto the DEXSORB® polymer.<sup>190</sup> Karoyo and Wilson (2017) confirmed that PFOS and PFOA will aggregate in hemicelles and exhibit self-assembly into multiple adsorptive layers at the interface of the β-CD-incorporated polymers when exposed to high aqueous PFAS concentrations.<sup>190</sup> Notably, the other PFAS-selective commercial media, PSR2+ IX and the SMC, also displayed S-type sorption envelopes of the 18-PFAS mix, in that at greater aqueous PFAS loadings these media exhibited greater adsorption capacities for certain longer-chain PFAS, particularly for PFSAAs (see individual isotherm plots in SI). In a review of peer-reviewed studies focusing on the remediation of PFAS via separation mechanisms, Abbasian and Foudazi (2022) highlighted that micelle and hemicelle formation are significant removal mechanisms for hydrophobic PFAS by GACs, IX resins, and polymeric adsorbents at sufficiently high concentrations, implying that PFAS-PFAS interactions are the likely mechanism controlling the S-type isotherm profile displayed by DEXSORB®.<sup>102</sup>

The hypothesized key mechanistic role host-guest complexation with the  $\beta$ -CD cavity<sup>135,137,146,175,177,194,195</sup> is not supported by the results of the UP isotherm tests conducted for the 18-PFAS mix, as is implied by the “S-shaped” isotherm profile. The sorption isotherm envelope for DEXSORB® for the entire 18-PFAS mix exhibited a better fit to the non-linear Langmuir isotherm model ( $r^2 = 0.980$ ), relative to the Freundlich model ( $r^2 = 0.910$ ), suggesting single-layer adsorption to homogeneous adsorption sites was a dominant removal mechanism,<sup>53,105,117</sup> which could arise as a result of host-guest complexation. Indeed, Wang et al. (2017) reported that a  $\beta$ -CDP crosslinked with 4,4'-difluorodiphenylsulfone (DFPS) rapidly removed >99 % of diverse organic micropollutants (e.g., BPA, 2-naphthol, 2,4-DCP, propranolol) from water through monolayer chemisorption consistent with the Langmuir model and pseudo-second-order kinetics. This and other studies reporting on the development of  $\beta$ -CDPs for PFAS treatment demonstrate that the  $\beta$ -cyclodextrin monomer alone is ineffective for PFAS removal, but incorporation of fluorinated crosslinkers or cationic groups significantly improved the rapid, selective PFAS removal even in moderately complex matrices. Therefore, alternative mechanisms to host-guest complexation with the  $\beta$ -CD monomer cannot be ruled out as the dominant PFAS removal mechanisms for DEXSORB. Evidence from atomistic molecular dynamics simulations published by Choudhary et al (2022) suggest that synergistic effects between (1) PFOA attraction to the modeled decafluorobiphenyl (DFB) polymer cross-linkers and (2) strong electrostatic interactions between polar segments in the model  $\beta$ -CD-based polymer network and the headgroup of the PFOA anion create more energetically favorable interactions, than the formation of PFOA- $\beta$ -CD host-guest complexes.<sup>196</sup> Their modeled results are corroborated by Ching et al. (2022)<sup>197</sup> who evaluated 34  $\beta$ -CDPs synthesized with 14 different crosslinkers. The evaluation determined that  $\beta$ -CDPs consisting of TFN-CDP and amine- or amide-containing crosslinkers demonstrated the

greatest adsorption affinity and most rapid adsorption kinetics for removal of PFOS, PFHxS, PFBS, PFOA, PFHxA, and PFBA from ultrapure water with respect to the other crosslinkers investigated. The continued development of modified  $\beta$ -CDP highlights that the  $\beta$ -CD monomers alone do not provide sufficient PFSA treatment, and that  $\beta$ -CDP surface charge, porosity, surface area, cross-linker content, and cross-linker hydrophobicity are the most significant parameters governing PFAS sorption to  $\beta$ -CDPs.<sup>197</sup>

#### 2.3.1.3. *Non-PFAS-selective IX resin has highest PFAS adsorption capacity*

The non-PFAS-selective IRA910 IX had by far the greatest adsorption capacity of any of the sorbents when considering the total adsorption of the entire 18-PFAS mix in the UP water isotherm tests, eclipsing the maximum adsorption capacities of the PFA694 IX, GACs, and DEXSORB® by at least a factor of 2.8. The maximum achieved adsorption capacity for the IRA910 IX resin was 321.7  $\mu\text{g PFAS/mg sorbent}$ , compared to 115.3  $\mu\text{g PFAS/mg sorbent}$  for the F400 GAC, 87.1  $\mu\text{g PFAS/mg sorbent}$  for the PFA694 IX resin, and 18.0  $\mu\text{g PFAS/mg sorbent}$  for the PSR2+ IX resin. The isotherm envelope for IRA910 IX demonstrates similarly good fits to both the non-linear Langmuir ( $r^2 = 0.923$ ) and non-linear Freundlich ( $r^2 = 0.900$ ) isotherm models, suggesting the involvement of electrostatic as well as hydrophobic mechanisms of PFAS removal.<sup>53,90,117</sup> A slightly better fit to the non-linear Langmuir model suggests single-layer adsorption to homogeneous adsorption sites as the dominant removal mechanism, consistent with manufacturer-reported chloride exchange capacities and the fundamental operational principles of IX resins (i.e. 1:1 replacement of target ions with counter-ions onto homogenous functional groups); however, the simultaneously good fit to the Freundlich isotherm model also suggests adsorption via multiple interaction mechanisms to the resin surface.<sup>53,117,122</sup> In literature reviews focusing on PFAS removal by IX resins conducted by Dixit et al. (2021)<sup>91</sup>, Boyer et al.(2021)<sup>122</sup>,

and Zhang et al. (2019)<sup>90</sup> each validate that intra-PFAS competition for adsorption sites, electrostatic interactions, hydrophobic interactions, and hemicelle formation are all interacting components governing PFAS removal by IX resins, which can result in either antagonistic or synergistic interferences depending on matrix and target PFAS characteristics. To more accurately encapsulate the combined mechanisms involved in the treatment of PFAS by IX resins, Freundlich isotherms often successfully model the observed experimental sorption data.<sup>90,122</sup>

When exposed to artificially high aqueous PFAS concentrations, the PFAS-selective IX resins exhibit (1) substantially reduced adsorption capacities relative to the non-selective IX resin, and (2) poor fits to either the Langmuir or Freundlich adsorption models (**Figure 2.1 and Figures S.16A-C**). Both of the evaluated PFAS-selective IX resins demonstrated high capacities (comparable to that of IRA910 IX) to remove the 18-PFAS mix to low residual aqueous concentrations in the UP water batch tests with relatively low initial aqueous concentrations of PFAS. However, for the PFAS-selective IX resins, the total PFAS isotherms in **Figure 2.1**, as well as the multi-component and individual PFAS isotherms in the SI, reveal that after an apparent point of maximum adsorption capacity with resulting low residual aqueous PFAS concentrations, the adsorption capacities decrease by an average of approximately 47% between their maximum achieved adsorption capacity and the adsorption capacity achieved in the 2 mg PFAS/L nominal initial concentrations batch tests. The adsorption capacity of PFA694 IX for the 18-PFAS mix shows a 48% reduction from a maximum of 87.1  $\mu\text{g PFAS/mg}$  sorbed to 45.2  $\mu\text{g PFAS/mg}$  after equilibration in the batch test with a nominal initial concentration of 2 mg PFAS/L. Similarly, PSR2+ IX resin has a maximum adsorption capacity of 18.0  $\mu\text{g/mg}$  in the 110  $\mu\text{g PFAS/L}$  nominal initial concentration batch test, but only a capacity of 8.0  $\mu\text{g PFAS/mg}$  after equilibration in the batch test with a nominal initial concentration of 2 mg PFAS/L (~45% reduction). The isotherms

generated by the PFAS-selective IX resins demonstrate their initially high adsorption capacities to achieve low residual aqueous PFAS concentrations resulting in an initial linear portion of the isotherm with a near infinite slope are classified as “H-type” isotherms, implying exceptionally high sorbate affinity for the sorbent.<sup>188,189,198,199</sup> H-type isotherms characterize the PFAS-selective IX resin isotherm profiles and corroborate their reported high-affinity for PFAS; yet, their diminished capacity beyond a certain threshold of aqueous PFAS loading distinguishes their performance significantly from that of the non-selective IRA910 IX resin, as well as the other traditional and novel adsorbents evaluated.

Significantly, IRA910 IX resin exhibited the least adsorption of the three smallest PFCAs and the smallest PFSA, suggesting a slight discernible preference for long-chain PFAS as a result of greater hydrophobic interactions—further validating that not only electrostatic interactions control PFAS removal via IX resin. In the UP water batch tests with 10 µg/L and 200 µg/L nominal initial PFAS concentrations, IRA910 IX demonstrated greater than 90% removal for the entire suite of PFAS, with the exception of TFMS (82%) in the 200 µg/L batch test (**Figure 2.4**). In the 2 mg/L UP batch test, IRA910 IX removed all of the PFAS in excess of 80%, with the exception of short-chain PFBA and ultrashort-chain PFPrA and TFA. The IRA910 IX resin has elsewhere demonstrated high adsorption capacities for long- and short-chain PFAS as a result of favorable electrostatic interactions, while PFAS hydrophobicity and resin porosity have been shown to be important factors contributing to the efficacy of IRA910 IX for PFAS removal from aqueous matrices.<sup>76,112,120,200</sup> The exceptionally high removal percentages achieved by IRA910 IX for all but the shortest PFCAs are in alignment with previously reported batch tests conducted by Liu and Sun (2021), where IRA910 IX, removed greater than 90% of all short- and long-chain PFAAs included in the study with 0.6 µg/L initial PFAS concentrations (C4 PFBS—C8 PFOS and C3

PFBA—C7 PFOA).<sup>112</sup> These authors report a maximum adsorption capacity of greater than 1,400 mg/g for PFOA and PFOS, >360 mg/g for PFBA and >1,000 mg/g for PFBS – which exceed the maximum reported adsorption capacities for F400 GAC by up to a factor of 5.<sup>76,92,122</sup> Although electrostatic interactions and ion exchange were important mechanisms for PFAS removal, Liu and Sun concluded that the relative mesoporosity of IRA910 IX was favorable for the diffusion and adsorption of PFAS and the formation of hemicelles or PFAS aggregations on the resin surface, resulting in its high adsorption capacity, particularly for long-chain PFAS.<sup>112</sup>

Although hemicelle and micelle formation is not expected to be a relevant mechanism in the removal of PFAS treating realistic concentrations in the context of municipal wastewater treatment, they are a possible mechanism to explain the results of the UP water matrix batch tests where the total PFAS concentration exceeded 36 mg PFAS/L. Artificially high PFAS concentrations can induce hemicelle formation at interfaces at 0.1-1% of the compound's critical micelle concentrations (CMCs), which for PFOS and PFOA the reported values are 4,573 and 15,696 mg/L.<sup>90,187,201–205</sup> Maimaiti et al. (2018) cited the formation of hemicelles as the mechanism leading to the increased adsorption capacity of IX resins at high initial aqueous concentrations of PFOS.<sup>120</sup> In addition, Deng et al. (2010) reported that the ratio of PFOS sorbed to chloride released via ion exchange was greater than 1.0 at high PFAS loadings indicating that hemicelle formation in the inner pore spaces of IX resins contributed to the high adsorption capacities of long-chain PFAS to IX resins in systems that exceeded environmentally relevant concentrations by many orders of magnitude.<sup>119</sup> High initial PFAS concentrations were used in this study to determine the maximum sorption capacity of each sorbent despite exceedance of environmentally relevant PFAS concentrations, although influent PFAS concentrations used in the RSSCTs more closely resemble realistic concentrations reflecting a heavily contaminated groundwater impacted by release of

AFFF, which can contain mixtures of PFAS with concentrations in the range of 10—50 µg PFAS/L.<sup>50,206</sup>

The large adsorption capacity of the non-selective IRA910 IX resin in the UP water matrix in comparison with the PFAS-selective IX resins can be explained by their fundamentally different structures. IRA910 IX resin is classified as macroporous, while the PFAS-selective IX resins are both classified as microporous (aka gel-like). Similar to the distinction between macroporous/mesoporous versus microporous GAC – the macroporous structure of non-selective IRA910 IX can accommodate the accumulation of a much greater mass of PFAS through multi-layer adsorption and/or aggregations of PFAS hemicelles to the resin surface.<sup>90,92,120,122,187,207</sup> In the UP water matrix batch tests with exceedingly high initial concentrations of the 18-PFAS mix, the IRA910 IX resin better accommodated multi-layer adsorption and hemicelle formation, thus achieving significantly greater total adsorption capacities compared to PFA694 or PSR2+ IX resins.<sup>90,92,120,122,187</sup> The fundamental macroporous structure of IRA910 IX is likely a key component in its design purpose as a general purpose industrial de-mineralization IX resin, while another contributing factor to the greater PFAS adsorption capacity of the non-selective IX resin is potentially due to its inherently smaller dimehtylethanolammonium functional groups.<sup>120,172,173,208</sup> The small (relative to the tri-n-butyl ammonium functional groups of PSR2+ IX), hydrophilic (alcohol-based) functional groups on the IRA910 IX are potentially favorable for reducing pore blockages allowing for greater and quicker access to interior pore spaces for the (ultra)short-chain PFAS, particularly in the UP matrix batch tests.<sup>90,122</sup>

The contrasting results between the non-selective IRA910 IX resin and PFAS-selective IX resins can be further explained by a similar phenomenon contributing to pore blockages on the microporous (or gel-like) PFAS-selective IX resins. The microporous structures of the PFAS-

selective IX resins likely limited the overall access to binding sites for the 18-PFAS mix, leading to the nearly halved total adsorption capacities in the 2 mg/L nominal initial concentration UP water batch tests compared to their maximum achieved adsorption capacities in batch tests with lower initial PFAS concentrations.<sup>90,209</sup> Preferential adsorption of long-chain PFAS, particularly PFSAs, to the PFAS-selective IX resins contributed to pore blockages and reduced adsorption capacities for each of the long-, short-, and ultrashort-chain PFCAs (**Figure S.16-S.17**). Each of the IX resins evaluated demonstrated a similar surface zeta potential across a broad range of pHs (**Figure S.1**), and had similar manufacturer-reported chloride ion exchange capacities, thus differences in electrostatic interaction or total anion exchange capacity are not likely to account for the differences in PFAS adsorption capacities of the different resin types. In contrast to the effects exhibited by the macroporous IX resin, the formation of hemicelles or aggregation of long-chain PFAS (particularly PFSAs) on the surface of the microporous PFAS-selective IX resins contributed to pore blockage and reduced access to PFAS binding sites via diffusion within the inner pore spaces of the PFAS-selective, microporous resins, and reduced the overall PFAS adsorption capacity at high aqueous PFAS loadings.<sup>56,91,103,105,120,187</sup>

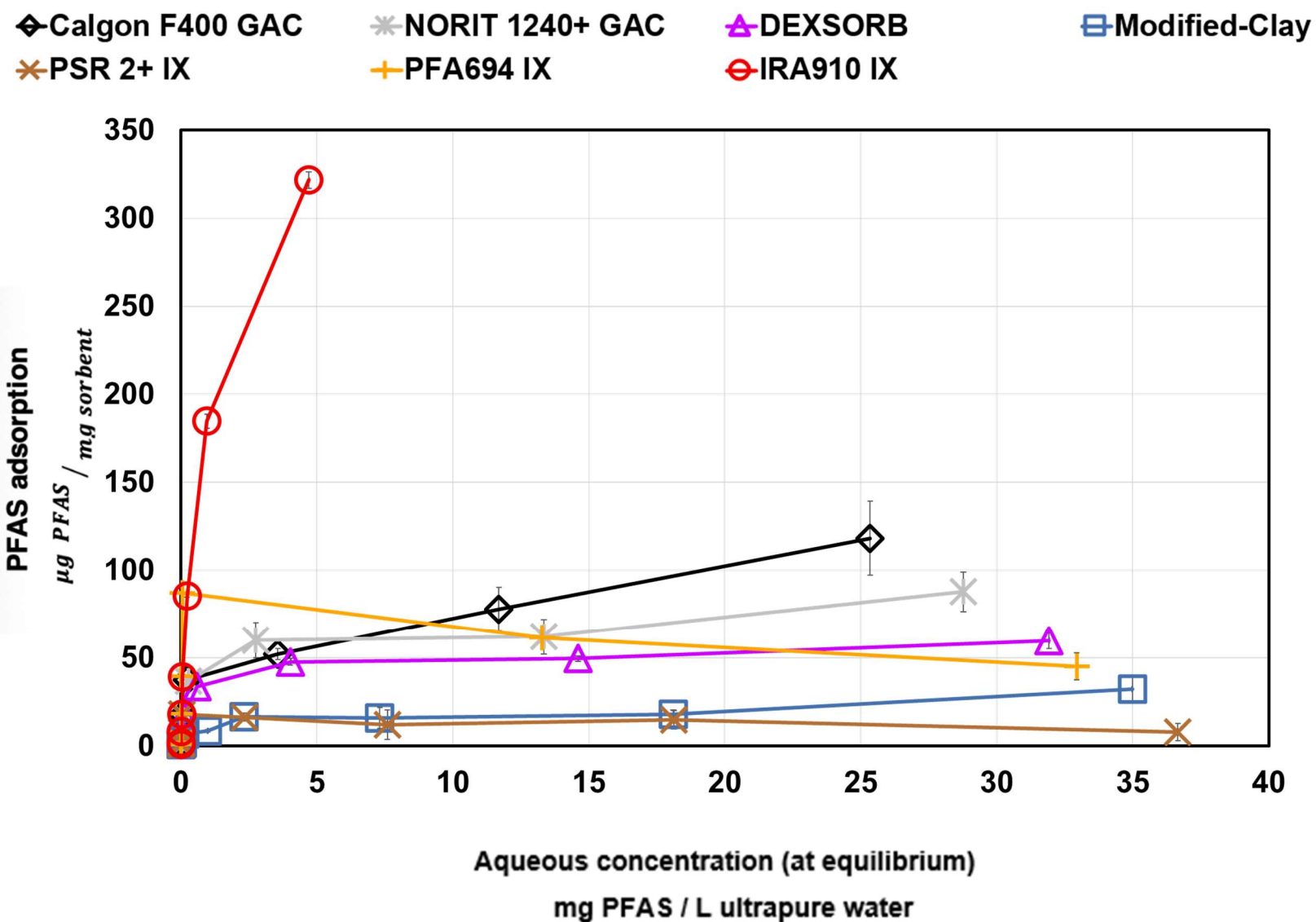


**Figure 2.1** – Total PFAS Adsorption Isotherms in the ultrapure water matrix. The sum of all 18-PFAS total adsorption capacities for each of the seven commercial sorbents analyzed in this study.

Experimental Conditions: Ultrapure water, 18-PFAS mixed system (**Table S.1**), 100 mg/L (5mg) as-received sorbent dose in 50 mL Polypropylene test tube. Equilibration time: 4 days (96 hours), while rotating at 40 rpm, room temperature.

### 2.3.2. *Intra-PFAS competition in an ultrapure matrix: long-chain PFAS outcompete (ultra)short-chain PFAS*

Competitive interferences between the long-, short-, and ultrashort-chain PFAS occurred for each of the sorbent media evaluated, where the longer-chain PFAS tend to show higher maximum adsorption capacities than any of the other compounds, inhibiting sorption of shorter-chain PFAS—even causing the desorption of (ultra)short-chain PFAS. The multi-component isotherms for each of the seven sorbents shown in the **Figures S.11A-S.17A** present a more detailed visualization of the distribution of the PFAS mass sorbed for the 18-PFAS mix in the UP water batch isotherm tests. **Figure 2.2** displays the cumulative percentage of PFAS mass sorbed to each media considering groupings by PFAS chain-length classification and functional group for each UP water batch test from the isotherm experiments with increasing nominal initial PFAS concentrations. Importantly, it is crucial to recognize that when evaluating the plots in **Figure 2.2**, the relevant quantities to track are the change in the proportions of each sub-group adsorbed as the PFAS loading is increased.

Considering F400 GAC in **Figure 2.2**, as the initial PFAS aqueous concentrations increased in subsequent batch tests, there was a marked decrease in total PFAS removal percentage in the 500 µg PFAS/L batch test, and the effects of competitive adsorption were apparent. For instance, in the relatively low nominal initial PFAS concentration batch tests (i.e. up to 225 µg PFAS/L), F400 GAC achieved greater than 95% removal for the entire 18-PFAS mix; while there was virtually no change in the relative proportions of ultrashort-chain PFCAs to short-chain PFSAs sorbed. Between the 500 µg PFAS/L and 1 mg PFAS/L nominal initial concentration batch tests, there was a smaller percentage of (ultra)short-chain PFAS sorbed to F400 GAC in favor of long-chain PFSAs, and to a lesser extent, long-chain PFCAs and short-chain PFSAs. Overall, F400

GAC demonstrated a preference for removal of the long-chain PFASs and the longer-chain PFCAs, achieving nearly complete removal of long- and short-chain PFCAs along with the full spectrum of PFASs in the 10 µg/L and 200 µg/L UP water batch tests, while achieving only approximately 80% removal of ultrashort-chain TFA and PFPrA (**Figure 2.4**). In batch tests with the greatest initial aqueous PFAS concentrations (2 mg/L each PFAS), F400 GAC demonstrated a preference for removal of the long-chain PFAAs, simultaneously demonstrating less than 20% removal of short-chain PFPeA, PFBA, and PFBS, and ultrashort-chain PFPrA, TFA, PFPrS, PFEtS, and TFMS, corroborating the preference of GAC to sorb long-chain PFAS.<sup>53,76</sup> Zhang, et al. demonstrated that the effect of preferential sorption versus desorption of certain PFAS to GACs and IX resins arises due rapid initial adsorption of more hydrophilic (ultra)short-chain PFAS to outer sorption sites or via faster diffusion into internal pore area before subsequent competitive displacement by long-chain PFAS, particularly PFSAs.<sup>98,105</sup> The progression of (ultra)short-chain PFAS sorption to the media followed by displacement by longer-chain PFAS, and the preferential displacement of PFCAs by PFSAs are reflected in the adsorption kinetics data in the SI, while the increasing proportions of long-chain PFAS sorbing to GAC in each subsequent batch test (**Figure 2.2**) highlight the strong affinity of GAC to sorb long-chain PFAS relative to (ultra)short-chain homologues.

Compared with F400 GAC, DEXSORB® exhibited a similar, yet more pronounced, preference for PFSAs over PFCAs, as well as a preference for long- and short-chain PFAS over ultrashort-chain PFAS. Suppression of the individual adsorption isotherms of the (ultra)short-chain PFAS for each of the evaluated media was attributed to competitive displacement by PFSAs of PFCAs, and by long-chain PFAS displacement of (ultra)short-chain PFAS. (**Figures S.11—S.17**). Our finding that DEXSORB® and the other media evaluated all show preferential removal of

longer-chain PFAS and PFAS with sulfonic acid head groups is consistent with previous findings that suggest that GACs, IX resins, and alternative adsorbents all demonstrate greater treatment efficacy for PFASs over PFCAs and long-chain PFAS over (ultra)short-chain PFAS.<sup>49,53,76,81</sup> Similar results between F400 GAC and DEXSORB® are validated by the commonly reported result of greater adsorption and uptake of PFASs relative to PFCAs due to greater electrostatic effect and larger size of the sulfonic acid functional group which contributes to the tendency for PFASs to be more hydrophobic than corresponding PFCAs.<sup>93,95</sup>

Amongst the four adsorbents evaluated, each exhibit preferences similar to F400 GAC for the uptake of long-chain PFASs over other PFAS through the process of competitive displacement; however, even at concentrations where the PFAS-selective and non-selective IX resins begin to experience reduced removal percentages, there is a more balanced distribution of different PFAS chain-lengths sorbed to any of the IX resins compared to the GACs and alternative adsorbents. For instance, considering PFA694 IX in **Figure 2.2**, the average percentage of long-chain PFCA mass sorbed is consistently between 6.5 – 10.7%, until the 2 mg PFAS/L UP batch test where the fraction of long-chain PFCA mass sorbed decreases to 3.4%. Similar trends for PFA694 IX resin are observed when considering the (ultra)short-chain PFCAs, and ultrashort-chain PFASs; whereas the opposite trend is observed for the long-chain PFASs. Initially, long-chain PFASs sorbed to PFA694 IX constituted approximately 11% of the total PFAS mass sorbed; yet by the 2 mg PFAS/L nominal initial concentration batch test, the percentage of PFAS mass sorbed contributed by the long-chain PFASs increased to 37%. Meanwhile, the percentage of short-chain PFSA mass sorbed by PFA694 IX is relatively consistent across all initial concentration ranges (between 24.2% and 27.4%). The IX resins demonstrated chain-length dependent sorption that was significantly less pronounced than the strong preferential adsorption of longer-chain PFAS and PFASs to the GACs,

DEXSORB, or SMC, thus highlighting the unique role of electrostatic interactions as a PFAS removal mechanism for IX resins.<sup>90,91,94</sup> Results reported here are in agreement with consistently observed trends regarding PFAA removal by IX resin, that IX resins exhibit greater removal efficiency of PFASs over PFCAs and their greater uptake with increasing PFAA chain-length, specifically del Moral et al. (2020) demonstrated that PS IX resins exhibit greater removal of C8 PFAS than C4 PFAS.<sup>60,113,126</sup>

The IX resins exhibit greater maximum achieved adsorption capacities for long-chain PFAS, similar to the GACs, DEXSORB® and SMC – while demonstrating more comparable maximum achieved adsorption capacities for the (ultra)short-chain PFAS, suggesting less chain-length dependent sorption on IX resin media. To compare the relative affinities between the suite of PFAS evaluated and the four selected sorbent media, we compare the maximum achieved adsorption capacity ( $q_{max}$ ) for each of the eight UP water batch tests with increasing initial nominal concentrations of the 18-PFAS mix to the molecular weight (MW) of each PFAS analyte (**Figure 2.3**). Note that comparing the Freundlich or Langmuir model fits were inadequate to describe the observed phenomena regarding competitive adsorption and desorption of the (ultra)short-chain PFAS. The GAC and alternative adsorbents each show a strong exponential increase in maximum achieved adsorption capacity as the MW of the PFAS homologue increases, suggesting hydrophobic interactions as the primary mechanism governing PFAS uptake for those media. Conversely, **Figure 2.3** (also **Figure S.5C**) reveals that both the PFAS-selective and non-selective IX resins have relatively consistent sorption affinity across the spectrum of PFAS chain-lengths, suggesting that MW (a proxy for hydrophobicity) is less of a factor for the sorption of PFAS to the IX resins, than it is for GAC, DEXSORB, or SMC; and that electrostatic interactions are the primary driving mechanism governing PFAS adsorption to those media. Hydrophobic interactions

are evidently still an important mechanism for the sorption of the longest-chain PFAS to the IX resins, as shown by the greater maximum adsorption capacities achieved for the long-chain PFASs and PFCAs by all three of the evaluated IX resins.

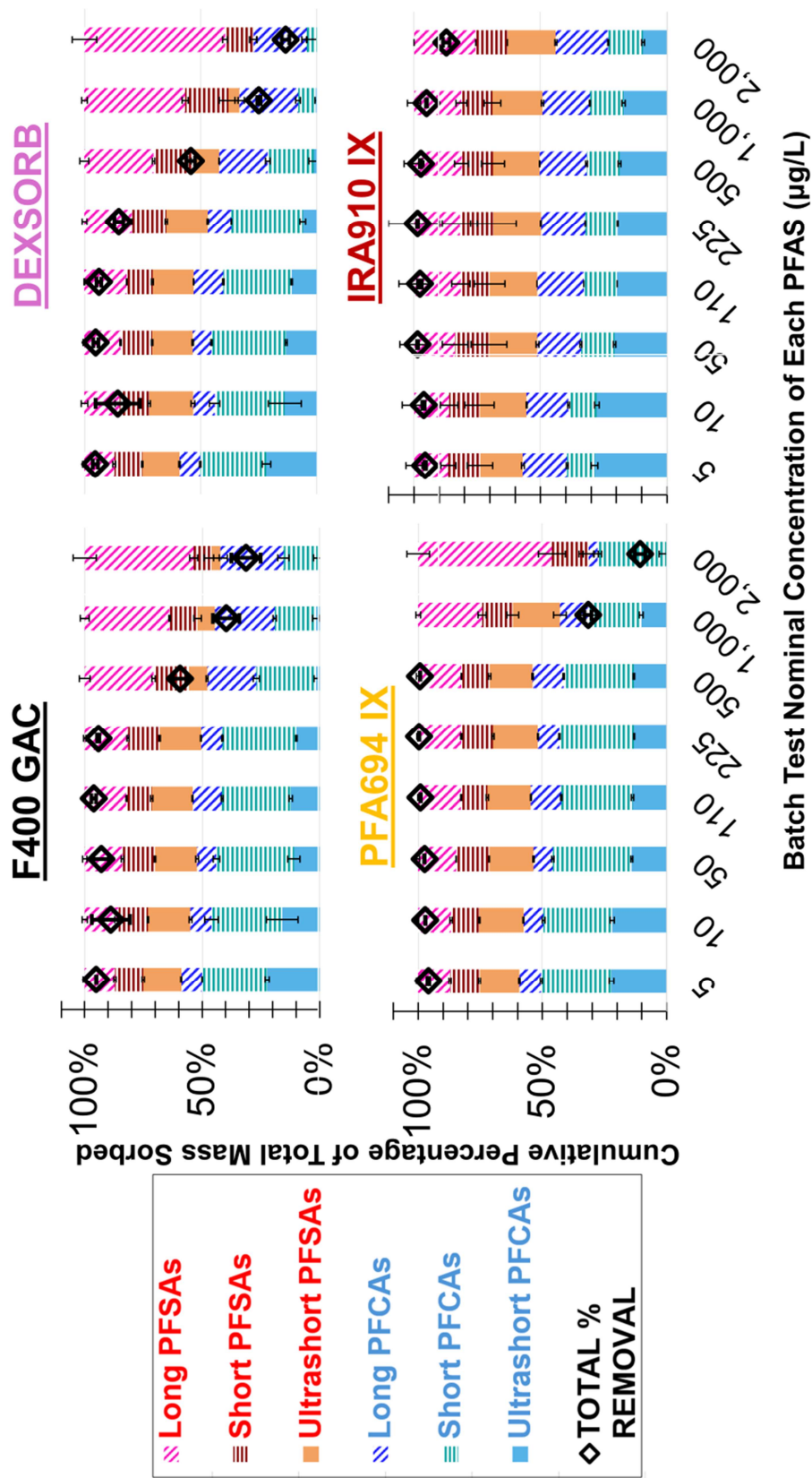


**Figure 2.2** Cumulative percentage of the total PFAS mass adsorbed for the eight nominal initial PFAS concentrations evaluated in the ultrapure water isotherms for the 18-PFAS mix. Plots for remaining media (Norit 1240+ GAC, SMC, and PSR2+) IX are provided in the SI **Figure S.19**

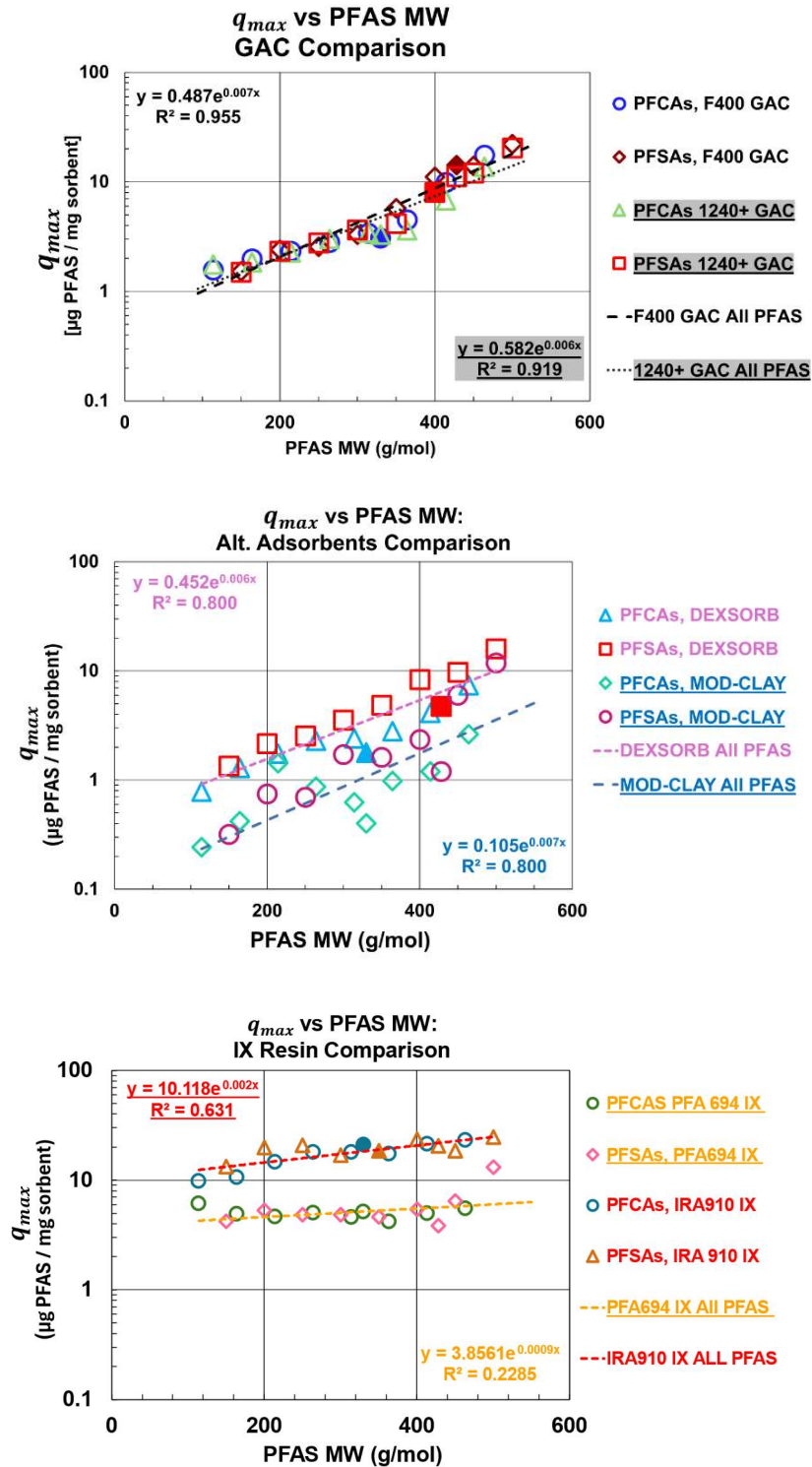


**Figure 2.3.** Maximum achieved adsorption capacity ( $q_{max}$ ) for the UP water matrix adsorption capacity batch tests in the 18-PFAS mixed system. Comparisons between the two evaluated GACs (top); SMC vs DEXSORB® (middle); and non-selective IRA910 IX vs PFAS-selective PFA694 IX (bottom). Solid symbols represent HFPO-DA and 6:2-FTS, respectively. Exponential equation regressions shown with corresponding correlation coefficient for each of the sorbent media.

### *2.3.3. Fast sorption of (Ultra)short-chain PFAS, suppressed and displaced by longer-chain PFAS in ultrapure matrix via intra-PFAS competition*

In the UP water adsorption kinetics tests, preferential adsorption of longer-chain PFAS combined with inhibited sorption and competitive displacement of (ultra)short-chain PFAS was apparent for DEXSORB®, GAC, and the SMC, while intra-PFAS competitive interferences did not clearly manifest for the IX resins due to greater overall sorption capacities for the 18-PFAS mix (**Figures 2.5.1 and 2.5.2**). Intra-PFAS competition for sorption sites is dependent on properties of the particular PFAS, sorbent media, and matrix characteristics. Short- and ultrashort-chain PFAS will tend to diffuse quickly, and can more quickly access the internal pore spaces to initially sorb primarily to accessible electrostatically-favorable sites, but may be displaced by more slowly diffusing, yet more preferentially sorbed, hydrophobic long-chain PFAS.<sup>53,98</sup> Each of the media demonstrated more rapid PSO initial adsorption velocities for (ultra)short-chain PFAS relative to longer-chain homologues (**Figures S.6C – S.10C**), while the longer-chain PFAS were adsorbed to DEXSORB® and GAC (and SMC) to a greater extent in the kinetics tests, supporting the theorized sorption kinetics progression for those media.

Suppression of adsorption capacities and competitive displacement due to intra-PFAS competition in the kinetics tests was most pronounced for the shortest PFAS on the GAC and DEXSORB® media. The F400 GAC UP water multi-component kinetic profiles (**Figure 2.5.1 - A**) exhibit de-sorption of PFPrA between 24 and 96 hours, and suppression of the equilibrium adsorptive capacities of the ultrashort-chain PFAAs, PFBA, and PFPeA. DEXSORB® exhibits de-sorption of TFA, PFPrA, and TFMS between 6 and 24 hours, and suppressed sorption of PFBA, PFPeA, and HFPO-DA. The preferential sorption of PFSA and longer-chain PFAS displayed by

F400 GAC and DEXSORB® which resulted in displacement and reduced adsorption capacities for the (ultra)short-chain PFAS is also an observed effect for the IX resins in the UP isotherm batch tests (**Figure 2.2, Figure S.11, S.13**). The IX resins exhibited lower equilibrium adsorption capacities in the isotherm tests, and more rapid PSO initial adsorption velocities for (ultra)short-chain PFAS relative to long-chain PFAS (**Figures S.8C and S.9C**), supporting the hypothesized mechanistic kinetic progression of PFAS removal. Regardless of the sorbent type, shorter, more hydrophilic PFAS diffuse more quickly and weakly sorb primarily onto electrostatically favorable sorption sites; they are likely to experience inhibited sorption and competitive displacement by longer, more hydrophobic PFAS as available sorption sites on the media become exhausted.

Each of the five media evaluated provided better fits to the non-linear PSO kinetic model as is commonly reported for GAC, IX resin, and alternative media adsorptive processes, although PFO models also commonly provide good fits to experimental data.<sup>52,89–91,117,121,122,125,154,192</sup> The non-linear PSO model provided the best fits to the experimental data for all five media considering the entire 18-PFAS mix, thus comparison of PSO model kinetic parameters allowed for direct comparison of kinetics data across the different media types (**Figure 2.5.0**). Only PFA694 IX had a coefficient of determination ( $r^2$ ) which was slightly greater for the non-linear PFO kinetic model fit ( $r^2 = 0.996$ ) compared to the non-linear PSO kinetic model ( $r^2 = 0.994$ ). The PSO parameter  $v_0$ , known as the “initial adsorption velocity,” (units of: [ $\mu\text{g PFAS} / \text{mg sorbent} / \text{hour}$ ]) is derived from the denominator of the first term in the linearized PSO kinetic model (**Section S.6, Eq. 8**). The initial adsorption velocity describes the relative affinity between a sorbent-analyte pair in the early stages of an adsorption process adequately modeled by the PSO kinetics, and is defined in Equation (1):<sup>90,210</sup>

$$v_o = k_2 * q_e^2 \equiv \text{initial adsorption velocity} \left[ \frac{\mu\text{g PFAS}}{\text{mg sorbent} * \text{hour}} \right] \quad (1)$$

Where  $k_2$ , and  $q_e$  are the non-linear PSO model rate constant and equilibrium adsorption capacity. For each of the five adsorbents evaluated for their adsorption kinetics of the 18-PFAS mix in the UP water matrix,  $v_o$  is plotted against the PFAS MW in **Figures S.6C – S.10C**. (**Tables S.9 – S.13** present data regarding the kinetic rate of adsorption in the UP water batch tests, along with the PFO and PSO kinetics model fits for each of the PFAS analytes for the five adsorbent media).

(Ultra)short-chain PFAS demonstrated a tendency for faster PSO initial adsorption velocities for all five of the sorbent media, consistent with previously reported trends. Generally, the non-selective IRA910 IX resin and F400 GAC (“traditional sorbents”) exhibited contrasting trends in terms of the variation of the PSO initial adsorption velocities with increasing PFAS MW. Whereas, the PFAS-selective PFA694 IX resin and DEXSORB® displayed comparable patterns across the spectrum of PFAS chain-lengths. For the non-selective IRA910 IX resin (**Figures S.8C**), comparable PSO initial adsorption velocities across the spectrum of PFAS chain-lengths provided a poor fit to an exponential decay function ( $r^2 = 0.151$ ), indicating consistent sorption affinity for PFAS compounds regardless of chain-length due to domination of electrostatic interactions as the primary PFAS removal mechanism for the non-selective IX resin. Comparatively, F400 GAC (**Figure S.6C**) displays a moderately good fit ( $r^2 = 0.627$ ) to an exponential decay function where for longer-chain PFAS (i.e. those with greater MW)  $v_o$  decreases exponentially with MW, suggesting that slower adsorption of larger PFAS to interior GAC pore sites is driven by slower rates of intra-particle or pore diffusion despite greater overall capacities for longer-chained PFAS.<sup>97,177</sup>

Fundamentally different adsorptive mechanisms likely explain the contrasting trends displayed between the non-selective IRA910 IX resin (**Figure S.8C**) and F400 GAC (**Figure S.6C**), in terms of the degree to which the PSO  $v_0$  varied exponentially with PFAS MW. For the IRA910 IX, the entire suite of 18 PFAS have relatively equal access to abundant sorption sites, as evidenced by the exceptionally high removal percentages achieved by IRA910 IX for both long- and (ultra)short-chain PFAS in the UP water batch test with nominal initial PFAS concentrations of 225 and 500  $\mu\text{g PFAS/L}$  ( $99.7\% \pm .02\%$ , and  $99.3\% \pm .08\%$  removal of entire 18-PFAS mix). Compared to the relative hydrophobicities of the PFAS of varying perfluorinated chain-lengths, the electric charges are less variable across the suite of PFAS. The combination of an abundance of accessible adsorption sites and consistently strong electrostatic attraction imparted by IRA910 IX to the PFAS anions regardless of perfluorinated chain-length resulted in the consistent adsorption velocities across the suite of PFAS chain-lengths demonstrated in **Figure S.8C**, supporting electrostatic interactions as the primary mechanism of adsorption of PFAS to the non-selective IX resin in the UP matrix. On the other hand, for F400 GAC, the PSO initial adsorption velocities have a better fit to an exponential decay function with increasing PFAS MW, suggesting hydrophobic interactions as the main driving adsorption mechanisms. Long-chain PFAS primarily sorbed via hydrophobic interactions initially encounter limited easily and quickly accessible sorption sites on GAC, hindering their PSO initial adsorption velocities due to slower diffusion to potential sorption sites. The contrasting trends between the PSO initial adsorption velocities across the suite of PFAS chain-lengths for the non-selective traditional sorbent media, IRA910 IX and F400 GAC, can be explained by their contrasting primary mechanisms of PFAS removal.

Similar trends displayed between the sorbent media designed and marketed for targeted PFAS removal from aqueous matrices (PFA694 IX and DEXSORB®), regarding their sorption

kinetics of the 18-PFAS mix, can be explained by their similar design considerations combining elements of electrostatic, hydrophobic, and potentially fluorophilic interactions<sup>94</sup>. PFA694 IX ( $r^2 = 0.317$ ) resin and DEXSORB® ( $r^2 = 0.331$  [PFOS excluded]) exhibited improved fits to an exponential decay function relative to IRA910 IX when comparing  $v_0$  as a function of PFAS MW (**Figure S.7C** and **Figure S.9C**). DEXSORB® has demonstrated improved uptake of short-chain PFAS as a result of design modifications made to  $\beta$ -CD-based polymers.<sup>146</sup> Modifications intended to improve the PFAS treatment efficacy of such polymers include imparting positive surface charge and fluorophilic interactions via integration into the polymer matrix of quaternary ammonium functional groups and fluorinated cross-linkers.<sup>94</sup> The attraction for PFAS imparted by the  $\beta$ -CD monomer in combination with the fluorophilic interactions is strongly linked to chain-length, comparable to the correlation between chain-length and hydrophobicity,<sup>94</sup> while PFAS anion attraction with positively quaternary ammonium groups on the DEXSORB® resembles their interactions with the non-selective IX resin. The positive surface charge of DEXSORB® (**Figure S.1**) increases the initial sorption affinity of more hydrophilic PFAS allowing (ultra)short-chain PFAS to more rapidly diffuse to access internal sorption sites on the DEXSORB similar to their behavior on GAC. The combination of electrostatic, hydrophobic and fluorophilic interactions manifest in the PSO sorption velocity trends being intermediate to those of the non-selective IX and the GAC.<sup>53,92,122</sup>

Similar design modifications can be made to IX resins to increase their uptake and selectivity for PFAS. Increasing the size of the IX resin functional groups (i.e. increasing the number of methyl groups on the alkyl chains attached to the cationic group) can increase the adsorption of PFAS by increasing the non-electrostatic interactions of the resin with more hydrophobic PFAS<sup>91,121,122,206,211</sup> Specialized functional groups can be designed to selectively

adsorb short-chain PFAS, as is likely the case for the emergent commercially available PFAS-selective IX resins.<sup>55,93,94,125,128</sup> Lobitz et al. (2025), reported on how a commercial IX resin can be functionalized with novel fluorinated functional groups to enhance the adsorption capacity and kinetics of ultrashort-chain and short-chain PFAS compared to an un-modified resin.<sup>55</sup> Although complete composition information is not available for the proprietary functional groups of the PFA694 IX resin, the similar trends between the adsorption kinetics data across the suite of PFAS chain-lengths for DEXSORB® and PFA694 IX suggest similar combinations of PFAS removal mechanisms for the two media. Obviously, PFA694 IX resin is designed primarily to remove PFAS via ion exchange, though it is likely that it contains large, potentially fluorinated, functional groups attached to the base PS-DVB polymer matrix. The similar PSO initial adsorption velocity trends displayed by the PFA694 IX and DEXSORB® reflect the commonalities between the intentionally designed PFAS-selective media targeting a combination of hydrophobic, electrostatic, and fluorophilic interactions for adequate simultaneous treatment of legacy PFAS and emerging (ultra)short-chain PFAS.<sup>94,103,128</sup>

Notably, DEXSORB® displayed the greatest initial adsorption velocity ( $v_0 = 5.7 \mu\text{g PFAS} / \text{mg sorbent} / \text{hour}$ ) for PFOS (**Table S.10, Figure S.7B**), indicating a particularly high affinity for PFOS in a mixed system with a variety of PFAS of different chain-lengths, and that this strong affinity overcomes potential sorption limitations due to slower pore diffusion of longer-chain PFAS. Additionally, when considering the PSO initial adsorption velocity determined for the entire 18-PFAS mix, DEXSORB® had the greatest initial adsorption velocity ( $v_0 = 20.2 \mu\text{g PFAS} / \text{mg sorbent} / \text{hour}$ ), double that of IRA910 IX ( $10.1 \mu\text{g PFAS} / \text{mg sorbent} / \text{hour}$ ), while F400, and the SMC, demonstrated  $v_0$  parameter values of 9.5, 7.4  $\mu\text{g PFAS} / \text{mg sorbent} / \text{hour}$ . The fast sorption kinetics of DEXSORB® are in agreement with kinetics batch test results reported by Wu

et al. (2020) and Ling et al. (2017) that  $\beta$ -CDP exhibit PFAS sorption kinetics similar to powdered activated carbon (PAC) as a result of the polymer's porosity allowing easy access to adsorption sites.<sup>177,178</sup> Our finding of a relatively high initial adsorption velocity for IR910 IX compared to PFA694 IX, which demonstrated the lowest PSO initial adsorption velocity of 6.6  $\mu\text{g}$  PFAS / mg sorbent / hour, is in agreement with trends that microporous (gel-like) resins exhibit lower initial adsorption rates than macroporous resin.<sup>122</sup>

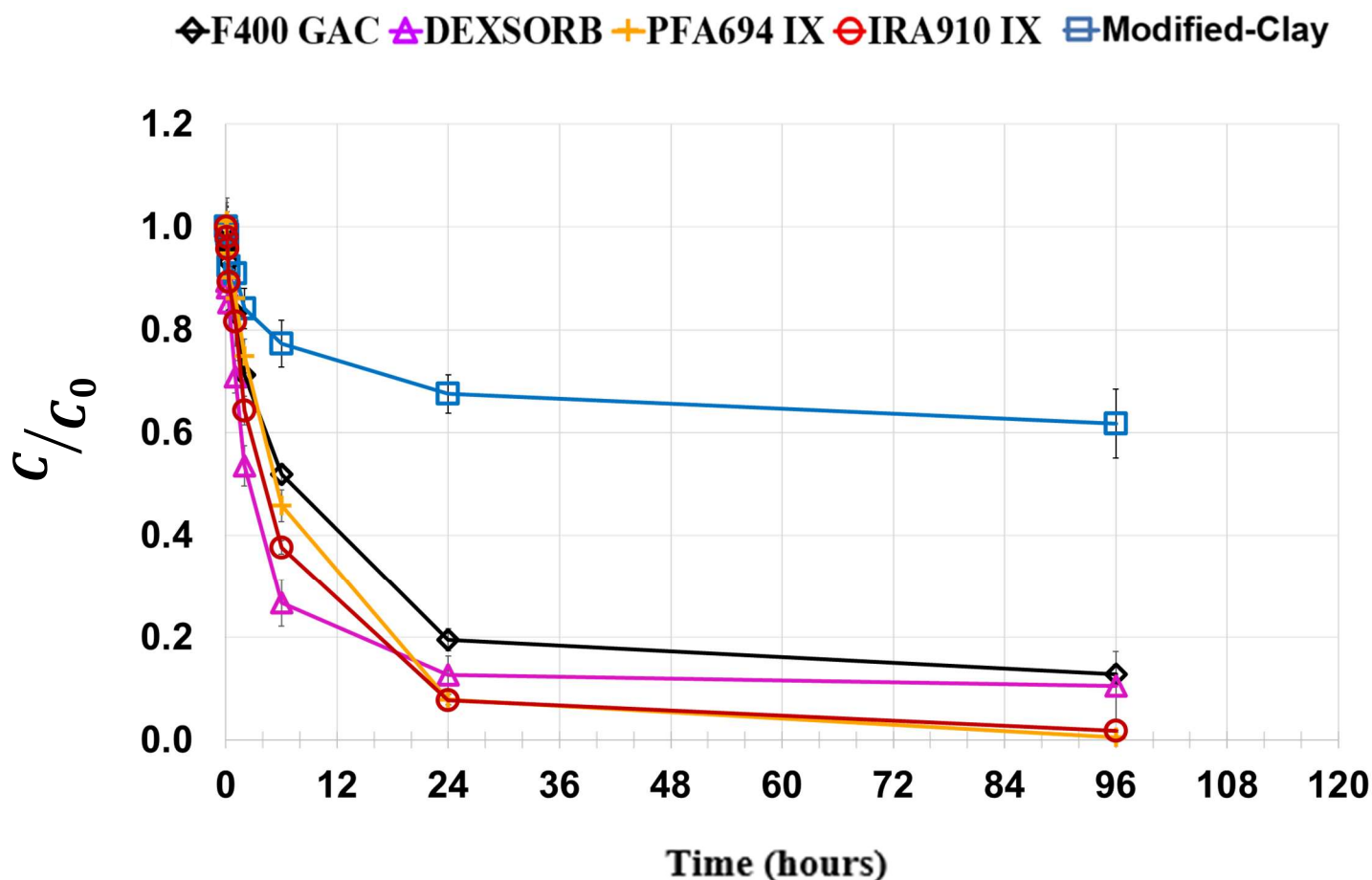


**Figure 2.5.0 Adsorption Kinetics Results** – Sum of all 18-PFAS initial concentration normalized adsorption kinetics for each of the five adsorbent media evaluated in the UP water matrix. Approximately 200  $\mu\text{g}/\text{L}$  (each) PFAS as starting concentration ( $C_0$ ). **Figure 2.5.0** depicts the total PFAS removal kinetics, normalized to the initial PFAS concentration for each of the five adsorbent media evaluated in the UP water matrix.

Experimental Conditions: Ultrapure water, 18-PFAS mixed system (**Table S.1**), 100 mg/L (5mg) as-received sorbent dose in 50 mL polypropylene test tube. Sacrificial data points collected after 1 min, 5 min, 10 min, 20 min, 1 hour, 2 hours, 6 hours, 24 hours, and 96 hours of equilibration, rotated at 40 rpm, room temperature.

◆ PFNA    ▲ PFOA    □ PFHpA    ● PFHxA    ✱ HFPO-DA    ○ PFPeA    ■ PFBA    ▲ PFPrA    ✱ TFA  
 ◆ PFOS    ▲ PFHpS    □ PFHxS    ✱ 6:2-FTS    ○ PFPeS    ○ PFBS    ■ PFPPrS    ▲ PFEtS    ✱ TFMS

$C/C_0$

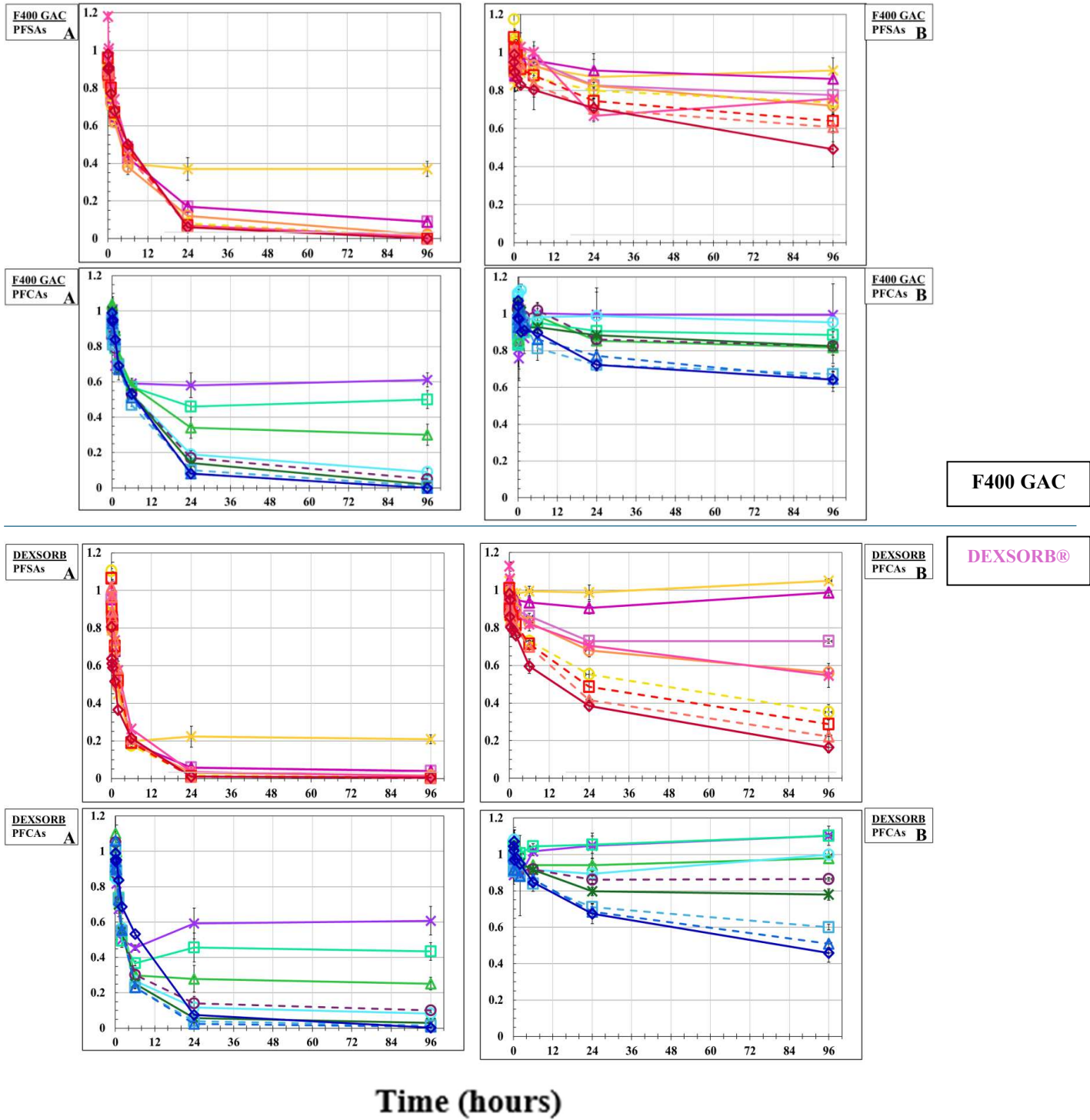
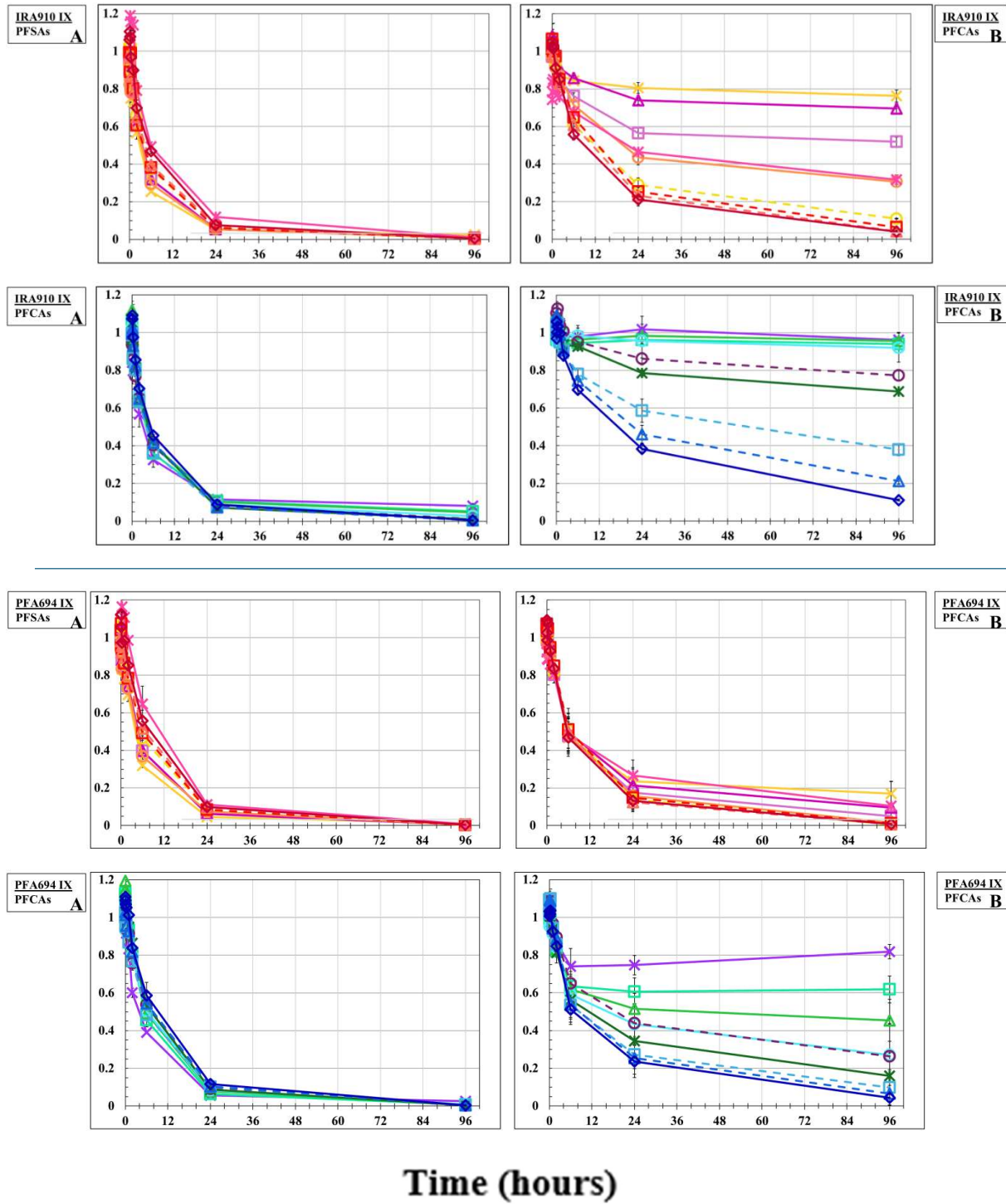


**Figure 2.5.1** Adsorption Kinetics Results - Calgon F400 GAC (above) and DEXSORB® (below). Multi-component normalized adsorption kinetics plots for PFCAs and PFASs comparing the adsorption kinetics for removal of 18-PFAS between ultrapure water matrix (A), and synthetic wastewater matrix (B).

◆-PFNA    ▲-PFOA    □-PFHpA    ●-PFHxA    \*~HFPO-DA    ○-PFPeA    ▣-PFBA    ▲-PFPrA    \*~TFA  
 ◆-PFOS    ▲-PFHpS    □-PFHxS    \*~6:2-FTS    ○-PFPeS    ○-PFBS    □-PFPrS    ▲-PFEtS    \*~TFMS

$C/C_0$



IRA910 IX

PFA694 IX

**Figure 2.5.2 Adsorption Kinetics Results** - non-selective IX IRA910 (above) and PFAS-selective IX PFA694 (below) Multi-component normalized adsorption kinetics plots for PFCAs and PFSAs comparing the adsorption kinetics for removal of 18-PFAS between ultrapure water matrix (A), and synthetic wastewater matrix (B).

#### *2.3.4. Less inhibition by synthetic wastewater matrix on PFAS-selective media sorption capacities, kinetics*

Significantly, results demonstrating the adequacy of PFA694 IX to treat all but the shortest PFCAs to high degree of removal in the synthetic wastewater matrix, offer insight into resolving two of the primary challenges regarding adsorptive PFAS treatment from aqueous matrices: (1) limited removal of PFAS and limited PFAS selectivity due to competitive sorption of other co-contaminants, and (2) low overall effectiveness in the removal of short-chain PFAS.<sup>94</sup> Sorption capacity and kinetics tests conducted in the synthetic wastewater matrix suggest that F400 GAC, IRA910 IX are severely limited in their capacity for PFAS in the SW matrix, DEXSORB® exhibits minor inhibition for sorption of long-chain PFASs in particular, while PFA694 IX demonstrated the least sorption inhibition across the entire suite of PFAS with only reduced performance for the shortest PFCAs in the SW matrix.

In regard to F400 GAC, PFAS removal capacity was dramatically impaired by the SW matrix constituents. F400 GAC achieved average removal percentages below 50% for each of the 18 PFAS in each of the SW matrix batch tests, with the exception of PFOS and PFHpS, which were removed to 65% and 52% from initial concentrations of 20 µg PFAS/L (**Figure 2.4**). In comparison, nearly complete removal was achieved for the long- and short-chain PFCAs and the full spectrum of PFASs in the 10 and 200 µg PFAS/L initial concentration batch tests conducted in UP water. Inhibited uptake by F400 GAC, especially for (ultra)short-chain PFAS, in the synthetic wastewater effluent is consistent with results that GACs are a more suitable treatment for hydrophobic long-chain PFAS, but suffer in their ability to treat short-chain PFAS.<sup>53</sup> Due to its tendency for non-selective adsorption of a variety of contaminants, GAC efficiency for PFAS removal is often limited by the presence of other co-contaminants, which exhausts the adsorptive capacity of the GAC particularly for less hydrophobic (ultra)short-chain PFAS.<sup>94</sup> Inhibited PFAS

removal by F400 GAC in the SW matrix is consistent with results reported by Zhang et al. that the presence of inorganic ions can significantly inhibit the adsorption of short-chain PFAS to GAC by reducing weakly present electrostatic interactions that would be favorable to adsorption in cleaner matrices.<sup>98</sup> As is evident from the low PFAS removal percentages for F400 GAC in each of our SW batch tests, the effect is most pronounced for short-chain PFPeA, PFBA, and PFBS, and all five of the ultrashort-chain PFAAs. Inhibited PFAS removal in the synthetic wastewater effluent for F400 GAC is consistent with results reported by Lenka et al. who observed that GACs suffer in their ability to treat short-chain PFAS especially when co-occurring inorganic ions will compete for limited electrostatically favorable adsorption sites on.<sup>53</sup> Overall, across all three of the SW batch adsorption capacity tests the suppressed removal percentages for the F400 GAC, illustrate the limitations of GAC to treat ultrashort-, short-, and long-chain PFAS as a result of interferences introduced by complex matrices simulating wastewater effluent.

DEXSORB® was inhibited in a similar manner to F400 GAC in the uptake of (ultra)short-chain PFCAs in the SW matrix batch tests; however, the  $\beta$ -CDP-based media demonstrated diminished inhibitory effects for the uptake of PFSAs and long-chain PFCAs in the complex aqueous matrix. In the SW matrix batch test with the lowest nominal initial aqueous PFAS concentrations (20  $\mu\text{g}$  PFAS/L), the removal percentages achieved by DEXSORB® were:

68.6% for PFOA, 16.7% for PFBA, 11.5% for TFA,

96.5% for PFOS, 68.6% for PFBS, and 10.2% for TFMS,

compared to the removal percentages achieved by F400 GAC:

50.1% for PFOA, 17.6% for PFBA, 20.5% for TFA,

63.9% for PFOS, 33.1% for PFBS, 10.8% for TFMS

This trend between the GAC and DEXSORB® observed in the 20 µg PFAS/L SW batch test was also exhibited in the 200 µg PFAS/L SW matrix batch tests (**Figure 2.4**). When tested at 2 mg PFAS/L in the SW matrix, DEXSORB® exhibited only slightly diminished removal percentages for long-chain PFASs, short-chain PFPeA, and long-chain PFOA and PFHpA, while exhibiting greatly reduced removal percentages for all the remaining PFCAs and (ultra)short-chain PFASs compared to its performance in the 2 mg PFAS/L UP batch test. The relatively high and comparable removal percentages in both the SW matrix and UP water batch tests for PFOS, PFHpS, PFHxS, PFPeS, PFNA, and PFOA highlight the preferential removal of long-chain PFAS by DEXSORB® relative to (ultra)short-chain PFAS despite matrix interferences in the form of co-occurring EfOM and inorganic ions. Our finding that DEXSORB experiences limited inhibition in the SW matrix for the uptake of long-chain PFAS suggests that DEXSORB® demonstrates DOM exclusion effects due to the β-cyclodextrin cavity. Lack of inhibition by DOM is consistent with previous results reported by others for β-CDPs,<sup>13,48,135,138,139,146,177,193,212</sup> while the lack of uptake of (ultra)short-chain PFAAs by β-CDPs in the complex water matrix remains an established limitation for their implementation as PFAS treatment. Reduced inhibition of DEXSORB® relative to GAC in the SW tests may be attributable to F-F interaction mechanisms imparted by fluorinated polymer components, which purportedly can improve uptake capacity and kinetics of (ultra)short-chain PFAS in the presence of co-contaminants.<sup>93</sup>

Consistent with the SW batch test results for F400 GAC and DEXSORB®, the non-selective IRA910 IX resin displayed the most sorption inhibition for the (ultra)short-chain PFCAs and the ultrashort-chain PFASs in the SW matrix (**Figure 2.4**). Although IRA910 IX still had the greatest overall PFAS removal efficiency in the 2 mg PFAS/L SW batch test amongst all the evaluated adsorbents, it displayed removal percentages below 40% for PFHxA, HFPO-DA,

PFPeA, PFBA, PFPrA, and TFA across each of the SW batch tests. In comparison, IRA910 IX achieved greater than 80% removal for the entire suite of PFAS in the UP water batch tests (with the exception of short-chain PFBA (71.4%) and ultrashort-chain PFPrA (54.3%), and TFA (12.8%) in the 2 mg PFAS/L UP batch test). Competitive sorption with other co-contaminants can foul IX resins severely impacting their PFAS sorption capacity, and inhibited PFAS uptake due to co-occurring inorganic ions have been previously demonstrated for IRA910 IX by Maimaiti et al.<sup>120</sup> Kothawala et al. (2017) also showed that the 2—8 mg C/L of DOM resulted in approximately 10% reduction in PFAA uptake by polystyrene AER.<sup>58</sup>

Despite exhibiting removal percentages above 80% in each of the SW batch tests for PFOS, PFHpS, PFHxS and PFPeS, the degree of PFAS uptake inhibition caused by the SW matrix exhibited by IRA910 IX was more pronounced than then inhibition exhibited by the PFA694 IX in the 20 µg PFAS/L and 200 µg PFAS/L SW batch tests. Although IRA910 IX resin out-performed PFA694 IX resin for the removal of all PFAS in the 2 mg/L batch tests conducted in both the UP water matrix and SW matrix for all of the PFCAs and PFSAs, such high concentrations of PFAS are not environmentally relevant, suggesting that IRA910 IX may not necessarily be suitable for treating low ng/L concentrations of PFAS in highly complex matrices as would be encountered in municipal wastewater treatment plants.<sup>24,30,56,62,63,65,66,69,70,122</sup> In each of the SW matrix batch tests, IRA910 IX displayed similar percent removals in each of the three tests, with generally decreasing removal percentages for PFAS with shorter perfluorinated chain-lengths, indicating that co-occurring inorganic ions preferentially sorbed to the non-selective IX resin in place of many of (ultra)short-chain PFAS.

The PFAS-selective PFA694 IX demonstrated the least adsorptive capacity reduction across the entire suite of PFAS as a result of the SW matrix in the batch tests conducted with the

most environmentally relevant nominal initial PFAS concentrations (**Figure 2.4**). In the SW matrix batch tests with nominal initial concentrations of 20 and 200 µg PFAS/L, PFA694 IX achieved greater than 80% removal for all of the PFASs, while greater than 70% removal was achieved for all but the shortest PFCAs (PFBA, PFPrA and TFA which were removed at 74%, 48%, and 35%, respectively). The principal finding from the SW batch tests was that near complete removal was achieved by PFA694 IX in the 20 µg PFAS/L SW batch test for PFOA, PFHpA, HFPO-DA, PFOS, PFHpS, PFHxS, 6:2-FTS, PFPeS, and PFBS. Comparatively, for PFA694 IX in the 10 and 200 µg PFAS/L nominal initial concentration batch test conducted in the UP water matrix, greater than 90% removal was achieved for the entire spectrum of PFAS, except for TFA (84% removal in the 200 µg/L nominal initial concentration batch test).

The relatively consistent performance of PFA694 IX for the uptake of all but the ultrashort-chain PFCAs between the batch tests conducted in UP water and the SW matrix suggest that the PFAS-selective IX resin would be most effective in removing environmentally-relevant concentrations of PFAS from municipal wastewater effluents. In the peer-reviewed literature, batch test evaluations of PFA694 IX in complex matrices are lacking, yet one previous study conducted by Wang et al. using ultrapure water batch tests demonstrated that PFA694E IX has a greater capacity for the sorption of the full spectrum of PFASs over (ultra)short-chain PFCAs, and a slightly greater capacity for long-chain PFAS, in general, over (ultra)short-chain PFAS.<sup>48</sup> Additionally, in a pilot system treating landfill leachate, Malovany et al.-reported that the PFAS-selective IX resin showed little removal of DOC, compared to F400 GAC; and 2—10 times longer treatment of PFOS and PFOA by PFA694E IX, indicating minimal sorption inhibition due to dissolved organics for the removal of long-chain PFAS.<sup>107</sup> Consistent with other reports on the performance of the PFAS-selective IX resin in relatively complex matrices, we find that PFA694

IX exhibits very little sorption inhibition for all but the shortest PFCAs (PFBA, PFPrA, and TFA) in the SW matrix with the most realistic PFAS concentrations, suggesting this sorbent media will be most effective at treating the full suite of PFAS in a continuous flow setting treating real wastewaters.<sup>75,107</sup> Kothawala et al. (2017) reported that PFAS uptake on IX resin was independent of DOM content, while GACs are clearly limited for PFAS treatment<sup>58</sup> In each of the SW matrix batch tests, IRA910 IX displayed similar percent removals in each of the three tests, with generally decreasing removal percentages for PFAS with shorter perfluorinated chain-lengths, indicating that co-occurring inorganic ions preferentially sorbed to the non-selective IX resin in place of many of (ultra)short-chain PFAS.

% Removal



**Figure 2.4** compares the results from three of the batch adsorption capacity tests in UP water with nominal initial PFAS concentrations of 10  $\mu\text{g/L}$ , 200  $\mu\text{g/L}$ , and 2  $\text{mg/L}$  (each PFAS) with the three batch adsorption capacity tests conducted in the SW matrix with nominal initial PFAS concentrations of 20  $\mu\text{g/L}$ , 200  $\mu\text{g/L}$ , and 2  $\text{mg/L}$  (each PFAS).

The more complex water matrix inhibited the PFAS adsorption kinetics and adsorption capacities compared to the UP water batch tests across the spectrum of PFAS chain-lengths for each of the evaluated sorbents, especially for PFCAs and (ultra)short-chain PFAS. **Figures 2.5.1 and 2.5.2** illustrate the deleterious effects on the adsorption kinetics imparted by the SW matrix for each of the four adsorbents evaluated. DEXSORB® and PFA694 IX demonstrated the least kinetic rate inhibition in the SW matrix, while the conventional non-selective adsorbents (i.e. F400 GAC and IRA910 IX) demonstrated more pronounced effects of dynamic competitive equilibrium in the SW matrix, in regards to the sorption and de-sorption of shorter-chain compounds as they are displaced from the sorbent by either longer-chain PFAS or EfOM. As discussed in *Section 2.3.2* the competitive displacement of short-chain PFAS on GAC and IX arises due to the slower, yet preferential, sorption of long-chain PFAS.<sup>98</sup> The intra-PFAS competitive effects observed in the UP water batch tests are amplified in the SW matrix kinetics tests, with no PFAS being removed below 40% of the initial aqueous concentration by F400 GAC.

Sorption kinetics can also be reduced due to interferences from complex matrices, while our results indicate the PFAS-selective PFA694 IX and DEXSORB® are generally less impacted by the more complex matrix. Overall, the similar kinetic adsorption rates demonstrated by PFA694 IX between the UP water and SW matrix batch tests, particularly for the PFASs and long-chain PFCAs imply that the PFAS-selective IX resin will be most effective for removing those compounds in the continuous-flow tests treating a complex real wastewater, with the greatest limitations for treating (ultra)short-chain PFCAs. In a review of PFAS removal via IX by Dixit et al. (2021), the authors highlighted that the presence of DOM can decrease PFAS removal efficacy, and that the type and composition of the DOM can influence the degree of inhibition,<sup>91,122</sup> while some IX resins have been shown to be less inhibited by DOM, or effective at simultaneous removal

of DOM and PFAS.<sup>34,91,127</sup> Co-occurring divalent cations (e.g.  $\text{CaCl}_2$ ) can decrease the PFAS adsorption capacity and kinetics for both GAC and IX resin via direct competition, compression of the electrical double-layer surrounding dissolved PFAS ions, and adsorbent surface charge suppression.<sup>53</sup> A primary knowledge gap for PFAS treatment regarding PFAS-selective IX is a lack of understanding of the impacts of dissolved ions, additional contaminants, and wastewater-derived organic matter present in the aqueous matrix,<sup>74,124</sup> thus this evaluation of PFA694 IX in batch and continuous-flow tests in complex matrices for the removal of a wide range of PFAS chain-lengths works to close this gap.

In the SW matrix, F400 GAC exhibited multi-staged sorption-desorption processes for a majority of the PFAS; while, in the UP water kinetics tests, equilibrium was attained relatively rapidly and directly via PSO kinetics processes for the majority of the 18-PFAS mix (excluding PFPrA and TFA) (**Figure 2.5.1**). For example, PFBA was reduced to 86.1% of the initial concentration ( $C_0 = 232.6$ ) after 20 minutes of contact time in the SW matrix, after 1 hour the concentration was found to have returned to 98.6% of  $C_0$ , before eventually equilibrating to 81.6 %  $C_0$  as the final equilibrated concentration after 96 hours. All of the PFAS, except PFOS and PFNA, exhibited a sudden decrease in the removal fraction within 2 hours of equilibration contact time with F400 GAC, which indicates sequential sorption of shorter-chain PFAS followed by desorption and displacement by longer-chained PFAS. Additionally, the average time to achieve equilibrium exceeded 48 hours in the SW matrix. In comparison, in the UP matrix, F400 GAC achieved equilibrium between 24—48 hours for the PFCAs, and by 24 hours for the PFSAs. Inhibitory effects manifesting as slow adsorption kinetics are consistent with results reported by Zhang et al. which demonstrated (1) that long-chain PFAS can displace shorter-chain adsorbed PFAS already adsorbed to the GAC surface, and (2) short-chain PFAS sorption to GAC is inhibited

by the presence of co-occurring cations.<sup>98</sup> Reduced adsorption capacities and slower sorption kinetics profiles in the SW matrix further corroborates the significant reduction in GAC as a viable PFAS treatment in municipal wastewater as a result of inhibition introduced by dissolved EfOM or co-occurring inorganic ions.<sup>30,70,74</sup>

DEXSORB® exhibited greater overall removal percentages for all of the PFAS in the SW matrix compared to F400 GAC; however, its kinetic rates of adsorption are greatly diminished in the SW batch tests, particularly for the removal of (ultra)short-chain PFAS. In terms of the sorption-desorption processes occurring in the early phases of the SW kinetics tests DEXSORB® displays similar trends to those of F400 GAC. For example, TFMS, PFPrA, and TFA were the only PFAS to demonstrate de-sorption from DEXSORB between 6—24 hours in the UP water batch test with equilibrium attained by 24—48 hours. Meanwhile, in the SW matrix, the same ultrashort-chain PFAS exhibit de-sorption earlier (between 2—6 hours), with continued equilibrium exchanges and reduction in removal fractions continuing to approximately 72—96 hours. The early and more widespread de-sorption in the SW matrix demonstrated by both F400 GAC and DEXSORB is a likely result of the additional matrix constituents reducing access to available adsorption sites via pore blockage or direct competition, and reducing the overall sorption capacities for the 18-PFAS mix and severely limiting PFAS sorption kinetics. The inhibitory effects of the SW matrix are consistent with batch tests conducted by Ruckbeil et al. evaluating ACs, IX resins, and various alternative adsorbents for PFAS and other organic micro-pollutant (OMP) removal from German drinking water (4.5 mg/L TOC).<sup>131</sup> In their evaluation, DEXSORB® demonstrated low DOC removal, but was significantly outperformed by various GACs and five PFAS-selective IX resins for the removal of short-chain PFCAs and PFSA and barely removed ultrashort-chain TFMS (~4% removal).<sup>131</sup> Despite demonstrating promising results for long-chain

PFCAs and long- and short-chain PFASs regarding a lack of sorption inhibition introduced by co-occurring EfOM and inorganic ions, the performance of DEXSORB® is suppressed to the point of complete ineffectiveness in the SW matrix for (ultra)short-chain PFASs and ultrashort-chain PFCAs – implying reduced treatment efficacy for those compounds in the continuous-flow tests.

The combined results of the kinetics and adsorption capacity batch tests in the SW matrix imply that the PFA694 IX resin would be the best performing media for the removal of the 18-PFAS mix in a continuous-flow setting treating a wastewater effluent containing realistic concentrations of dissolved organic matter and typically occurring inorganic ions. In the SW matrix, IRA910 IX resin demonstrated (1) reductions in the removal rate and the fraction of PFAS removed at equilibration for all but the long-chain PFASs, and (2) de-sorption between 12 and 24 hours of ultrashort-chain TFA and PFPrA, and of short-chain PFBA. By comparison, PFA694 IX exhibited only slightly decreased adsorption kinetics and removal fractions at equilibrium for the entire suite of PFASs in the SW batch kinetics tests. While, for the PFCAs, PFA694 IX equilibrium was achieved later and the overall removal fraction at equilibrium was reduced—particularly for the (ultra)short-chain compounds, suggesting that PFA694 IX may provide reduced treatment efficacy for (ultra)short-chain PFCAs. PFPrA and TFA were the only PFAS that demonstrated the de-sorption effect on PFA694 IX in the SW matrix, beginning between 6 and 24 hours of equilibration contact time, further indicating poor expected treatment performance in the continuous-flow tests. Although both the non-selective IRA910 IX resin and PFAS-selective PFA694 IX display markedly consistent kinetic rates of adsorption to near complete removal for the entire suite of 18 PFAS in the UP water batch tests, the PFAS-selective IX resin demonstrates the most comparable adsorption kinetic profiles between the UP water and SW matrix batch tests, indicating the least sorption inhibition due to the SW matrix constituents. The similar kinetic

adsorption rates demonstrated by PFA694 IX between the UP water and SW matrix batch tests, particularly for the PFASs and long-chain PFCAS, imply that the PFAS-selective IX resin will be most effective for treating those compounds in the continuous-flow tests treating a complex real wastewater.

#### *2.3.5. PFA694 IX outperforms all adsorbents in RSSCTs for majority of 18-PFAS Mix*

The breakthrough curves normalized to the average influent concentration, presented in **Figures 2.6A and 2.6B** illustrate the superior performance of the PFAS-selective PFA694 IX resin for the majority of the PFAS evaluated in this study. The batch test results in the UP and SW matrices corroborated the RSSCT findings in that PFA694IX was the least inhibited in terms of adsorption kinetics and capacities for the full suite of PFAS, and that DEXSORB® is marginally the next most effective adsorbent. Similarly, the non-selective F400 GAC and IRA910 IX exhibited the greatest inhibition due to the SW constituents in the batch tests, and subsequently performed very poorly relative to PFA694IX in the RSSCTs. The non-zero effluent concentrations for the RSSCTs indicate that the mass-transfer zone for each of the PFAS evaluated was not captured within the commercial media test columns.<sup>49,120</sup> This effect could be due to a combination of inhibited adsorption kinetics and capacities due to the complexities introduced by the real wastewater matrix,<sup>53,58,74</sup> as well as insufficient media contact time as a result of using 1wt% active media mass.<sup>49</sup>

The F400 GAC breakthrough curves demonstrate near immediate breakthrough for all of the PFAS, with the exception of PFOS, which still broke through relatively rapidly. Considering the PFASs (**Figure 2.6A**), F400 GAC slightly underperformed non-selective IRA910 IX resin for all but 6:2-FTS, which demonstrated near immediate breakthrough in the non-selective IX resin

columns. F400 GAC similarly slightly underperformed or had similar removal efficiencies in the RSSCTs when compared to DEXSORB® for all 18 of the PFAS considered in this study.

Overall, the breakthrough curves for the DEXSORB® columns are similar to those for GAC and non-selective IX resin, while showing the best treatment performance for PFOS in the continuous flow tests. DEXSORB's relative functionality for treating PFOS in a tertiary-treated municipal wastewater effluent is consistent with previous reports suggesting that DEXSORB® may be a suitable technology for PFOS treatment in complex matrices, but lacks suitability for treatment of other co-occurring short-chain, and ultrashort-chain PFAS.<sup>131</sup> PFA694 IX resin was by far the best performing adsorbent media for the treatment of each of the 18 PFAS in this complex multi-component system, with the exception of PFOS and TFA. Regarding PFOS, PFA694 IX was able to treat approximately three times as many column pore volumes (PVs) (250) prior to effluent concentrations surpassing 50% of the average influent concentration (i.e. 50% breakthrough), compared to the remaining three test media, which surpassed 50% breakthrough after treating approximately 75 PVs.

For the rest of the PFASs PFA694 IX demonstrated much lower effluent concentrations for significantly longer operational times, including for the ultrashort-chain compounds TFMS, PFETs, and PFPrS. Overall, the F400 GAC, DEXSORB, and IRA910 IX resin had no significant difference in performance, in that 50% breakthrough occurred at approximately 50 PVs treated for all of the PFASs (other than PFOS). IRA910 IX exhibited near immediate breakthrough of 6:2-FTS.

Considering TFA, breakthrough occurred nearly immediately for all four of the test media, and also demonstrated a pronounced chromatographic effect for each of the test media<sup>25,97</sup>. The chromatographic effect is caused by displacement of sorbed compounds as the treatment operation

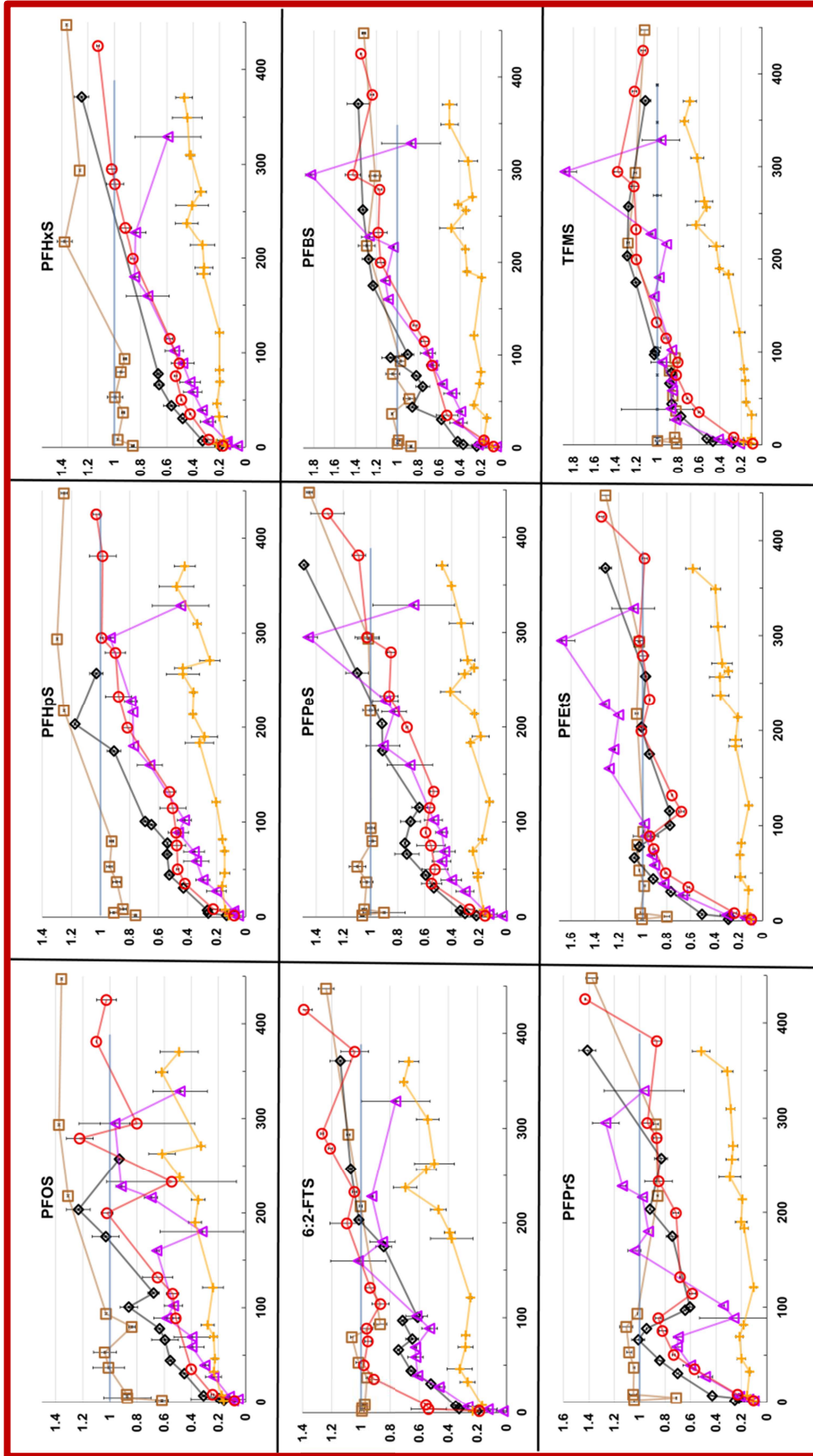
is on-going resulting in effluent concentrations that are greater than the measured influent concentrations. The chromatographic effect may also play a role in the breakthrough curve profiles for the rest of the compounds in the 18 PFAS system, however normalized effluent concentrations greater than 1.0 in the later portions of the RSSCTs are more likely the result of unintentionally spiking of the third influent reservoir (Reservoir E/F) with an excess of PFAS compared to the targeted concentration of 10 µg/L in the first two influent reservoirs (Reservoirs A/B and C/D).

The trend of decreasing time to breakthrough with decreasing PFAS chain-length is generally followed for the PFA694 IX resin and the deviation from the order of the PFAS breaking through based solely on the perfluorinated chain length are likely a result of unequal PFAS concentrations in the test columns' influent. As has been previously reported, the breakthrough of anionic PFAS when treated by GAC or IX resin typically occurs for ultrashort-chain first, then short-chain, and long-chain PFAS.<sup>49,51,107,114,116</sup> Evaluating the breakthrough curves of the PFCAs for PFA694 IX (**Figure 2.6B**), 50% breakthrough occurred first (nearly immediately) for the ultrashort-chain TFA, then breakthrough occurred for PFPrA (~60 PVs), PFPeA (~125 PVs), PFBA (~125 PVs) PFHxA (~220 PVs), HFPO-DA (~230 PVs), PFNA (~250 PVs), PFHpA (~270 PVs), and PFOA (~320 PVs). Considering the PFSAs (**Figure 2.6A**), the breakthrough pattern was less dependent on the chain-length of the particular PFAS, but showed a more consistent number of PVs treated across the spectrum of ultrashort- to long-chain PFSAs. The breakthrough order from earliest to latest was: TFMS (~220 PVs), 6:2-FTS (~240 PVs), PFEtS, PFPrS, PFBS, PFOS (~350 PVs), PFPeS, PFHxS, PFHpS (>370 PVs). Overall, PFA694 IX had the greatest treatment operational times for a majority of the long-, short-, and ultrashort-chain PFSAs, while only treating one PFCA to nearly the same extent (PFOA) and showing lack of capacity to treat (ultra)short-chain PFCAs, particularly.

The strong performance of PFA694 IX is generally in agreement with previous results investigating PFAS-selective IX resins (including several peer-reviewed studies which evaluated a similar product Purolite™ Purofine™ PFA694E IX, purportedly designed and marketed for use in drinking water treatment systems with unspecified differences from PFA694 IX designed for PFAS removal from wastewaters.<sup>169</sup> For instance, Chow et al. (2022) reported on the relatively short service times for successful treatment of PFEtS, PFPeA, PFBA, and PFPrA in pilot-scale, continuous flow tests treating PFAS-impacted groundwater for PFAS-selective Purolite® PFA694 IX and Amberlite PSR2+ IX, with a substantially lower number of bed volumes (BVs) treated prior to PFAS breakthrough for Norit 1240+ GAC.<sup>51</sup> PFAS-selective IX resins treated PFEtS, PFPeA, PFBA, and PFPrA occurred after treatment of 120,000 BVs, 60,000 BVs, 20,000 BVs, and <15,000 BVs, respectively, with no long-chain PFSA breakthrough above 10% after treating more than 210,000 BVs.<sup>51</sup> Comparatively, the 1240+ GAC exhibited breakthrough above 10% for PFEtS, PFPeA, PFBA, PFPrA after treatment of 13,000 BVs, 20,000 BVs, 10,000 BVs, and <5000 BVs, respectively.<sup>51</sup> In a pilot test for a drinking water treatment of PFAS contaminated groundwater in California, Medina et al. (2022) confirmed that (1) PFAS-selective IX resins, including PFA694E IX, outperform a variety of GACs in terms of BVs treated prior to breakthrough; (2) that shorter-chain PFAS breakthrough earlier than longer-chain compounds; and that (3) PFCAs of same fluorocarbon chain length will breakthrough earlier than corresponding PFASs.<sup>114</sup> Similarly, for treating a landfill leachate, Malovany et al. (2023) demonstrated that PFA694E IX can treat PFOS for ~22,000 BVs and PFOA for ~8,000 BVs prior to breakthrough in continuous flow tests, compared to less than 2,000 BVs for each compound for the F400 GAC. The PFAS-selective resin showed little removal of DOC, compared to F400 GAC; and only

slightly outperformed the GAC for removal of the sum of 11 other PFAS detected in the influent groundwater.<sup>107</sup>

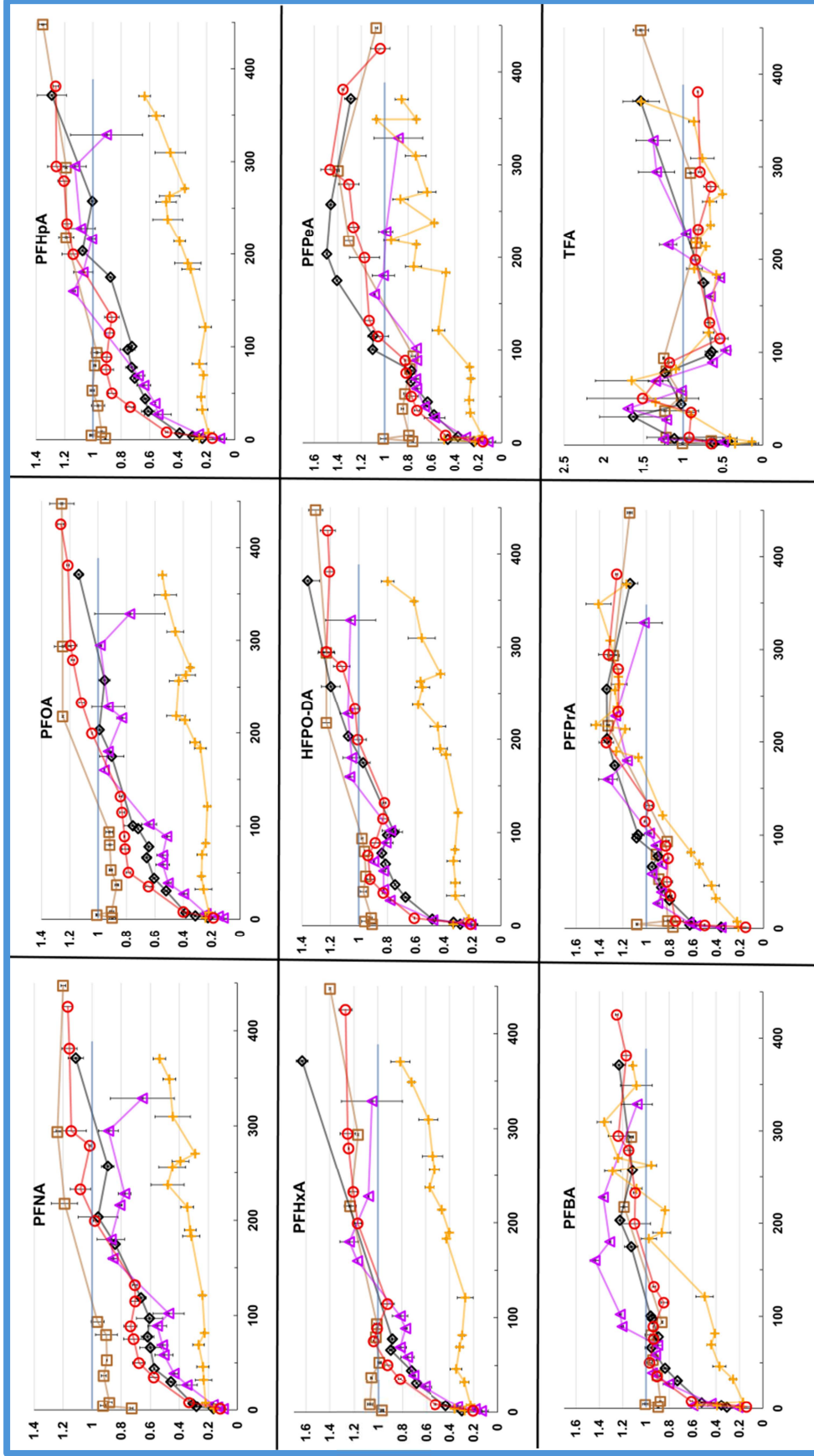
■ Sand Control ◊ F400 GAC ▲ DEXSORB + PFA694 IX ○ IRA910 IX — Influent



### # Treated Pore Volumes

**Figure 2.6A.** RSSCT Results - PFSAs: Influent concentration-normalized RSSCT Breakthrough curves for the PFSAs for each of the four evaluated sorbents and the sand control.  $C_0$  calculated as the average measured influent concentration, sampled throughout test. Symbols represent average values, and error bars are the standard deviation of duplicate test columns for each media and control.

■ Sand Control ◊ F400 GAC ▲ DEXSORB + PFA694 IX ⊖ IRA910 IX — Influent



$C/C_0$

## # Treated Pore Volumes

**Figure 2.6B.** RSSCT Results - PFCAs: Influent concentration-normalized RSSCT Breakthrough curves for the PFCAs for each of the four evaluated sorbents and the sand control.  $C_0$  calculated as the average measured influent concentration, sampled throughout test. Symbols represent average values, and error bars are the standard deviation of duplicate test columns for each media and control

#### 2.4. Conclusion

We find that despite demonstrating exceptionally high adsorption capacity for long-, short-, and ultrashort-chain PFCAs and PFSAAs in ultrapure water tests evaluating a combined 18-PFAS system, the non-PFAS-selective IRA910 IX resin performs similarly to GAC and DEXSORB® when operated in a continuous flow setting, treating a complex wastewater matrix. In the SW matrix batch tests, all the adsorbents were negatively impacted in terms of a decrease in the total adsorption capacity, and a decrease in the rate of adsorption. Inhibition of the sorption capacity and sorption rate was more pronounced for the PFCAs, compared to the PFSAAs; and the PFAS-selective DEXSORB® and PFA694 IX demonstrated the least inhibition in batch tests conducted in the SW matrix. When considering a spectrum of PFAAs from ultrashort-chain to long-chain compounds in continuous flow column tests, F400 GAC, DEXSORB®, and IRA910 IX were significantly outperformed by PFAS-selective PFA694 IX in terms of the total number of column pore volumes treated prior to exceedance of 50% breakthrough of the influent PFAS concentrations of the 18-PFAS mix. PFA694 IX did only slightly outperform the other adsorbents in terms of removing short-chain and ultrashort-chain PFCAs in the RSSCTs. The results of this study suggest that in an ideally designed treatment train scenario installation of a PFAS-selective IX resin, such as PFA694 IX, employed as a polishing step following tertiary treatment of secondary wastewater effluent could be a feasible alternative to reverse osmosis systems when considering PFAS treatment in the potable or non-potable re-use of reclaimed wastewater.<sup>74</sup>

The evaluated PFAS-selective PFA694 IX resin demonstrated comparable adsorption kinetics to the non-selective IRA910 IX resin and to the F400 GAC in ultrapure water and was the least inhibited in terms of adsorption kinetics and adsorption capacity at near environmentally relevant conditions along with DEXSORB®. DEXSORB® exhibited the fastest overall pseudo-

second order initial adsorption velocity of all the adsorbents, and an exceptionally high initial adsorption velocity for PFOS compared across the other co-occurring PFAS analyte-sorbent pairs evaluated in this study. In the SW matrix, DEXSORB® showed reduced inhibition relative to F400 GAC and had comparable PFAS uptake performance in the lower initial concentration batch tests, relative to the UP matrix, for the spectrum of PFAS chain-lengths except for some of the short-chain PFASs and all the ultrashort-chain PFAAs.

Despite the relatively promising results for DEXSORB® in the SW matrix batch tests, the media performed very similarly to GAC in the RSSCTs. The overall success of PFA694 IX in treating the 18-PFAS mix spiked into a real wastewater effluent sample could be predicted by the results of the adsorption SW adsorption kinetics and the SW adsorption capacity batch tests conducted at lower initial aqueous PFAS concentrations (or, in the case of this study, at near experimentally relevant concentrations for the RSSCTs). The agreement between the SW capacity and kinetics tests and the results of the continuous-flow tests using real wastewater highlight the importance of evaluating treatment systems in as realistic a setting as possible due to the differences in performance between batch and continuous-flow tests, and between laboratory studies using synthetic or ultrapure matrices versus pilot-scale studies treating real, likely more complex matrices with typical environmentally relevant PFAS concentrations.

### *2.5. Recommendations for Future Work*

There are many possible future evaluations that would enhance the understanding behind the mechanisms involved in the adsorption of each of the PFAS; in addition to quantification of the inhibitory effects on PFAS treatment attributed to each of the individual components constituting the synthetic and real wastewater matrices for the PFAS-selective adsorbent media evaluated in this study. Another key progression that stems from this work would be to confirm

the performance results reported here at lower, more environmentally relevant concentrations in the ~100 ng/L to 1 µg/L (total PFAS, depending on the number of PFAS detected or targeted for detection), which are more likely to represent typical concentrations detected in wastewater samples around the globe.

While the results of the RSSCTs suggest the superior performance of the Purolite® PFA694 IX resin, the early and non-zero effluent concentrations for all of the PFAS throughout a majority of the continuous-flow test are not fully indicative of its suitability for application in full-scale treatment trains targeting PFAS removal from municipal wastewater effluent without further evaluation. Modifications to the continuous-flow tests which would supplement our results and potentially verify the feasibility of full-scale implementation include conducting RSSCTs with greater active media contact times through increasing the percent wt% active media, to evaluate PFA694 IX with many of the other commercially available IX resins that are marketed as PFAS-selective, and to increase the scope from laboratory small-scale tests to pilot scale tests treating concentrations of PFAS that are actually present in the wastewater effluent.

Regardless of the demonstrated potential for PFAS-selective IX resins to successfully treat ultrashort-, short- and long-chain PFAS to some degree, other studies suggest that GAC may still be a key component in treatment train approaches because of its capacity for nonselective removal of DOM, PFAS with cationic or zwitterionic functional groups and other non-PFAS contaminants.<sup>25,53,54,74,112,115</sup> Therefore, evaluation of a treatment train approach utilizing RSSCTs with a combination of adsorptive media in series - such as GAC, DEXSORB, cation exchange resins, and PFAS-specific IX resin(s) in various configurations - could provide further insight into the full-scale feasibility of adsorptive removal of PFAS from municipal wastewater effluent for a broader range of PFAS that are likely to co-exist in real effluents globally. Further pretreatment

approaches may also increase the feasibility of adsorptive removal of PFAS such as electrochemical oxidation,<sup>110</sup> membrane bioreactor (MBR), biologically-activated filtration (BAF), ozonation, or a combined with novel PFAS destructive technologies such as hydrothermal alkaline treatment (HALT)<sup>213, 74</sup>.

Fundamentally, further characterization and elucidation of the physical and chemical characteristics of the adsorbent media, particularly the proprietary PFAS-selective IX resins, in addition to evaluations of single-PFAS solute systems in ultrapure and complex aqueous matrices, will help improve the mechanistic understanding of the removal of ultrashort-, short-, and long-chain PFAAs and other PFAS widespread in the environment and municipal wastewater effluents. Another fundamental knowledge gap that requires attention to better frame the targets for PFAS treatment is the lack of characterizations of the occurrence of ultrashort-chain PFAS in WWTPs and the water discharged to the environment and how that may impact PFAS contamination in drinking water sources. Finally, preparation of experimental composite media consisting of many of the elements discussed herein designed to increase the capacity, kinetics, and affinity of the adsorbent media for the full spectrum of PFAS chain-lengths could be worth exploring. For example, a media that immobilized a quaternary ammonium functionalized PFAS-templated molecularly-imprinted polymer (MIP)<sup>185</sup> with TFN and  $\beta$ -cyclodextrin comonomers onto a macroporous or mesoporous GAC could synthesize a novel media with potentially superior performance in complex matrices to PFA694 IX.

## References

- (1) *PFAS National Primary Drinking Water Regulation Rulemaking*. Federal Register. <https://www.federalregister.gov/documents/2023/03/29/2023-05471/pfas-national-primary-drinking-water-regulation-rulemaking> (accessed 2025-09-01).
- (2) Glüge, J.; Scheringer, M.; Cousins, I. T.; DeWitt, J. C.; Goldenman, G.; Herzke, D.; Lohmann, R.; Ng, C. A.; Trier, X.; Wang, Z. An Overview of the Uses of Per- and Polyfluoroalkyl Substances (PFAS). *Environ. Sci. Process. Impacts* **2020**, *22* (12), 2345–2373. <https://doi.org/10.1039/d0em00291g>.
- (3) *CompTox Chemicals Dashboard*. <https://comptox.epa.gov/dashboard/chemical-lists/PFASSTRUCT> (accessed 2025-08-28).
- (4) Gaines, L. G. T. Historical and Current Usage of Per- and Polyfluoroalkyl Substances (PFAS): A Literature Review. *Am. J. Ind. Med.* **2023**, *66* (5), 353–378. <https://doi.org/10.1002/ajim.23362>.
- (5) Giesy, J. P.; Kannan, K. Perfluorochemical Surfactants in the Environment. *Environ. Sci. Technol.* **2002**, *36* (7), 146A–152A. <https://doi.org/10.1021/es022253t>.
- (6) Prevedouros, K.; Cousins, I. T.; Buck, R. C.; Korzeniowski, S. H. Sources, Fate and Transport of Perfluorocarboxylates. *Environ. Sci. Technol.* **2006**, *40* (1), 32–44. <https://doi.org/10.1021/es0512475>.
- (7) Lindstrom, A. B.; Strynar, M. J.; Libelo, E. L. Polyfluorinated Compounds: Past, Present, and Future. *Environ. Sci. Technol.* **2011**, *45* (19), 7954–7961. <https://doi.org/10.1021/es2011622>.
- (8) Taves, D. R. Evidence That There Are Two Forms of Fluoride in Human Serum. *Nature* **1968**, *217* (5133), 1050–1051. <https://doi.org/10.1038/2171050b0>.
- (9) Buck, R. C.; Franklin, J.; Berger, U.; Conder, J. M.; Cousins, I. T.; de Voigt, P.; Jensen, A. A.; Kannan, K.; Mabury, S. A.; van Leeuwen, S. P. J. Perfluoroalkyl and Polyfluoroalkyl Substances in the Environment: Terminology, Classification, and Origins. *Integr. Environ. Assess. Manag.* **2011**, *7* (4), 513–541. <https://doi.org/10.1002/ieam.258>.
- (10) Botelho, J. C.; Kato, K.; Wong, L.-Y.; Calafat, A. M. Per- and Polyfluoroalkyl Substances (PFAS) Exposure in the U.S. Population: NHANES 1999–March 2020. *Environ. Res.* **2025**, *270* (120916), 120916. <https://doi.org/10.1016/j.envres.2025.120916>.
- (11) Ritter, S. K. FLUOROCHEMICALS GO SHORT: Shorter Perfluoroalkyl Chain Lengths Improve ENVIRONMENTAL PROFILE of Versatile Stain-, Grease-, and Water-Repelling Chemicals. *Chem. Eng. News Archive* **2010**, *88* (5), 12–17. <https://doi.org/10.1021/cen-v088n005.p012>.
- (12) Renner, R. The Long and the Short of Perfluorinated Replacements. *Environ. Sci. Technol.* **2006**, *40* (1), 12–13. <https://doi.org/10.1021/es062612a>.
- (13) Wang, Z.; DeWitt, J. C.; Higgins, C. P.; Cousins, I. T. A Never-Ending Story of per- and Polyfluoroalkyl Substances (PFASs)? *Environ. Sci. Technol.* **2017**, *51* (5), 2508–2518. <https://doi.org/10.1021/acs.est.6b04806>.
- (14) *PFAS and Forever Chemicals*. Drinking Water Inspectorate. <https://www.dwi.gov.uk/pfas-and-forever-chemicals/> (accessed 2025-08-26).
- (15) Neuwald, I. J.; Hübner, D.; Wiegand, H. L.; Valkov, V.; Borchers, U.; Nödler, K.; Scheurer, M.; Hale, S. E.; Arp, H. P. H.; Zahn, D. Ultra-Short-Chain PFASs in the Sources of German Drinking Water: Prevalent, Overlooked, Difficult to Remove, and Unregulated. *Environ. Sci. Technol.* **2022**, *56* (10), 6380–6390. <https://doi.org/10.1021/acs.est.1c07949>.

- (16) *PFAS contamination and soil remediation (Signal)*. <https://www.eea.europa.eu/en/european-zero-pollution-dashboards/indicators/pfas-contamination-and-soil-remediation-signal> (accessed 2025-09-02).
- (17) Us Epa, O. W. *Per- and Polyfluoroalkyl Substances (PFAS)*. US EPA. <https://www.epa.gov/sdwa/and-polyfluoroalkyl-substances-pfas> (accessed 2025-09-02).
- (18) Vakili, M.; Bao, Y.; Gholami, F.; Gholami, Z.; Deng, S.; Wang, W.; Kumar Awasthi, A.; Rafatullah, M.; Cagnetta, G.; Yu, G. Removal of HFPO-DA (GenX) from Aqueous Solutions: A Mini-Review. *Chem. Eng. J.* **2021**, *424* (130266), 130266. <https://doi.org/10.1016/j.cej.2021.130266>.
- (19) Xiao, F. Emerging Poly- and Perfluoroalkyl Substances in the Aquatic Environment: A Review of Current Literature. *Water Res.* **2017**, *124*, 482–495. <https://doi.org/10.1016/j.watres.2017.07.024>.
- (20) Wang, Z.; Cousins, I. T.; Scheringer, M.; Hungerbühler, K. Fluorinated Alternatives to Long-Chain Perfluoroalkyl Carboxylic Acids (PFCAs), Perfluoroalkane Sulfonic Acids (PFSA) and Their Potential Precursors. *Environ. Int.* **2013**, *60*, 242–248. <https://doi.org/10.1016/j.envint.2013.08.021>.
- (21) Hopkins, Z. R.; Sun, M.; DeWitt, J. C.; Knappe, D. R. U. Recently Detected Drinking Water Contaminants: GenX and Other Per- and Polyfluoroalkyl Ether Acids. *J. Am. Water Works Assoc.* **2018**, *110* (7), 13–28. <https://doi.org/10.1002/awwa.1073>.
- (22) Fast, A.; Calderon, I. EPA Will Roll Back Limits on 4 “forever Chemicals.” See If They Were Found in Your Water. *USA Today*. USA TODAY May 15, 2025. <https://www.usatoday.com/story/news/investigations/2025/05/15/trump-epa-scraps-pfas-forever-chemical-limits/83627286007/> (accessed 2025-09-02).
- (23) Us Epa, O. A. *EPA Announces It Will Keep Maximum Contaminant Levels for PFOA, PFOS*. US EPA. <https://www.epa.gov/newsreleases/epa-announces-it-will-keep-maximum-contaminant-levels-pfoa-pfos> (accessed 2025-09-02).
- (24) *PFAS in wastewater*. Washington State Department of Ecology. <https://ecology.wa.gov/waste-toxics/reducing-toxic-chemicals/addressing-priority-toxic-chemicals/pfas/wastewater> (accessed 2025-09-02).
- (25) Cantoni, B.; Turolla, A.; Wellmitz, J.; Ruhl, A. S.; Antonelli, M. Perfluoroalkyl Substances (PFAS) Adsorption in Drinking Water by Granular Activated Carbon: Influence of Activated Carbon and PFAS Characteristics. *Sci. Total Environ.* **2021**, *795*, 148821. <https://doi.org/10.1016/j.scitotenv.2021.148821>.
- (26) *2.2 Chemistry, Terminology, and Acronyms*. <https://pfas-1.itrcweb.org/2-2-chemistry-terminology-and-acronyms/> (accessed 2025-09-05).
- (27) Ateia, M.; Maroli, A.; Tharayil, N.; Karanfil, T. The Overlooked Short- and Ultrashort-Chain Poly- and Perfluorinated Substances: A Review. *Chemosphere* **2019**, *220*, 866–882. <https://doi.org/10.1016/j.chemosphere.2018.12.186>.
- (28) *Remediation Management for Local and Wide-Spread PFAS Contaminations (Texte 205/2020)*. UBA. Retrieved from Umweltbundesamt Website; 2020.
- (29) Us Epa, O. *Fact Sheet: 2010/2015 PFOA Stewardship Program*. US EPA. <https://www.epa.gov/assessing-and-managing-chemicals-under-tsca/fact-sheet-20102015-pfoa-stewardship-program> (accessed 2025-08-26).
- (30) Lenka, S. P.; Kah, M.; Padhye, L. P. A Review of the Occurrence, Transformation, and Removal of Poly- and Perfluoroalkyl Substances (PFAS) in Wastewater Treatment Plants. *Water Res.* **2021**, *199*, 117187. <https://doi.org/10.1016/j.watres.2021.117187>.

- (31) Heydebreck, F.; Tang, J.; Xie, Z.; Ebinghaus, R. Alternative and Legacy Perfluoroalkyl Substances: Differences between European and Chinese River/Estuary Systems. *Environ. Sci. Technol.* **2015**, *49* (14), 8386–8395. <https://doi.org/10.1021/acs.est.5b01648>.
- (32) Strynar, M.; Dagnino, S.; McMahan, R.; Liang, S.; Lindstrom, A.; Andersen, E.; McMillan, L.; Thurman, M.; Ferrer, I.; Ball, C. Identification of Novel Perfluoroalkyl Ether Carboxylic Acids (PFECAs) and Sulfonic Acids (PFESAs) in Natural Waters Using Accurate Mass Time-of-Flight Mass Spectrometry (TOFMS). *Environ. Sci. Technol.* **2015**, *49* (19), 11622–11630. <https://doi.org/10.1021/acs.est.5b01215>.
- (33) *What is GenX?* <https://www.chemours.com/en/about-chemours/genx> (accessed 2025-09-01).
- (34) Dixit, F.; Barbeau, B.; Mostafavi, S. G.; Mohseni, M. Efficient Removal of GenX (HFPO-DA) and Other Perfluorinated Ether Acids from Drinking and Recycled Waters Using Anion Exchange Resins. *J. Hazard. Mater.* **2020**, *384*, 121261. <https://doi.org/10.1016/j.jhazmat.2019.121261>.
- (35) Wang, Y.; Chang, W.; Wang, L.; Zhang, Y.; Zhang, Y.; Wang, M.; Wang, Y.; Li, P. A Review of Sources, Multimedia Distribution and Health Risks of Novel Fluorinated Alternatives. *Ecotoxicol. Environ. Saf.* **2019**, *182* (109402), 109402. <https://doi.org/10.1016/j.ecoenv.2019.109402>.
- (36) Gomis, M. I.; Vestergren, R.; Borg, D.; Cousins, I. T. Comparing the Toxic Potency in Vivo of Long-Chain Perfluoroalkyl Acids and Fluorinated Alternatives. *Environ. Int.* **2018**, *113*, 1–9. <https://doi.org/10.1016/j.envint.2018.01.011>.
- (37) Epa, U. S. *Final PFAS NPDWR*; <https://www.epa.gov/sdwa/and-polyfluoroalkyl-substances-pfas>, 2024.
- (38) Zhi, Y.; Lu, X.; Munoz, G.; Yeung, L. W. Y.; De Silva, A. O.; Hao, S.; He, H.; Jia, Y.; Higgins, C. P.; Zhang, C. Environmental Occurrence and Biotic Concentrations of Ultrashort-Chain Perfluoroalkyl Acids: Overlooked Global Organofluorine Contaminants. *Environ. Sci. Technol.* **2024**, *58* (49), 21393–21410. <https://doi.org/10.1021/acs.est.4c04453>.
- (39) Frenzel, I.; Nöltge, D.; Freeling, F.; Müller, M.; Lange, J. Diffuse Sources of TFA: Atmospheric and Terrestrial Inputs, Retention and Pathways at the Catchment Scale, 2025. <https://doi.org/10.5194/egusphere-2025-2882>.
- (40) Chow, S. J.; Ojeda, N.; Jacangelo, J. G.; Schwab, K. J. Detection of Ultrashort-Chain and Other per- and Polyfluoroalkyl Substances (PFAS) in U.S. Bottled Water. *Water Res.* **2021**, *201*, 117292. <https://doi.org/10.1016/j.watres.2021.117292>.
- (41) Liang, S.-H.; Steimling, J. A.; Chang, M. Analysis of Ultrashort-Chain and Short-Chain (C1 to C4) per- and Polyfluorinated Substances in Potable and Non-Potable Waters. *Journal of Chromatography Open* **2023**, *4*, 100098. <https://doi.org/10.1016/j.jcoa.2023.100098>.
- (42) Zheng, G.; Eick, S. M.; Salamova, A. Elevated Levels of Ultrashort- and Short-Chain Perfluoroalkyl Acids in US Homes and People. *Environ. Sci. Technol.* **2023**, *57* (42), 15782–15793. <https://doi.org/10.1021/acs.est.2c06715>.
- (43) Jagani, R.; Chovatiya, J.; Patel, H.; Andra, S. S. Trifluoroacetic Acid: An Ultra-Short PFAS with Emerging Environmental and Public Health Concerns. *ACS ES T Water* **2025**, *5* (7), 3533–3537. <https://doi.org/10.1021/acsestwater.5c00599>.
- (44) Arp, H. P. H.; Gredelj, A.; Glüge, J.; Scheringer, M.; Cousins, I. T. The Global Threat from the Irreversible Accumulation of Trifluoroacetic Acid (TFA). *Environ. Sci. Technol.* **2024**, *58* (45), 19925–19935. <https://doi.org/10.1021/acs.est.4c06189>.
- (45) Scheurer, M.; Nödler, K.; Freeling, F.; Janda, J.; Happel, O.; Riegel, M.; Müller, U.; Storck, F. R.; Fleig, M.; Lange, F. T.; Brunsch, A.; Brauch, H.-J. Small, Mobile, Persistent:

- Trifluoroacetate in the Water Cycle - Overlooked Sources, Pathways, and Consequences for Drinking Water Supply. *Water Res.* **2017**, *126*, 460–471. <https://doi.org/10.1016/j.watres.2017.09.045>.
- (46) Cozzolino, L.; Benassi, C.; Falletta, A.; Di Francesco, C. V.; Mancarella, S.; Casali, M. B. Ultrashort Pfas: A Review of the Topic. *Clin. Ter.* **2024**, *175 Suppl 1(4)* (4), 109–112. <https://doi.org/10.7417/CT.2024.5095>.
- (47) Ateia, M.; Chiang, D.; Cashman, M.; Acheson, C. Total Oxidizable Precursor (TOP) Assay-Best Practices, Capabilities and Limitations for PFAS Site Investigation and Remediation. *Environ. Sci. Technol. Lett.* **2023**, *10* (4), 292–301. <https://doi.org/10.1021/acs.estlett.3c00061>.
- (48) Wang, R.; Ching, C.; Dichtel, W. R.; Helbling, D. E. Evaluating the Removal of Per- and Polyfluoroalkyl Substances from Contaminated Groundwater with Different Adsorbents Using a Suspect Screening Approach. *Environ. Sci. Technol. Lett.* **2020**, *7* (12), 954–960. <https://doi.org/10.1021/acs.estlett.0c00736>.
- (49) Murray, C. C.; Marshall, R. E.; Liu, C. J.; Vatankhah, H.; Bellona, C. L. PFAS Treatment with Granular Activated Carbon and Ion Exchange Resin: Comparing Chain Length, Empty Bed Contact Time, and Cost. *Journal of Water Process Engineering* **2021**, *44*, 102342. <https://doi.org/10.1016/j.jwpe.2021.102342>.
- (50) Ellis, A. C.; Liu, C. J.; Fang, Y.; Boyer, T. H.; Schaefer, C. E.; Higgins, C. P.; Strathmann, T. J. Pilot Study Comparison of Regenerable and Emerging Single-Use Anion Exchange Resins for Treatment of Groundwater Contaminated by per- and Polyfluoroalkyl Substances (PFASs). *Water Res.* **2022**, *223* (119019), 119019. <https://doi.org/10.1016/j.watres.2022.119019>.
- (51) Chow, S. J.; Croll, H. C.; Ojeda, N.; Klamerus, J.; Capelle, R.; Oppenheimer, J.; Jacangelo, J. G.; Schwab, K. J.; Prasse, C. Comparative Investigation of PFAS Adsorption onto Activated Carbon and Anion Exchange Resins during Long-Term Operation of a Pilot Treatment Plant. *Water Res.* **2022**, *226* (119198), 119198. <https://doi.org/10.1016/j.watres.2022.119198>.
- (52) Ghorbani Gorji, S.; Hawker, D. W.; Mackie, R.; Higgins, C. P.; Bowles, K.; Li, Y.; Kaserzon, S. Sorption Affinity and Mechanisms of Per-and Polyfluoroalkyl Substances (PFASs) with Commercial Sorbents: Implications for Passive Sampling. *J. Hazard. Mater.* **2023**, *457* (131688), 131688. <https://doi.org/10.1016/j.jhazmat.2023.131688>.
- (53) Lenka, S. P.; Kah, M.; Chen, J. L.-Y.; Tiban-Anrango, B. A.; Padhye, L. P. Adsorption Mechanisms of Short-Chain and Ultrashort-Chain PFAS on Anion Exchange Resins and Activated Carbon. *Environmental Science: Water Research & Technology* **2024**. <https://doi.org/10.1039/D3EW00959A>.
- (54) Tajdini, B.; Vatankhah, H.; Pezoulas, E. R.; Zhang, C.; Higgins, C. P.; Bellona, C. Adsorbability of a Wide Range of Per- and Polyfluoroalkyl Substances on Granular Activated Carbon, Ion Exchange Resin, and Surface Modified Clay. *Water Res.* **2025**, *268* (Pt B), 122774. <https://doi.org/10.1016/j.watres.2024.122774>.
- (55) Lobitz, A.; Steuber, A.; Chen, M.; Maohajer, M. A.; Feng, R.; Barry, M.; Harris, B.; Zou, M.; Jia, S.; Guo, L. Fluorous Modification of Commercial Resins for Ultrashort and Short Chain PFAS Removal. *ChemRxiv*, 2025. <https://doi.org/10.26434/chemrxiv-2025-6zgbk>.
- (56) Phong Vo, H. N.; Ngo, H. H.; Guo, W.; Hong Nguyen, T. M.; Li, J.; Liang, H.; Deng, L.; Chen, Z.; Hang Nguyen, T. A. Poly-and Perfluoroalkyl Substances in Water and Wastewater: A Comprehensive Review from Sources to Remediation. *Journal of Water Process Engineering* **2020**, *36*, 101393. <https://doi.org/10.1016/j.jwpe.2020.101393>.

- (57) Tshangana, C. S.; Nhlengethwa, S. T.; Glass, S.; Denison, S.; Kuvarega, A. T.; Nkambule, T. T. I.; Mamba, B. B.; Alvarez, P. J. J.; Muleja, A. A. Technology Status to Treat PFAS-Contaminated Water and Limiting Factors for Their Effective Full-Scale Application. *Npj Clean Water* **2025**, *8* (1), 1–30. <https://doi.org/10.1038/s41545-025-00457-3>.
- (58) Kothawala, D. N.; Köhler, S. J.; Östlund, A.; Wiberg, K.; Ahrens, L. Influence of Dissolved Organic Matter Concentration and Composition on the Removal Efficiency of Perfluoroalkyl Substances (PFASs) during Drinking Water Treatment. *Water Res.* **2017**, *121*, 320–328. <https://doi.org/10.1016/j.watres.2017.05.047>.
- (59) Lei, X.; Lian, Q.; Zhang, X.; Karsili, T. K.; Holmes, W.; Chen, Y.; Zappi, M. E.; Gang, D. D. A Review of PFAS Adsorption from Aqueous Solutions: Current Approaches, Engineering Applications, Challenges, and Opportunities. *Environ. Pollut.* **2023**, *321*, 121138. <https://doi.org/10.1016/j.envpol.2023.121138>.
- (60) Franke, V.; Ullberg, M.; McCleaf, P.; Wålander, M.; Köhler, S. J.; Ahrens, L. The Price of Really Clean Water: Combining Nanofiltration with Granular Activated Carbon and Anion Exchange Resins for the Removal of Per- And Polyfluoroalkyl Substances (PFASs) in Drinking Water Production. *ACS EST Water* **2021**, *1* (4), 782–795. <https://doi.org/10.1021/acsestwater.0c00141>.
- (61) Lenntech. MBERSEP® 900 OH Strong Base Anion Exchanger PRODUCT DATA SHEET. 1999. <https://www.lenntech.com/Data-sheets/Ambersep-900-OH-L.pdf>.
- (62) Duru, C. I.; Sherchan, S. P. A Systematic Review and Meta Analysis on the Occurrence of Per- and Polyfluoroalkyl Substances (PFAS) in Wastewater Treatment Plants. *Water Air Soil Pollut.* **2025**, *236* (10), 627. <https://doi.org/10.1007/s11270-025-08225-2>.
- (63) Thompson, K. A.; Mortazavian, S.; Gonzalez, D. J.; Bott, C.; Hooper, J.; Schaefer, C. E.; Dickenson, E. R. V. Poly- and Perfluoroalkyl Substances in Municipal Wastewater Treatment Plants in the United States: Seasonal Patterns and Meta-Analysis of Long-Term Trends and Average Concentrations. *ACS EST Water* **2022**, *2* (5), 690–700. <https://doi.org/10.1021/acsestwater.1c00377>.
- (64) Winchell, L. J.; Wells, M. J. M.; Ross, J. J.; Fonoll, X.; Norton, J. W., Jr; Kuplicki, S.; Khan, M.; Bell, K. Y. Per- and Polyfluoroalkyl Substances Presence, Pathways, and Cycling through Drinking Water and Wastewater Treatment. *J. Environ. Eng. (New York)* **2022**, *148* (1). [https://doi.org/10.1061/\(asce\)ee.1943-7870.0001943](https://doi.org/10.1061/(asce)ee.1943-7870.0001943).
- (65) Kim, J.; Xin, X.; Mamo, B. T.; Hawkins, G. L.; Li, K.; Chen, Y.; Huang, Q.; Huang, C.-H. Occurrence and Fate of Ultrashort-Chain and Other Per- and Polyfluoroalkyl Substances (PFAS) in Wastewater Treatment Plants. *ACS EST Water* **2022**, *2* (8), 1380–1390. <https://doi.org/10.1021/acsestwater.2c00135>.
- (66) Schaefer, C. E.; Hooper, J. L.; Strom, L. E.; Abusallout, I.; Dickenson, E. R. V.; Thompson, K. A.; Mohan, G. R.; Drennan, D.; Wu, K.; Guelfo, J. L. Occurrence of Quantifiable and Semi-Quantifiable Poly- and Perfluoroalkyl Substances in United States Wastewater Treatment Plants. *Water Res.* **2023**, *233*, 119724. <https://doi.org/10.1016/j.watres.2023.119724>.
- (67) Brendel, S.; Fetter, É.; Staude, C.; Vierke, L.; Biegel-Engler, A. Short-Chain Perfluoroalkyl Acids: Environmental Concerns and a Regulatory Strategy under REACH. *Environ Sci Eur* **2018**, *30* (1), 9. <https://doi.org/10.1186/s12302-018-0134-4>.
- (68) Gewurtz, M. *Molly Lamb Bobak*; The Canadian Art Library; Canadian Art Library, 2019.

- (69) Cookson, E. S.; Detwiler, R. L. Global Patterns and Temporal Trends of Perfluoroalkyl Substances in Municipal Wastewater: A Meta-Analysis. *Water Res.* **2022**, *221*, 118784. <https://doi.org/10.1016/j.watres.2022.118784>.
- (70) Mortazavian, S.; Hooper, J.; Abusallout, I.; Hofmann, R. Granular Activated Carbon for PFAS Removal in Municipal Wastewater: A Rapid Small-Scale Column Test Study. *ACS EST Water* **2025**. <https://doi.org/10.1021/acsestwater.4c00919>.
- (71) Comber, S. D. W.; Gardner, M. J.; Ellor, B. Perfluorinated Alkyl Substances: Sewage Treatment and Implications for Receiving Waters. *Sci. Total Environ.* **2021**, *791* (148391), 148391. <https://doi.org/10.1016/j.scitotenv.2021.148391>.
- (72) Gewurtz, S. B.; Auyeung, A. S.; De Silva, A. O.; Teslic, S.; Smyth, S. A. Per- and Polyfluoroalkyl Substances (PFAS) in Canadian Municipal Wastewater and Biosolids: Recent Patterns and Time Trends 2009 to 2021. *Sci. Total Environ.* **2024**, *912*, 168638. <https://doi.org/10.1016/j.scitotenv.2023.168638>.
- (73) Pontius, J.; McIntosh, A. Water Scarcity. In *Springer Textbooks in Earth Sciences, Geography and Environment*; Springer International Publishing: Cham, 2024; pp 87–103. [https://doi.org/10.1007/978-3-031-48762-0\\_8](https://doi.org/10.1007/978-3-031-48762-0_8).
- (74) Tajdini, B.; Vatankhah, H.; Murray, C. C.; Liethen, A.; Bellona, C. Impact of Effluent Organic Matter on Perfluoroalkyl Acid Removal from Wastewater Effluent by Granular Activated Carbon and Alternative Adsorbents. *Water Res.* **2023**, *241*, 120105. <https://doi.org/10.1016/j.watres.2023.120105>.
- (75) Dixit, F.; Barbeau, B.; Lompe, K. M.; Kheyrandish, A.; Mohseni, M. Performance of the HSDM to Predict Competitive Uptake of PFAS, NOM and Inorganic Anions by Suspended Ion Exchange Processes. *Environ. Sci. (Camb.)* **2021**, *7* (8), 1417–1429. <https://doi.org/10.1039/d1ew00145k>.
- (76) Gagliano, E.; Sgroi, M.; Falciglia, P. P.; Vagliasindi, F. G. A.; Roccaro, P. Removal of Poly- and Perfluoroalkyl Substances (PFAS) from Water by Adsorption: Role of PFAS Chain Length, Effect of Organic Matter and Challenges in Adsorbent Regeneration. *Water Res.* **2020**, *171*, 115381. <https://doi.org/10.1016/j.watres.2019.115381>.
- (77) Sharma, N.; Kumar, V.; Sugumar, V.; Umesh, M.; Sondhi, S.; Chakraborty, P.; Kaur, K.; Thomas, J.; Kamaraj, C.; Maitra, S. S. A Comprehensive Review on the Need for Integrated Strategies and Process Modifications for Per- and Polyfluoroalkyl Substances (PFAS) Removal: Current Insights and Future Prospects. *Case Studies in Chemical and Environmental Engineering* **2024**, *9*, 100623. <https://doi.org/10.1016/j.cscee.2024.100623>.
- (78) Ahrens, L.; Lundgren, S.; McCleaf, P.; Köhler, S. Removal of Perfluoroalkyl Substances (PFAS) from Different Water Types by Techniques Based on Anion Exchange (AIX), Powdered Activated Carbon (PAC), Iron(III) Chloride and Nanofiltration (NF) Membrane - A Systematic Comparison. *Sci. Total Environ.* **2025**, *970* (179004), 179004. <https://doi.org/10.1016/j.scitotenv.2025.179004>.
- (79) Ross, I.; McDonough, J.; Miles, J.; Storch, P.; Thelakkat Kochunarayanan, P.; Kalve, E.; Hurst, J.; S. Dasgupta, S.; Burdick, J. A Review of Emerging Technologies for Remediation of PFASs. *Remediation* **2018**, *28* (2), 101–126. <https://doi.org/10.1002/rem.21553>.
- (80) Houtz, E.; Wang, M.; Park, J.-S. Identification and Fate of Aqueous Film Forming Foam Derived Per- and Polyfluoroalkyl Substances in a Wastewater Treatment Plant. *Environ. Sci. Technol.* **2018**, *52* (22), 13212–13221. <https://doi.org/10.1021/acs.est.8b04028>.
- (81) Nzeribe, B. N.; Crimi, M.; Mededovic Thagard, S.; Holsen, T. M. Physico-Chemical Processes for the Treatment of per- and Polyfluoroalkyl Substances (PFAS): A Review. *Crit.*

- Rev. Environ. Sci. Technol.* **2019**, *49* (10), 866–915. <https://doi.org/10.1080/10643389.2018.1542916>.
- (82) Hooper, J.; Funk, D.; Bell, K.; Noibi, M.; Vickstrom, K.; Schulz, C.; Machek, E.; Huang, C.-H. Pilot Testing of Direct and Indirect Potable Water Reuse Using Multi-Stage Ozone-Biofiltration without Reverse Osmosis. *Water Res.* **2020**, *169* (115178), 115178. <https://doi.org/10.1016/j.watres.2019.115178>.
- (83) Smith, S. J.; Wiberg, K.; McCleaf, P.; Ahrens, L. Pilot-Scale Continuous Foam Fractionation for the Removal of per- and Polyfluoroalkyl Substances (PFAS) from Landfill Leachate. *ACS ES T Water* **2022**, *2* (5), 841–851. <https://doi.org/10.1021/acsestwater.2c00032>.
- (84) Smith, S. J.; Lewis, J.; Wiberg, K.; Wall, E.; Ahrens, L. Foam Fractionation for Removal of Per- and Polyfluoroalkyl Substances: Towards Closing the Mass Balance. *Sci. Total Environ.* **2023**, *871* (162050), 162050. <https://doi.org/10.1016/j.scitotenv.2023.162050>.
- (85) Austin, C.; Li, J.; Moore, S.; Purohit, A.; Pinkard, B. R.; Novosselov, I. V. Destruction and Defluorination of PFAS Matrix in Continuous-Flow Supercritical Water Oxidation Reactor: Effect of Operating Temperature. *Chemosphere* **2023**, *327* (138358), 138358. <https://doi.org/10.1016/j.chemosphere.2023.138358>.
- (86) Austin, C.; Purohit, A. L.; Thomsen, C.; Pinkard, B. R.; Strathmann, T. J.; Novosselov, I. V. Hydrothermal Destruction and Defluorination of Trifluoroacetic Acid (TFA). *Environ. Sci. Technol.* **2024**, *58* (18), 8076–8085. <https://doi.org/10.1021/acs.est.3c09404>.
- (87) Liu, F.; Pignatello, J. J.; Sun, R.; Guan, X.; Xiao, F. A Comprehensive Review of Novel Adsorbents for Per- and Polyfluoroalkyl Substances in Water. *ACS EST Water* **2024**, *4* (4), 1191–1205. <https://doi.org/10.1021/acsestwater.3c00569>.
- (88) Grieco, S. A.; Chang, J.; Maio, E. (lily) Y.; Hwang, M. Comparing Conventional and Emerging Adsorbents for Per- and Polyfluoroalkyl Substances: Kinetic, Equilibrium, and Column Experiments. *AWWA Water Sci.* **2021**, *3* (6). <https://doi.org/10.1002/aws2.1256>.
- (89) Karbassiyazdi, E.; Kasula, M.; Modak, S.; Pala, J.; Kalantari, M.; Altaee, A.; Esfahani, M. R.; Razmjou, A. A Juxtaposed Review on Adsorptive Removal of PFAS by Metal-Organic Frameworks (MOFs) with Carbon-Based Materials, Ion Exchange Resins, and Polymer Adsorbents. *Chemosphere* **2023**, *311* (Pt 1), 136933. <https://doi.org/10.1016/j.chemosphere.2022.136933>.
- (90) Zhang, D. Q.; Zhang, W. L.; Liang, Y. N. Adsorption of Perfluoroalkyl and Polyfluoroalkyl Substances (PFASs) from Aqueous Solution - A Review. *Sci. Total Environ.* **2019**, *694*, 133606. <https://doi.org/10.1016/j.scitotenv.2019.133606>.
- (91) Dixit, F.; Dutta, R.; Barbeau, B.; Berube, P.; Mohseni, M. PFAS Removal by Ion Exchange Resins: A Review. *Chemosphere* **2021**, *272*, 129777. <https://doi.org/10.1016/j.chemosphere.2021.129777>.
- (92) Calore, F.; Badetti, E.; Bonetto, A.; Pozzobon, A.; Marcomini, A. Non-Conventional Sorption Materials for the Removal of Legacy and Emerging PFAS from Water: A Review. *Emerging Contaminants* **2024**, *10* (3), 100303. <https://doi.org/10.1016/j.emcon.2024.100303>.
- (93) Kassar, C.; Graham, C.; Boyer, T. H. Removal of Perfluoroalkyl Acids and Common Drinking Water Contaminants by Weak-Base Anion Exchange Resins: Impacts of Solution PH and Resin Properties. *Water Res X* **2022**, *17*, 100159. <https://doi.org/10.1016/j.wroa.2022.100159>.
- (94) He, Y.; Cheng, X.; Gunjal, S. J.; Zhang, C. Advancing PFAS Sorbent Design: Mechanisms, Challenges, and Perspectives. *ACS Mater Au* **2024**, *4* (2), 108–114. <https://doi.org/10.1021/acsmaterialsau.3c00066>.

- (95) McCleaf, P.; Englund, S.; Östlund, A.; Lindegren, K.; Wiberg, K.; Ahrens, L. Removal Efficiency of Multiple Poly- and Perfluoroalkyl Substances (PFASs) in Drinking Water Using Granular Activated Carbon (GAC) and Anion Exchange (AE) Column Tests. *Water Res.* **2017**, *120*, 77–87. <https://doi.org/10.1016/j.watres.2017.04.057>.
- (96) Vu, C. T.; Wu, T. Recent Progress in Adsorptive Removal of Per- and Poly-Fluoroalkyl Substances (PFAS) from Water/Wastewater. *Crit. Rev. Environ. Sci. Technol.* **2022**, *52* (1), 90–129. <https://doi.org/10.1080/10643389.2020.1816125>.
- (97) Park, M.; Wu, S.; Lopez, I. J.; Chang, J. Y.; Karanfil, T.; Snyder, S. A. Adsorption of Perfluoroalkyl Substances (PFAS) in Groundwater by Granular Activated Carbons: Roles of Hydrophobicity of PFAS and Carbon Characteristics. *Water Res.* **2020**, *170*, 115364. <https://doi.org/10.1016/j.watres.2019.115364>.
- (98) Zhang, Y.; Thomas, A.; Apul, O.; Venkatesan, A. K. Coexisting Ions and Long-Chain per- and Polyfluoroalkyl Substances (PFAS) Inhibit the Adsorption of Short-Chain PFAS by Granular Activated Carbon. *J. Hazard. Mater.* **2023**, *460*, 132378. <https://doi.org/10.1016/j.jhazmat.2023.132378>.
- (99) Xiao, X.; Ulrich, B. A.; Chen, B.; Higgins, C. P. Sorption of Poly- and Perfluoroalkyl Substances (PFASs) Relevant to Aqueous Film-Forming Foam (AFFF)-Impacted Groundwater by Biochars and Activated Carbon. *Environ. Sci. Technol.* **2017**, *51* (11), 6342–6351. <https://doi.org/10.1021/acs.est.7b00970>.
- (100) Kempisty, D. M.; Arevalo, E.; Spinelli, A. M.; Edeback, V.; Dickenson, E. R. V.; Husted, C.; Higgins, C. P.; Summers, R. S.; Knappe, D. R. U. Granular Activated Carbon Adsorption of Perfluoroalkyl Acids from Ground and Surface Water. *AWWA Water Sci.* **2022**, *4* (1). <https://doi.org/10.1002/aws2.1269>.
- (101) Appleman, T. D.; Higgins, C. P.; Quiñones, O.; Vanderford, B. J.; Kolstad, C.; Zeigler-Holady, J. C.; Dickenson, E. R. V. Treatment of Poly- and Perfluoroalkyl Substances in U.S. Full-Scale Water Treatment Systems. *Water Res.* **2014**, *51*, 246–255. <https://doi.org/10.1016/j.watres.2013.10.067>.
- (102) Abbasian Chaleshtari, Z.; Foudazi, R. A Review on Per- and Polyfluoroalkyl Substances (PFAS) Remediation: Separation Mechanisms and Molecular Interactions. *ACS EST Water* **2022**, *2* (12), 2258–2272. <https://doi.org/10.1021/acsestwater.2c00271>.
- (103) Yu, H.; Chen, H.; Fang, B.; Sun, H. Sorptive Removal of Per- and Polyfluoroalkyl Substances from Aqueous Solution: Enhanced Sorption, Challenges and Perspectives. *Sci. Total Environ.* **2023**, *861* (160647), 160647. <https://doi.org/10.1016/j.scitotenv.2022.160647>.
- (104) Gao, Y.; Deng, S.; Du, Z.; Liu, K.; Yu, G. Adsorptive Removal of Emerging Polyfluoroalkyl Substances F-53B and PFOS by Anion-Exchange Resin: A Comparative Study. *J. Hazard. Mater.* **2017**, *323* (Pt A), 550–557. <https://doi.org/10.1016/j.jhazmat.2016.04.069>.
- (105) Du, Z.; Deng, S.; Bei, Y.; Huang, Q.; Wang, B.; Huang, J.; Yu, G. Adsorption Behavior and Mechanism of Perfluorinated Compounds on Various Adsorbents--a Review. *J. Hazard. Mater.* **2014**, *274*, 443–454. <https://doi.org/10.1016/j.jhazmat.2014.04.038>.
- (106) Ellis, A. C. Anion Exchange Remediation of Per- and Polyfluoroalkyl Substances From Groundwater Impacted by Aqueous Film-Forming Foams, Colorado School of Mines, Ann Arbor, United States, 2023. <https://www.proquest.com/dissertations-theses/anion-exchange-remediation-per-polyfluoroalkyl/docview/2895679168/se-2>.
- (107) Malovanyy, A.; Hedman, F.; Bergh, L.; Liljeros, E.; Lund, T.; Suokko, J.; Hinrichsen, H. Comparative Study of Per- and Polyfluoroalkyl Substances (PFAS) Removal from Landfill

- Leachate. *J. Hazard. Mater.* **2023**, *460*, 132505. <https://doi.org/10.1016/j.jhazmat.2023.132505>.
- (108) Schaefer, C. E.; Nguyen, D.; Culina, V. M.; Guelfo, J.; Kumar, N. Application of Rapid Small-Scale Column Tests for Treatment of Perfluoroalkyl Acids Using Anion-Exchange Resins and Granular Activated Carbon in Groundwater with Elevated Organic Carbon. *Ind. Eng. Chem. Res.* **2020**, *59* (38), 16832–16837. <https://doi.org/10.1021/acs.iecr.0c02290>.
- (109) Thompson, M.; Hooper, C.; Cooper, M.; Hooper, C. M. *Child & Adolescent Mental Health: Theory & Practice*; Hodder Arnold: London, England, 2005. <https://doi.org/10.1201/b13430>.
- (110) Lu, D.; Sha, S.; Luo, J.; Huang, Z.; Zhang Jackie, X. Treatment Train Approaches for the Remediation of Per- and Polyfluoroalkyl Substances (PFAS): A Critical Review. *J. Hazard. Mater.* **2020**, *386* (121963), 121963. <https://doi.org/10.1016/j.jhazmat.2019.121963>.
- (111) Dixit, F.; Barbeau, B.; Mostafavi, S. G. PFOA and PFOS Removal by Ion Exchange for Water Reuse and Drinking Applications: Role of Organic Matter Characteristics. *Water Sci. Technol.* **2019**.
- (112) Liu, Y.-L.; Sun, M. Ion Exchange Removal and Resin Regeneration to Treat Per- and Polyfluoroalkyl Ether Acids and Other Emerging PFAS in Drinking Water. *Water Res.* **2021**, *207*, 117781. <https://doi.org/10.1016/j.watres.2021.117781>.
- (113) Zaggia, A.; Conte, L.; Falletti, L.; Fant, M.; Chiorboli, A. Use of Strong Anion Exchange Resins for the Removal of Perfluoroalkylated Substances from Contaminated Drinking Water in Batch and Continuous Pilot Plants. *Water Res.* **2016**, *91*, 137–146. <https://doi.org/10.1016/j.watres.2015.12.039>.
- (114) Medina, R.; Pannu, M. W.; Grieco, S. A.; Hwang, M.; Pham, C.; Plumlee, M. H. Pilot-scale Comparison of Granular Activated Carbons, Ion Exchange, and Alternative Adsorbents for Per- and Polyfluoroalkyl Substances Removal. *AWWA Water Sci.* **2022**, *4* (5). <https://doi.org/10.1002/aws2.1308>.
- (115) Fang, Y.; Ellis, A.; Choi, Y. J.; Boyer, T. H.; Higgins, C. P.; Schaefer, C. E.; Strathmann, T. J. Removal of Per- and Polyfluoroalkyl Substances (PFASs) in Aqueous Film-Forming Foam (AFFF) Using Ion-Exchange and Nonionic Resins. *Environ. Sci. Technol.* **2021**, *55* (8), 5001–5011. <https://doi.org/10.1021/acs.est.1c00769>.
- (116) Pannu, M. W.; Chang, J.; Medina, R.; Grieco, S. A.; Hwang, M.; Plumlee, M. H. Comparing PFAS Removal across Multiple Groundwaters for Eight GACs and Alternative Adsorbent. *AWWA Water Sci.* **2023**, *5* (3). <https://doi.org/10.1002/aws2.1345>.
- (117) Zhang, Z.; Joudiazar, S.; Satpathy, A.; Fernando, E. Y.; Rahmati, R.; Kim, J.; de Falco, G.; Datta, R.; Sarkar, D. Removal of Per- and Polyfluoroalkyl Substances Using Commercially Available Sorbents. *Materials (Basel)* **2025**, *18*. <https://doi.org/10.3390/ma18061299>.
- (118) Urbanas, D.; Baltrėnaitė-Gedienė, E. A Critical Review of the Methods Being Proposed to Solve the PFAS Problem in Drinking Water: Are They Practically Applicable in Real World? *Emerg. Contam.* **2025**, *11* (4), 100563. <https://doi.org/10.1016/j.emcon.2025.100563>.
- (119) Deng, S.; Yu, Q.; Huang, J.; Yu, G. Removal of Perfluorooctane Sulfonate from Wastewater by Anion Exchange Resins: Effects of Resin Properties and Solution Chemistry. *Water Res.* **2010**, *44* (18), 5188–5195. <https://doi.org/10.1016/j.watres.2010.06.038>.
- (120) Maimaiti, A.; Deng, S.; Meng, P.; Wang, W.; Wang, B.; Huang, J.; Wang, Y.; Yu, G. Competitive Adsorption of Perfluoroalkyl Substances on Anion Exchange Resins in Simulated AFFF-Impacted Groundwater. *Chem. Eng. J.* **2018**, *348*, 494–502. <https://doi.org/10.1016/j.cej.2018.05.006>.

- (121) Conte, L.; Falletti, L.; Zaggia, A.; Milan, M. Polyfluorinated Organic Micropollutants Removal from Water by Ion Exchange and Adsorption. *Chemical engineering transactions* **2015**, *43*, 2257–2262. <https://doi.org/10.3303/CET1543377>.
- (122) Boyer, T. H.; Fang, Y.; Ellis, A.; Dietz, R.; Choi, Y. J.; Schaefer, C. E.; Higgins, C. P.; Strathmann, T. J. Anion Exchange Resin Removal of Per- and Polyfluoroalkyl Substances (PFAS) from Impacted Water: A Critical Review. *Water Res.* **2021**, *200*, 117244. <https://doi.org/10.1016/j.watres.2021.117244>.
- (123) Yao, Y.; Volchek, K.; Brown, C. E.; Robinson, A.; Obal, T. Comparative Study on Adsorption of Perfluorooctane Sulfonate (PFOS) and Perfluorooctanoate (PFOA) by Different Adsorbents in Water. *Water Sci. Technol.* **2014**, *70* (12), 1983–1991. <https://doi.org/10.2166/wst.2014.445>.
- (124) Kugler, A. J.; Saslow, S. A.; Pearce, C. I.; Johnson, C. D. PFAS Removal by Ion Exchange Resins: Background and Knowledge Gaps with Respect to the Hanford Site. **2025**.
- (125) Junge, F.; Rückbeil, F. E.; Gnirss, R.; Haag, R.; Lorente, A.; Lorenz, F.; Menacherry, S. P. M.; Ruhl, A. S.; Sperlich, A.; Zidar, A.; Wagner, O. Effect of Hydrophobic Cross-Linkers in Strong Base Gel-Type Resins on the Adsorption Kinetics and Capacity for Perfluoroalkyl Substances. *ACS ES T Water* **2025**, *5* (8), 4435–4447. <https://doi.org/10.1021/acsestwater.5c00094>.
- (126) Laura Del Moral, L.; Choi, Y. J.; Boyer, T. H. Comparative Removal of Suwannee River Natural Organic Matter and Perfluoroalkyl Acids by Anion Exchange: Impact of Polymer Composition and Mobile Counterion. *Water Res.* **2020**, *178*, 115846. <https://doi.org/10.1016/j.watres.2020.115846>.
- (127) Dixit, F.; Barbeau, B.; Mohseni, M. Impact of Natural Organic Matter Characteristics and Inorganic Anions on the Performance of Ion Exchange Resins in Natural Waters. *Water Sci. Technol. Water Supply* **2020**, *20* (8), 3107–3119. <https://doi.org/10.2166/ws.2020.197>.
- (128) Fu, K.; Huang, J.; Luo, F.; Fang, Z.; Yu, D.; Zhang, X.; Wang, D.; Xing, M.; Luo, J. Understanding the Selective Removal of Perfluoroalkyl and Polyfluoroalkyl Substances via Fluorine-Fluorine Interactions: A Critical Review. *Environ. Sci. Technol.* **2024**. <https://doi.org/10.1021/acs.est.4c06519>.
- (129) Ellis, A. C.; Boyer, T. H.; Strathmann, T. J. Regeneration of Conventional and Emerging PFAS-Selective Anion Exchange Resins Used to Treat PFAS-Contaminated Waters. *Sep. Purif. Technol.* **2025**, *355* (129789), 129789. <https://doi.org/10.1016/j.seppur.2024.129789>.
- (130) Marshall, R. E. Performance and Cost-Effectiveness of Commercially Available Adsorptive Technologies for Treatment of Per- and Poly-Fluoroalkyl Substances (PFAS) Impacted Groundwater, Colorado School of Mines, Ann Arbor, United States, 2019. <https://www.proquest.com/dissertations-theses/performance-cost-effectiveness-commercially/docview/2382683585/se-2>.
- (131) Rückbeil, F. E.; Sperlich, A.; Gnirss, R.; Dittmann, D.; Kämpfe, A.; Höra, C.; Ruhl, A. S. Comparing Activated Carbons, Ion Exchange Resins and Alternative Adsorbents for the Removal of Perfluoroalkyl and Other Persistent and Mobile Substances. *Chem. Eng. J.* **2025**, *516* (164070), 164070. <https://doi.org/10.1016/j.cej.2025.164070>.
- (132) Anjum, S.; Arik, M.; Patel, A.; Abasali, N.; Wu, L.; Sarkar, A. Fluorinated Block Copolymer: An Important Sorbent Design Criteria for Effective PFOA Removal from Its Aqueous Solution. *ACS Appl. Polym. Mater.* **2025**, *7* (3), 1187–1193. <https://doi.org/10.1021/acsapm.4c03792>.

- (133) Pezoulas, E. R.; Tajdini, B.; Ko, Y.; Uliana, A. A.; Giovine, R.; Furukawa, H.; Vatankhah, H.; Börgel, J.; Kim, K. C.; Bellona, C.; Long, J. R. Functionalized Porous Polymer Networks as High-Performance PFAS Adsorbents. *J. Am. Chem. Soc.* **2025**, *147* (25), 21832–21843. <https://doi.org/10.1021/jacs.5c04689>.
- (134) Wanninayake, D. M. Comparison of Currently Available PFAS Remediation Technologies in Water: A Review. *J. Environ. Manage.* **2021**, *283* (111977), 111977. <https://doi.org/10.1016/j.jenvman.2021.111977>.
- (135) Ching, C.; Lin, Z.-W.; Dichtel, W. R.; Helbling, D. E. Evaluating the Performance of Novel Cyclodextrin Polymer Granules to Remove Perfluoroalkyl Acids (PFAAs) from Water. *ACS EST Eng.* **2023**, *3* (5), 661–670. <https://doi.org/10.1021/acsestengg.2c00379>.
- (136) Wang, R.; Ling, Y. DEXSORB: New Technology for PFAS, 2022. [https://www.holbrookma.gov/sites/g/files/vyhlf3261/f/news/cyclopure\\_tech\\_intro\\_01.20.2021.pdf](https://www.holbrookma.gov/sites/g/files/vyhlf3261/f/news/cyclopure_tech_intro_01.20.2021.pdf).
- (137) Ling, Y.; Barin, G.; Li, S.; Notter, M. J. Novel Cyclodextrin Polymer Adsorbents for PFAS Removal. In *Forever Chemicals*; CRC Press, 2021; pp 291–313. <https://doi.org/10.1201/9781003024521-17>.
- (138) Wang, R.; Lin, Z.-W.; Klemes, M. J.; Ateia, M.; Trang, B.; Wang, J.; Ching, C.; Helbling, D. E.; Dichtel, W. R. A Tunable Porous  $\beta$ -Cyclodextrin Polymer Platform to Understand and Improve Anionic PFAS Removal. *ACS Cent Sci* **2022**, *8* (5), 663–669. <https://doi.org/10.1021/acscentsci.2c00478>.
- (139) Lin, Z.-W.; Shapiro, E. F.; Barajas-Rodriguez, F. J.; Gaisin, A.; Ateia, M.; Currie, J.; Helbling, D. E.; Gwinn, R.; Packman, A. I.; Dichtel, W. R. Trace Organic Contaminant Removal from Municipal Wastewater by Styrenic  $\beta$ -Cyclodextrin Polymers. *Environ. Sci. Technol.* **2023**, *57* (48), 19624–19636. <https://doi.org/10.1021/acs.est.3c04233>.
- (140) Loeve, S.; Normand, M. How to Trust a Molecule? The Case of Cyclodextrins Entering the Nanorealm. *Quantum Engagements. Social reflections of nanoscience and emerging technologies* **2011**, 195–216.
- (141) Sedlak, J.; Chheda, S.; Green, C.; Okoh, E.; Zheng, Z. Malodor Management in High Exuding Chronic Wounds. In *2014 40th Annual Northeast Bioengineering Conference (NEBEC)*; IEEE, 2014; pp 1–3. <https://doi.org/10.1109/nebec.2014.6972933>.
- (142) Anderson, J. C.; Beyger, L.; Guchardi, J.; Holdway, D. Chronic Effects of Hydroxypropyl- $\beta$ -Cyclodextrin on Reproduction in the American Flagfish (*Jordanella Floridae*) over One Complete Life Cycle. *Environ. Toxicol. Chem.* **2016**, *35* (6), 1358–1363. <https://doi.org/10.1002/etc.3280>.
- (143) Xiao, L.; Ling, Y.; Alsbaiee, A.; Li, C.; Helbling, D. E.; Dichtel, W. R. B-Cyclodextrin Polymer Network Sequesters Perfluorooctanoic Acid at Environmentally Relevant Concentrations. *J. Am. Chem. Soc.* **2017**, *139* (23), 7689–7692. <https://doi.org/10.1021/jacs.7b02381>.
- (144) Wang, Z.; Zhang, P.; Hu, F.; Zhao, Y.; Zhu, L. A Crosslinked  $\beta$ -Cyclodextrin Polymer Used for Rapid Removal of a Broad-Spectrum of Organic Micropollutants from Water. *Carbohydr. Polym.* **2017**, *177*, 224–231. <https://doi.org/10.1016/j.carbpol.2017.08.059>.
- (145) Crini, G.; Fourmentin, S.; Fenyvesi, É.; Torri, G.; Fourmentin, M.; Morin-Crini, N. Cyclodextrins, from Molecules to Applications. *Environ. Chem. Lett.* **2018**, *16* (4), 1361–1375. <https://doi.org/10.1007/s10311-018-0763-2>.

- (146) Helbling, D. E.; Dichtel, W. R. Rational Design and Implementation of Novel Polymer Adsorbents for Selective Uptake of PFAS from Groundwater. *SERDP Project ER18-1026* **2022**.
- (147) Leung, S. C. E.; Wanninayake, D.; Chen, D.; Nguyen, N.-T.; Li, Q. Physicochemical Properties and Interactions of Perfluoroalkyl Substances (PFAS) - Challenges and Opportunities in Sensing and Remediation. *Sci. Total Environ.* **2023**, *905* (166764), 166764. <https://doi.org/10.1016/j.scitotenv.2023.166764>.
- (148) Ling, Y. Novel  $\beta$ -Cyclodextrin Polymer Adsorbents for Removal of PFAS from Diverse Water Matrices. *2021 Emerging Contaminants in the Environment Conference (ECEC21)* **2021**.
- (149) Anjum, A.; Gupta, D.; Singh, B.; Garg, R.; Pani, B.; Kashif, M.; Jain, S. Clay-Polymer Nanocomposites for Effective Water Treatment: Opportunities, Challenges, and Future Prospects. *Environ. Monit. Assess.* **2024**, *196* (7), 666. <https://doi.org/10.1007/s10661-024-12823-8>.
- (150) Ray, J. R.; Shabtai, I. A.; Teixidó, M.; Mishael, Y. G.; Sedlak, D. L. Polymer-Clay Composite Geomedia for Sorptive Removal of Trace Organic Compounds and Metals in Urban Stormwater. *Water Res.* **2019**, *157*, 454–462. <https://doi.org/10.1016/j.watres.2019.03.097>.
- (151) Okaikue-Woodi, F. E. K.; Cherukumilli, K.; Ray, J. R. A Critical Review of Contaminant Removal by Conventional and Emerging Media for Urban Stormwater Treatment in the United States. *Water Res.* **2020**, *187* (116434), 116434. <https://doi.org/10.1016/j.watres.2020.116434>.
- (152) Okaikue-Woodi, F. E. K.; Lumagui, R. M.; Ray, J. R. Simultaneous Oxidation of Trace Organics and Sorption of Trace Metals by Ferrate (Fe(VI))-Coated Sand in Synthetic Wastewater Effluent. *ACS Environ. Au* **2024**, *4* (5), 260–270. <https://doi.org/10.1021/acsenvironau.4c00024>.
- (153) Umeh, A. C.; Hassan, M.; Egbuatu, M.; Zeng, Z.; Al Amin, M.; Samarasinghe, C.; Naidu, R. Multicomponent PFAS Sorption and Desorption in Common Commercial Adsorbents: Kinetics, Isotherm, Adsorbent Dose, PH, and Index Ion and Ionic Strength Effects. *Sci. Total Environ.* **2023**, *904* (166568), 166568. <https://doi.org/10.1016/j.scitotenv.2023.166568>.
- (154) Das, P.; Arias E., V. A.; Kambala, V.; Mallavarapu, M.; Naidu, R. Remediation of Perfluorooctane Sulfonate in Contaminated Soils by Modified Clay Adsorbent—a Risk-Based Approach. *Water Air Soil Pollut.* **2013**, *224* (12). <https://doi.org/10.1007/s11270-013-1714-y>.
- (155) Zhou, Q.; Deng, S.; Yu, Q.; Zhang, Q.; Yu, G.; Huang, J.; He, H. Sorption of Perfluorooctane Sulfonate on Organo-Montmorillonites. *Chemosphere* **2010**, *78* (6), 688–694. <https://doi.org/10.1016/j.chemosphere.2009.12.005>.
- (156) Yan, B.; Munoz, G.; Sauv e, S.; Liu, J. Molecular Mechanisms of Per- and Polyfluoroalkyl Substances on a Modified Clay: A Combined Experimental and Molecular Simulation Study. *Water Res.* **2020**, *184*, 116166. <https://doi.org/10.1016/j.watres.2020.116166>.
- (157) Wang, C.; Yan, B.; Munoz, G.; Sauv e, S.; Liu, J. Modified Clays Reduce Leaching of Per- and Polyfluoroalkyl Substances from AFFF-contaminated Soils. *AWWA Water Sci.* **2021**, *3*. <https://doi.org/10.1002/aws2.1241>.
- (158) Najm, I.; Gallagher, B.; Vishwanath, N.; Blute, N.; Gorzalski, A.; Feffer, A.; Richardson, S. Per- and Polyfluoroalkyl Substances Removal with Granular Activated Carbon and a

- Specialty Adsorbent: A Case Study. *AWWA Water Sci.* **2021**, 3 (5). <https://doi.org/10.1002/aws2.1245>.
- (159) Pourabadehei, M.; Tarnocai, D.; Timlin, R.; Orquiza, R.; McRae, C.; Tam, A. In Situ Treatment-train Remediation of Per- and Polyfluoroalkyl Substance-Impacted Groundwater. *Remediation (N. Y.)* **2025**, 35 (2). <https://doi.org/10.1002/rem.70014>.
- (160) Leong, C. C. ... of Granular Activated Carbon and Alternative Adsorbents for Per-and Polyfluoroalkyl Substances Removal From Surface Water and Groundwater. **2024**.
- (161) El Mohtar, C. S.; Alvertos, A.; Panda, S. Stabilization of PFAS in Contaminated Soils Using Fluoro-Sorb® 100: A Bench-Scale Study. publishing.argo-e.com 2023. <https://doi.org/10.53243/ICEG2023-437>.
- (162) Fakioglu, M.; Golovko, O.; Baresel, C.; Ahrens, L.; Ozturk, I. Combination of Ozonation with GAC, AIX and Biochar Post-Treatment for Removal of Pharmaceuticals and Transformation Products from Municipal WWTP Effluent. *Environ. Sci. (Camb.)* **2024**, 10 (12), 3249–3262. <https://doi.org/10.1039/d4ew00702f>.
- (163) Calgon, C. FILTRASORB® 400 Granular Activated Carbon. 2024. <https://www.calgoncarbon.com/app/uploads/F400-Final.pdf>.
- (164) Ochoa-Herrera, V.; Sierra-Alvarez, R. Removal of Perfluorinated Surfactants by Sorption onto Granular Activated Carbon, Zeolite and Sludge. *Chemosphere* **2008**, 72 (10), 1588–1593. <https://doi.org/10.1016/j.chemosphere.2008.04.029>.
- (165) Zeng, C.; Atkinson, A.; Sharma, N.; Ashani, H.; Hjelmstad, A.; Venkatesh, K.; Westerhoff, P. Removing Per- and Polyfluoroalkyl Substances from Groundwaters Using Activated Carbon and Ion Exchange Resin Packed Columns. *AWWA Water Sci.* **2020**, 2 (1), e1172. <https://doi.org/10.1002/aws2.1172>.
- (166) Croll, H. C.; Chow, S.; Ojeda, N.; Schwab, K.; Prasse, C.; Capelle, R.; Klamerus, J.; Oppenheimer, J.; Jacangelo, J. G. Adaptation of Selected Models for Describing Competitive Per- and Polyfluoroalkyl Substances Breakthrough Curves in Groundwater Treated by Granular Activated Carbon. *J. Hazard. Mater.* **2022**, 433, 128804. <https://doi.org/10.1016/j.jhazmat.2022.128804>.
- (167) Coelho, C.; Oliveira, A. S.; Pereira, M. F. R.; Nunes, O. C. The Influence of Activated Carbon Surface Properties on the Adsorption of the Herbicide Molinate and the Bio-Regeneration of the Adsorbent. *J. Hazard. Mater.* **2006**, 138 (2), 343–349. <https://doi.org/10.1016/j.jhazmat.2006.05.062>.
- (168) Purolite. *Purofine® PFA694*. <https://www.purolite.com/product/pfa694> (accessed 2024-04-10).
- (169) Boodoo, F.; Campos, J.; Kennedy, S. Removal of PFOA, PFOS and Other PFAS Substances Using Ion Exchange. *bzchem.gr* **2017**.
- (170) DuPont™ AmberLite™ PSR2 Plus Ion Exchange Resin. <https://www.dupont.com/content/dam/water/amer/us/en/water/public/documents/en/IER-AmberLite-PSR2-Plus-PDS-45-D00899-en.pdf>.
- (171) DuPont™. AmberLite™ IRA910 Cl Ion Exchange Resin. February 2023. <https://www.dupont.com/content/dam/water/amer/us/en/water/public/documents/en/IER-AmberLite-IRA910-Cl-PDS-45-D01255-en.pdf>.
- (172) Liu, C.; Chu, J.; Cápiro, N. L.; Fortner, J. D.; Pennell, K. D. In-Situ Sequestration of Perfluoroalkyl Substances Using Polymer-Stabilized Ion Exchange Resin. *J. Hazard. Mater.* **2022**, 422, 126960. <https://doi.org/10.1016/j.jhazmat.2021.126960>.

- (173) Nguyen, D.; Schaefer, C. E. Application of Rapid, Small-Scale Column Tests to Assess Treatment of Perfluoroalkyl Acids in Groundwater Using A Novel Modified Clay Sorbent. *Ind. Eng. Chem. Res.* **2023**, *62* (34), 13314–13323. <https://doi.org/10.1021/acs.iecr.3c02159>.
- (174) Ching, C.; Klemes, M. J.; Trang, B.; Dichtel, W. R.; Helbling, D. E. B-Cyclodextrin Polymers with Different Cross-Linkers and Ion-Exchange Resins Exhibit Variable Adsorption of Anionic, Zwitterionic, and Nonionic PFASs. *Environ. Sci. Technol.* **2020**, *54* (19), 12693–12702. <https://doi.org/10.1021/acs.est.0c04028>.
- (175) Cyclopure. DEXSORB in Engineered Systems. May 31, 2022. [https://cyclopure.com/wp-content/uploads/2022/05/2022-05-31\\_Handout\\_DEXSORB-in-Engineered-Systems-v3.pdf](https://cyclopure.com/wp-content/uploads/2022/05/2022-05-31_Handout_DEXSORB-in-Engineered-Systems-v3.pdf).
- (176) Wu, C.; Klemes, M. J.; Trang, B.; Dichtel, W. R.; Helbling, D. E. Exploring the Factors That Influence the Adsorption of Anionic PFAS on Conventional and Emerging Adsorbents in Aquatic Matrices. *Water Res.* **2020**, *182*, 115950. <https://doi.org/10.1016/j.watres.2020.115950>.
- (177) Ling, Y.; Klemes, M. J.; Xiao, L.; Alsaiee, A.; Dichtel, W. R.; Helbling, D. E. Benchmarking Micropollutant Removal by Activated Carbon and Porous  $\beta$ -Cyclodextrin Polymers under Environmentally Relevant Scenarios. *Environ. Sci. Technol.* **2017**, *51* (13), 7590–7598. <https://doi.org/10.1021/acs.est.7b00906>.
- (178) Yang, A.; Ching, C.; Easler, M.; Helbling, D. E.; Dichtel, W. R. Cyclodextrin Polymers with Nitrogen-Containing Tripodal Crosslinkers for Efficient PFAS Adsorption. *ACS Mater. Lett.* **2020**, *2* (9), 1240–1245. <https://doi.org/10.1021/acsmaterialslett.0c00240>.
- (179) Zhang, C.; Hopkins, Z. R.; McCord, J.; Strynar, M. J.; Knappe, D. R. U. Fate of Per- and Polyfluoroalkyl Ether Acids in the Total Oxidizable Precursor Assay and Implications for the Analysis of Impacted Water. *Environ. Sci. Technol. Lett.* **2019**, *6* (11), 662–668. <https://doi.org/10.1021/acs.estlett.9b00525>.
- (180) Mullin, L.; Katz, D.; Riddell, N.; Plumb, R.; Burgess, J. A.; Yeung, L. W. Y.; Jogsten, I. E. Analysis of Hexafluoropropylene Oxide-Dimer Acid (HFPO-DA) by Liquid Chromatography-Mass Spectrometry (LC-MS): Review of Current Approaches and Environmental Levels. *Trends Analyt. Chem.* **2019**, *118*, 828–839. <https://doi.org/10.1016/j.trac.2019.05.015>.
- (181) Field, J. A.; Seow, J. Properties, Occurrence, and Fate of Fluorotelomer Sulfonates. *Crit. Rev. Environ. Sci. Technol.* **2017**, *47* (8), 643–691. <https://doi.org/10.1080/10643389.2017.1326276>.
- (182) Skinner, J. P.; Raderstorf, A.; Rittmann, B. E.; Delgado, A. G. Biotransforming the “Forever Chemicals”: Trends and Insights from Microbiological Studies on PFAS. *Environ. Sci. Technol.* **2025**, *59* (11), 5417–5430. <https://doi.org/10.1021/acs.est.4c04557>.
- (183) Henne, S.; Storck, F. R.; Wöhrnschimmel, H.; Leuenberger, M.; Vollmer, M. K.; Reimann, S. Trifluoroacetate (TFA) in Precipitation and Surface Waters in Switzerland: Trends, Source Attribution, and Budget. *EGUsphere* **2025**, *2025*, 1–43.
- (184) Steigerwald, J. M.; Peng, S.; Ray, J. R. Novel Perfluorooctanesulfonate-Imprinted Polymer Immobilized on Spent Coffee Grounds Biochar for Selective Removal of Perfluoroalkyl Acids in Synthetic Wastewater. *ACS EST Eng.* **2023**, *3* (4), 520–532. <https://doi.org/10.1021/acsestengg.2c00336>.
- (185) ZeeWeed 1500 -Experienced Evolution. [https://preprod.watertechnologies.com/document/document/contentdownload/?document\\_name=BRpwZeeWeed1500\\_GEA17506\\_EN.pdf&language=English&limit=25&security=Public](https://preprod.watertechnologies.com/document/document/contentdownload/?document_name=BRpwZeeWeed1500_GEA17506_EN.pdf&language=English&limit=25&security=Public).

- (186) Yu, Q.; Zhang, R.; Deng, S.; Huang, J.; Yu, G. Sorption of Perfluorooctane Sulfonate and Perfluorooctanoate on Activated Carbons and Resin: Kinetic and Isotherm Study. *Water Res.* **2009**, *43* (4), 1150–1158. <https://doi.org/10.1016/j.watres.2008.12.001>.
- (187) Giles, C. H.; MacEwan, T. H.; Nakhwa, S. N.; Smith, D. 786. Studies in Adsorption. Part XI. A System of Classification of Solution Adsorption Isotherms, and Its Use in Diagnosis of Adsorption Mechanisms and in Measurement of Specific Surface Areas of Solids. *J. Chem. Soc.* **1960**, No. 0, 3973. <https://doi.org/10.1039/jr9600003973>.
- (188) Limousin, G.; Gaudet, J.-P.; Charlet, L.; Szenknect, S.; Barthès, V.; Krimissa, M. Sorption Isotherms: A Review on Physical Bases, Modeling and Measurement. *Appl. Geochem.* **2007**, *22* (2), 249–275. <https://doi.org/10.1016/j.apgeochem.2006.09.010>.
- (189) Karoyo, A. H.; Wilson, L. D. Investigation of the Adsorption Processes of Fluorocarbon and Hydrocarbon Anions at the Solid–Solution Interface of Macromolecular Imprinted Polymer Materials. *J. Phys. Chem. C Nanomater. Interfaces* **2016**, *120* (12), 6553–6568. <https://doi.org/10.1021/acs.jpcc.5b12246>.
- (190) Pauletto, P. S.; Bandosz, T. J. Activated Carbon versus Metal–Organic Frameworks: A Review of Their PFAS Adsorption Performance. *J. Hazard. Mater.* **2022**, *425* (127810), 127810. <https://doi.org/10.1016/j.jhazmat.2021.127810>.
- (191) Zhang, Y.; Xu, Y.; Shi, B.; Huang, X. The Influence of Nitrogen-Containing Functional Groups and Pore Structure on the Adsorption of per- and Polyfluoroalkyl Substances in Ultrapure and Real Water. *J. Environ. Chem. Eng.* **2024**, *12* (2), 112082. <https://doi.org/10.1016/j.jece.2024.112082>.
- (192) Liu, C. J.; Werner, D.; Bellona, C. Removal of Per- and Polyfluoroalkyl Substances (PFASs) from Contaminated Groundwater Using Granular Activated Carbon: A Pilot-Scale Study with Breakthrough Modeling. *Environ. Sci. (Camb.)* **2019**, *5* (11), 1844–1853. <https://doi.org/10.1039/c9ew00349e>.
- (193) Weiss-Errico, M. J.; O’Shea, K. E. Enhanced Host–Guest Complexation of Short Chain Perfluoroalkyl Substances with Positively Charged  $\beta$ -Cyclodextrin Derivatives. *J. Incl. Phenom. Macrocycl. Chem.* **2019**, *95* (1–2), 111–117. <https://doi.org/10.1007/s10847-019-00930-w>.
- (194) Karoyo, A. H.; Sidhu, P.; Wilson, L. D.; Hazendonk, P. Characterization and Dynamic Properties for the Solid Inclusion Complexes of  $\beta$ -Cyclodextrin and Perfluorooctanoic Acid. *J. Phys. Chem. B* **2013**, *117* (27), 8269–8282. <https://doi.org/10.1021/jp402559n>.
- (195) Choudhary, A.; Dong, D.; Tsianou, M.; Alexandridis, P.; Bedrov, D. Adsorption Mechanism of Perfluorooctanoate on Cyclodextrin-Based Polymers: Probing the Synergy of Electrostatic and Hydrophobic Interactions with Molecular Dynamics Simulations. *ACS Mater. Lett.* **2022**, *4* (5), 853–859. <https://doi.org/10.1021/acsmaterialslett.2c00168>.
- (196) Ching, C.; Ling, Y.; Trang, B.; Klemes, M.; Xiao, L.; Yang, A.; Barin, G.; Dichtel, W. R.; Helbling, D. E. Identifying the Physicochemical Properties of  $\beta$ -Cyclodextrin Polymers That Determine the Adsorption of Perfluoroalkyl Acids. *Water Res.* **2022**, *209* (117938), 117938. <https://doi.org/10.1016/j.watres.2021.117938>.
- (197) Akkaya, R.; Ulusoy, U. Adsorptive Features of Chitosan Entrapped in Polyacrylamide Hydrogel for Pb<sup>2+</sup>, UO<sub>2</sub>(<sup>2+</sup>), and Th<sup>4+</sup>. *J. Hazard. Mater.* **2008**, *151* (2–3), 380–388. <https://doi.org/10.1016/j.jhazmat.2007.05.084>.
- (198) Roque, M. I.; Rocha, V.; Domingues, E.; Martins, R. C.; Durães, L. Effective Removal of Perfluoroalkyl Substances from Water by SilicaBased Aerogel Adsorbents.

- (199) Sun, M. Remove Per- and Polyfluoroalkyl Substance from Water by Combined Ion Exchange and UV/Sulfite Treatment. March 15, 2024. <https://repository.lib.ncsu.edu/server/api/core/bitstreams/a2f2b01b-0cec-496a-9a34-6ee879aa6145/content>.
- (200) Rayne, S.; Forest, K. Perfluoroalkyl Sulfonic and Carboxylic Acids: A Critical Review of Physicochemical Properties, Levels and Patterns in Waters and Wastewaters, and Treatment Methods. *J. Environ. Sci. Health A Tox. Hazard. Subst. Environ. Eng.* **2009**, *44* (12), 1145–1199. <https://doi.org/10.1080/10934520903139811>.
- (201) Johnson, R. L.; Anschutz, A. J.; Smolen, J. M.; Simcik, M. F.; Penn, R. L. The Adsorption of Perfluorooctane Sulfonate onto Sand, Clay, and Iron Oxide Surfaces. *J. Chem. Eng. Data* **2007**, *52* (4), 1165–1170. <https://doi.org/10.1021/je060285g>.
- (202) Tsianou, M.; Bedrov, D.; Alexandridis, P. Surfactants in the Environment: Self-Assembly of PFAS Pollutants in Solution and at Interfaces. In *ACS Symposium Series*; ACS symposium series. American Chemical Society; American Chemical Society: Washington, DC, 2023; pp 443–462. <https://doi.org/10.1021/bk-2023-1457.ch016>.
- (203) Kancharla, S.; Jahan, R.; Bedrov, D.; Tsianou, M.; Alexandridis, P. Role of Chain Length and Electrolyte on the Micellization of Anionic Fluorinated Surfactants in Water. *Colloids Surf. A Physicochem. Eng. Asp.* **2021**, *628* (127313), 127313. <https://doi.org/10.1016/j.colsurfa.2021.127313>.
- (204) Sobolewski, T. N.; Findlay, J. L.; Hemphill, J. E.; Walker, R. A. Aggregation, Not Micellization: Perfluorooctanoic Acid, Perfluorobutanesulfonic Acid, and Potassium Perfluorooctanesulfonate Behavior in Aqueous Solution. *Langmuir* **2024**, *40* (47), 24820–24831. <https://doi.org/10.1021/acs.langmuir.4c02566>.
- (205) Ellis, A. C.; Boyer, T. H.; Fang, Y.; Liu, C. J.; Strathmann, T. J. Life Cycle Assessment and Life Cycle Cost Analysis of Anion Exchange and Granular Activated Carbon Systems for Remediation of Groundwater Contaminated by Per- and Polyfluoroalkyl Substances (PFASs). *Water Res.* **2023**, *243* (120324), 120324. <https://doi.org/10.1016/j.watres.2023.120324>.
- (206) Karoyo, A. H.; Wilson, L. D. Tunable Macromolecular-Based Materials for the Adsorption of Perfluorooctanoic and Octanoic Acid Anions. *J. Colloid Interface Sci.* **2013**, *402*, 196–203. <https://doi.org/10.1016/j.jcis.2013.03.065>.
- (207) DuPont™ AmberLite™ IRA910 Cl. <https://www.dupont.com/products/amberliteira910cl.html> (accessed 2025-12-01).
- (208) Deng, S.; Zhang, Q.; Nie, Y.; Wei, H.; Wang, B.; Huang, J.; Yu, G.; Xing, B. Sorption Mechanisms of Perfluorinated Compounds on Carbon Nanotubes. *Environ. Pollut.* **2012**, *168*, 138–144. <https://doi.org/10.1016/j.envpol.2012.03.048>.
- (209) Zhang, D.; He, Q.; Wang, M.; Zhang, W.; Liang, Y. Sorption of Perfluoroalkylated Substances (PFASs) onto Granular Activated Carbon and Biochar. *Environ. Technol.* **2021**, *42* (12), 1798–1809. <https://doi.org/10.1080/09593330.2019.1680744>.
- (210) Schuricht, F.; Borovinskaya, E. S.; Reschetilowski, W. Removal of Perfluorinated Surfactants from Wastewater by Adsorption and Ion Exchange - Influence of Material Properties, Sorption Mechanism and Modeling. *J. Environ. Sci. (China)* **2017**, *54*, 160–170. <https://doi.org/10.1016/j.jes.2016.06.011>.
- (211) Chaudhary, M.; Sela-Adler, M.; Ronen, A.; Nir, O. Efficient PFOA Removal from Drinking Water by a Dual-Functional Mixed-Matrix-Composite Nanofiltration Membrane. *Npj Clean Water* **2023**, *6* (1), 1–10. <https://doi.org/10.1038/s41545-023-00286-2>.

- (212) Smith, S.; Pinkard, B.; Zweifel, T.; Dressel, L.; Vorarath, P.; Junes, C.; Gibeault, J.; Malinsky, J.; Hackbarth, T.; Halevi, A.; Thomsen, C.; Rhodes, C.; Mukherjee, S.; Ellis, A. Demonstration of Hydrothermal Alkaline Treatment for PFAS Destruction in Industrial Wastewater: Assessment of Degradation, Defluorination, Fluorine Mass Balance, and Potential .... **2025**.